

INFORMATION TO USERS

This material was produced from a microfilm copy of the original document. While the most advanced technological means to photograph and reproduce this document have been used, the quality is heavily dependent upon the quality of the original submitted

The following explanation of techniques is provided to help you understand markings or patterns which may appear on this reproduction.

- 1 The sign or "target" for pages apparently lacking from the document photographed is "Missing Page(s)". If it was possible to obtain the missing page(s) or section, they are spliced into the film along with adjacent pages. This may have necessitated cutting thru an image and duplicating adjacent pages to insure you complete continuity.
- 2 When an image on the film is obliterated with a large round black mark, it is an indication that the photographer suspected that the copy may have moved during exposure and thus cause a blurred image. You will find a good image of the page in the adjacent frame.
- 3 When a map, drawing or chart, etc., was part of the material being photographed the photographer followed a definite method in "sectioning" the material. It is customary to begin photoing at the upper left hand corner of a large sheet and to continue photoing from left to right in equal sections with a small overlap. If necessary, sectioning is continued again — beginning below the first row and continuing on until complete.
- 4 The majority of users indicate that the textual content is of greatest value, however, a somewhat higher quality reproduction could be made from "photographs" if essential to the understanding of the dissertation. Silver prints of "photographs" may be ordered at additional charge by writing the Order Department, giving the catalog number, title, author and specific pages you wish reproduced.
- 5 PLEASE NOTE: Some pages may have indistinct print. Filmed as received.

Xerox University Microfilms

300 North Zeeb Road
Ann Arbor, Michigan 48106

74-25,549

SCHWARTZ, Ira Sheldon, 1947-
INTERACTION OF DAUNOMYCIN AND DNA.

The City University of New York, Ph.D., 1974
Chemistry, biological

University Microfilms, A XEROX Company, Ann Arbor, Michigan

INTERACTION OF DAUNOMYCIN AND DNA

by

IRA SCHWARTZ

A dissertation submitted to the Graduate Faculty in Biochemistry in partial fulfillment of the requirements for the degree of Doctor of Philosophy. The City University of New York.

1974

This manuscript has been read and accepted for the Graduate Faculty in Biochemistry in satisfaction of the dissertation requirement for the degree of Doctor of Philosophy.

June 25, 1974
Date

Meyer Fishman
Chairman of Examining Committee

June 25, 1974
Date

Walter L. Brown
Executive Officer

Stanley Seltzer
Joseph Kern V
Harold J. Li
Charlotte S. Russell

ABSTRACT

Various aspects of the interaction between daunomycin and nucleic acids were studied. The addition of either Mg^{++} or Cu^{++} ions resulted in spectral changes for the daunomycin-DNA complex; the 505 nm peak disappeared with the appearance of new peaks at 540 nm and 582 nm and there was a marked decrease in the fluorescence intensity at 555 nm as well. However, the effects were different for each ion. Mg^{++} affected the complexes with both native and denatured DNA, whereas Cu^{++} was effective only for the denatured DNA-daunomycin complex. The maximum effect occurred at pH 7.8 with Mg^{++} , at pH 5.2 with Cu^{++} . In addition, the concentration of Mg^{++} necessary to induce these effects was 0.1 M, three orders of magnitude greater than that which was needed with Cu^{++} . Mg^{++} released DNA from the complex and replaced it by competing for binding sites on the daunomycin molecule, probably the chromophore oxygen atoms. On the other hand, Cu^{++} bound to the sugar amino group of daunomycin.

Daunomycin did not form a complex with nucleic acid bases, nucleosides, nucleoside monophosphates or nucleoside triphosphates. Complex formation was observed with polynucleotides indicating a requirement for a polymeric structure.

Spectral titration studies demonstrated the existence of two binding processes for the daunomycin-nucleic acid interaction, a strong binding, probably intercalation, and

a second binding mode, electrostatic in nature.

The maximum number of daunomycin binding sites/ phosphate, n , was greater for denatured DNA and polynucleotides than for native DNA. An increase in ionic strength resulted in lower n values. In native DNA and at high ionic strength there were geometrical constraints which resulted in lower n values. An ionic strength increase caused a greater decrease in n for the polynucleotides than for native or denatured DNA which indicated a large electrostatic contribution for the polynucleotide-daunomycin complex at low ionic strength ($\mu = 0.005$).

The intrinsic association constant, k , was three-fold greater for the native DNA interaction than for any other single-stranded nucleic acid (denatured DNA or polynucleotide). This indicated the importance of the double-helical structure for maximum interaction.

At $\mu = 0.5$, poly I, which is a triple-stranded structure at this ionic strength, did not bind to daunomycin at all.

The association constants for the polynucleotide interactions were all similar to each other which indicated a lack of base preference for the daunomycin-nucleic acid interaction. Similarly, no preference for the nucleic acid sugar moiety (ribose or deoxyribose) was observed.

The addition of daunomycin to a DNA solution resulted in an increase in the T_m of the solution. The extent of

renaturation also increased. The T_m increase leveled off as r , the number of daunomycin molecules bound/phosphate, approached the n value for strong binding. This indicated that the increased stabilization observed in the presence of daunomycin was the result of strong, type I binding.

The T_m results were similar for *Cl. perfringens* DNA (%GC = 32), calf thymus DNA (%GC = 43) and *M. lysodeikticus* (DNA (%GC = 72)). Thus, there was no base preference.

The results of these studies correlate well with an intercalation model. The major factor controlling the daunomycin-nucleic acid interaction was the secondary structure of the nucleic acid molecule.

ACKNOWLEDGEMENTS

I wish to thank Dr. Myer Fishman for his guidance and knowledge throughout the course of this work. I am indebted to him for imparting to me the basic principles of research and especially the rigorous treatment of experimental data.

I am also grateful to Dr. Charlotte Russell for many hours of helpful discussions and encouragement.

I would like to express my sincere thanks to the following people: Steven Allen for his capable assistance in performing some of the experiments presented here; Jory Lennox, for the many hours spent typing this thesis; Karol Chesney, for typing the first draft; and my father-in-law, Irving Ebner, for his artwork in drawing the figures.

Finally, my sincerest thanks to my family, Arlene and Kenny, for encouragement during the low points and for bearing with me through the nights and weekends spent in the laboratory.

TABLE OF CONTENTS

	<u>Page Number</u>
Abstract	i
Acknowledgements	iv
List of Tables	xii
List of Figures	xiii
INTRODUCTION	
I. Daunomycin	1
A. Chemical description and structure	1
B. Cytological effects	1
a. Inhibition of RNA and DNA synthesis	4
b. Antimitotic effect	5
II. Binding of Dyes to DNA	6
III. Acridines	7
A. Structure and cytological effects	7
B. Acridine - DNA interaction	7
a. Intercalation model	10
b. Effect of ionic strength	11
c. Binding to denatured DNA	12
d. Description of two modes of binding	13
e. Effect of Acridine and DNA structure	14
f. Effect of acridine binding on T_m	15
1. Description of T_m	15

TABLE OF CONTENTS (continued)

	<u>Page Number</u>
g. Effect of organic solvents	18
h. Dependence on DNA base composition	19
i. Kinetic studies	19
IV. Ethidium Bromide	20
A. Structure and cytological effects	20
B. Ethidium bromide - DNA interaction	20
a. Binding to polynucleotides	20
b. Binding to closed circular DNA	23
V. Actinomycin	24
A. Inhibition of RNA synthesis	24
B. Actinomycin - DNA interaction	27
a. Physicochemical changes induced in DNA	27
b. Requirement for guanine	28
c. Covalent binding model	29
d. Intercalation model	29
VI. Ion-DNA Interactions	31
A. General description	31
B. Binding of alkali metal ions and transi- tion metal ions	32
C. Effect of ion binding on T_m	33
D. Base specificity of Cu^{++} binding	35
E. Effect of ions on antibiotic-DNA complexes	36

TABLE OF CONTENTS (continued)

	<u>Page Number</u>
VII. Physicochemical Effect Caused by Daunomycin	
Binding to DNA	37
A. Effect on absorption spectra	37
B. Effect on fluorescence spectra	38
C. Effect on T_m	38
D. Effect on viscosity and sedimentation	39
E. Hydrogen bonding model of daunomycin binding	39
F. Requirement for unaltered daunomycin sugar amino group	39
G. Evidence for two binding modes	41
H. X ray diffraction studies	41
VIII. Purpose of Present Study	42
MATERIALS AND METHODS	
I. Materials	44
A. DNA	44
B. Daunomycin	44
C. Polynucleotides	44
II. Methods	45
A. Preparation of nucleic acid solutions	45
B. Denaturation of DNA	45
C. Preparation of daunomycin solutions	46

TABLE OF CONTENTS (continued)

	<u>Page Number</u>
D. Characterization of solutions	46
E. Spectral studies	47
a. Absorbance	47
b. Fluorescence	47
c. Titrations	47
F. Determination of binding equilibria	48
G. Equilibrium dialysis	52
H. pH studies	53
I. T_m studies	54
 RESULTS	
I. Spectral Studies	55
A. Ultraviolet and visible studies	55
B. Fluorescence	55
C. Concentration dependence	60
II. Effect of Cu^{++} on the Daunomycin-DNA Complex	60
A. Absorption studies	60
B. Effect of pH	77
C. Fluorescence studies	77
III. Effect of Mg^{++} on the Daunomycin-DNA Complex	82
A. Effect of pH	82
B. Fluorescence studies	85
IV. Binding of Daunomycin to Nucleic Acid Units	92

TABLE OF CONTENTS (continued)

	<u>Page Number</u>
A. Absorbance studies	92
B. Fluorescence studies	99
V. Spectrophotometric Titrations	99
A. Calf thymus DNA	99
B. Ribo-homopolynucleotides	110
VI. Spectrofluorimetric Titrations	114
A. Deoxy-homopolynucleotides	114
B. Polynucleotide duplexes	115
VII. <u>C1. perfringens</u> DNA	124
VIII. T _m Studies	129
A. Absorbance vs. temperature profiles	129
B. Effects of daunomycin concentration	134
a. Calf thymus DNA	134
b. <u>C1. perfringens</u> DNA	134
c. <u>M. lysodeikticus</u> DNA	134
d. Comparisons	148
C. Effect of ionic strength	148
a. Calf thymus DNA	148
b. <u>C1. perfringens</u> DNA	153
D. Renaturation	154
IX. Equilibrium Dialysis	154

TABLE OF CONTENTS (continued)

	<u>Page Number</u>
DISCUSSION	
I. Effect of Ions on the DNA-Daunomycin Complex	156
A. Effect of Cu^{++}	156
B. Effect of Mg^{++}	157
C. Comparison of the Cu^{++} and Mg^{++} effects	158
D. Binding sites for Cu^{++} and Mg^{++}	159
II. Binding of Nucleic Acid Units and Poly-nucleotides to Daunomycin	161
III. Spectrophotometric Titrations	162
A. Polynucleotides-daunomycin interaction	162
B. DNA-daunomycin interaction	163
C. Comparison of the DNA and polynucleotide complexes	164
IV. Spectrofluorimetric Titrations	166
A. Binding of ribo- vs. deoxy-ribopolymer duplexes to daunomycin	166
B. Base preference for the binding of polynucleotides to daunomycin	168
C. Criteria for formation of type I complex	169
V. T_m Studies	170
A. Biphasic melting profiles	170
B. Renaturation	171
C. Stabilization due to AT base content	172

TABLE OF CONTENTS (continued)

	<u>Page Number</u>
D. Effect of ionic strength on T_m' and ΔT_m	174
E. T_m stabilization is result of intercalation	175
REFERENCES	178

LIST OF TABLES

<u>Table Number</u>		<u>Page Number</u>
1	Fluorescence intensity of daunomycin-DNA complexes.....	61
2	Compounds tested for binding to daunomycin.....	95
3	Fluorescence intensity of polynucleotide-daunomycin complexes.....	102
4	Binding data for daunomycin complexes.	113
5	Binding data for daunomycin complexes.	118
6	T _m data for calf thymus DNA-daunomycin complex.....	135
7	T _m data for <u>C1. perfringens</u> DNA-daunomycin complex.....	140
8	T _m data for <u>M. lysodeikticus</u> DNA-daunomycin complex.....	145

LIST OF FIGURES

<u>Figure Number</u>		<u>Page Number</u>
1	Structure of Daunomycin.....	3
2	Structure of Acridine	9
3	Structure of Ethidium Bromide	22
4	Structure of Actinomycin D	26
5	Effect of addition of DNA on ultraviolet spectrum of daunomycin	57
6	Addition of DNA to Daunomycin	59
7	Effect of DNA addition on the visible spectrum of daunomycin	63
8	Effect of addition of DNA on fluorescence emission spectrum of daunomycin	65
9	Addition of Cu^{++} to daunomycin or daunomycin-DNA complex.....	68
10	Effect of denatured DNA concentration on the visible spectrum of the denatured DNA-daunomycin- Cu^{++} complex.....	70
11	Effect of concentration of denatured DNA on the visible spectra of the daunomycin- Cu^{++} complex.....	72
12	Effect of concentration of Cu^{++} on the visible spectra of the daunomycin-denatured DNA complex.....	74

LIST OF FIGURES (continued)

<u>Figure Number</u>		<u>Page Number</u>
13	Effect of concentration of Cu^{++} on the visible spectra of the daunomycin-denatured DNA complex.....	76
14	Effect of pH on the daunomycin ($2.5 \times 10^{-5}\text{M}$)-native DNA ($1.0 \times 10^{-4}\text{M}$)- Cu^{++} ($1.0 \times 10^{-4}\text{M}$) complex...	79
15	Effect of pH on the daunomycin ($2.5 \times 10^{-5}\text{M}$)-denatured DNA ($1.0 \times 10^{-4}\text{M}$)- Cu^{++} ($1.0 \times 10^{-4}\text{M}$) complex	81
16	Effect of pH on the daunomycin ($2.5 \times 10^{-5}\text{M}$)-DNA ($2 \times 10^{-4}\text{M}$)- Mg^{++} (0.1M) complex.....	84
17	Addition of Mg^{++} to the daunomycin-DNA complex at pH 2.4	87
18	Addition of Mg^{++} (0.1M) to daunomycin or daunomycin-DNA complex at pH 2.4	89
19	Effect of the addition of Mg^{++} on the fluorescence emission spectrum of daunomycin.....	91
20	Effect of pH on the fluorescence emission spectrum of the daunomycin- Mg^{++} complex.....	94

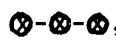
LIST OF FIGURES (continued)

<u>Figure Number</u>		<u>Page Number</u>
21	Effect of poly G on the visible spectrum of daunomycin.....	98
22	Effect of polynucleotides on the fluorescence emission spectrum of daunomycin.....	101
23	Binding isotherms for the calf thymus native DNA-daunomycin complex	104
24	Binding isotherms for the denatured calf thymus DNA-daunomycin complex	107
25	Scatchard plot for the calf thymus native DNA-daunomycin complex at $\mu = 0.005$	109
26	Binding isotherms for various polynucleotide-daunomycin complexes...	112
27	Binding isotherms for various polynucleotide-daunomycin complexes...	117
28	Binding isotherms for various polynucleotide duplex-daunomycin complexes.....	121
29	Binding isotherms for the poly dG·poly dC-daunomycin complex.....	123
30	Binding isotherms for the <u>C1. perfringens</u> DNA-daunomycin complexes.	126

LIST OF FIGURES (continued)

<u>Figure Number</u>		<u>Page Number</u>
31	Scatchard plots for the <u>Cl. perfringens</u> DNA-daunomycin complex...	129
32	Effect of daunomycin on the melting curve (T_m) of calf thymus DNA	131
33	Effect of daunomycin on the melting curve (T_m) of calf thymus DNA	133
34	Melting temperature (T_m') of the daunomycin-calf thymus DNA complexes as a function of daunomycin/DNA ratio.....	137
35	Change in the melting temperature of (ΔT_m) of calf thymus DNA due to complex formation with daunomycin as a function of daunomycin/DNA ratio (T_D/T_P).....	139
36	Melting temperature (T_m') of the daunomycin- <u>Cl. perfringens</u> DNA complexes as a function of daunomycin/DNA ratio (T_D/T_P).....	142
37	Change in the melting temperature (ΔT_m) of <u>Cl. perfringens</u> DNA due to complex formation with daunomycin as a function of daunomycin/DNA ratio (T_D/T_P).	144

LIST OF FIGURES (continued)

<u>Figure Number</u>		<u>Page Number</u>
38	Melting temperature (T_m') of the <u>M. lysodeikticus</u> DNA-daunomycin complex, o-o-o; and the change in the melting temperature (ΔT_m) of <u>M. lysodeikticus</u> DNA due to complex formation with daunomycin,  , as a function of daunomycin/DNA (T_D/T_p) ratio.....	147
39	Increase in the melting temperature (ΔT_m) of DNA due to complex formation with daunomycin.....	150
40	Melting temperature (T_m') of daunomycin-DNA complexes as a function of T_D/T_p ..	152

INTRODUCTION

I. Daunomycin

A. Chemical description and structure.

Daunomycin is an antibiotic isolated from *Streptomyces peucetius* first described by DiMarco, et al. (1). It was described as having an effect on both RNA and DNA synthesis and also possessing antimitotic activity. Daunomycin exhibited a strong tendency to form a complex with DNA (1).

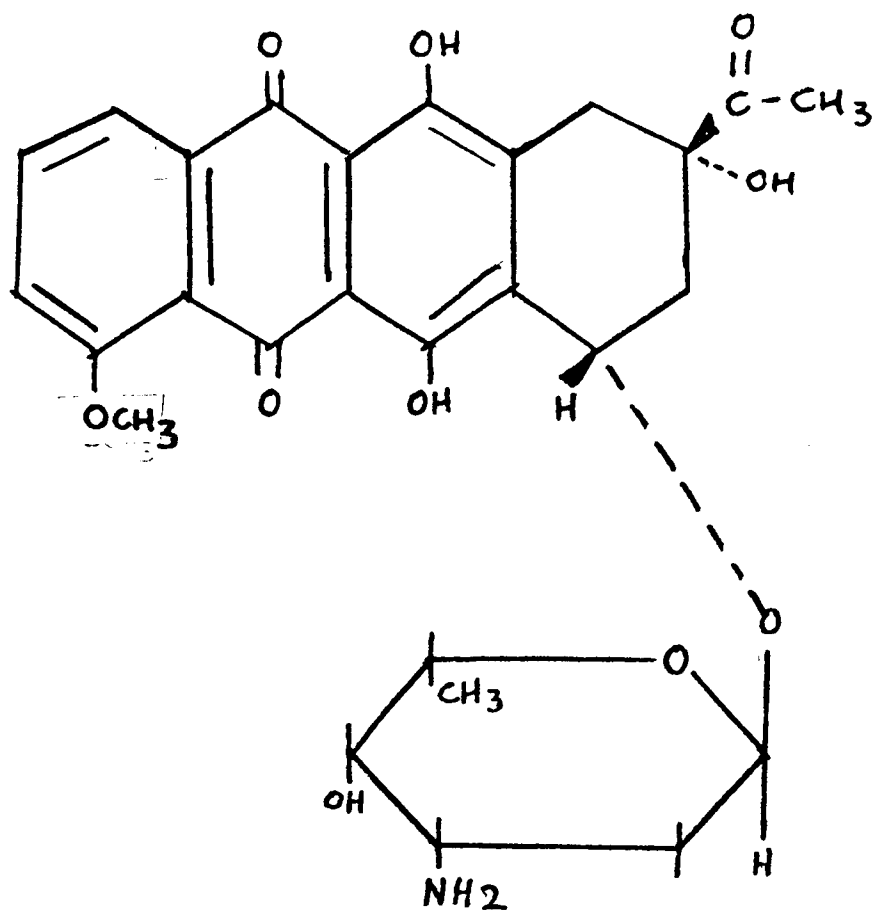
The antibiotic consists of a chromophore, daunomycinone, $C_{21}H_{18}O_8$ (2) and a sugar, daunosamine, $C_6H_{13}O_3N$ (3). These could be obtained by simply treating daunomycin with HCl for one hour at $90^{\circ}C$ (3). The chromophore has an anthraquinone nucleus with an additional saturated ring and daunosamine is a 3'-amino sugar. The nature of the glycosidic linkage and the absolute configuration of daunomycin were determined by Arcamone, et al. (4,5) and is shown in figure 1.

B. Cytological effects.

Daunomycin inhibited the growth of experimental tumors, such as Ehrlich ascites and Walker carcinoma (6) as well as tumor growth in animals (7). In conjunction with this it was found that daunomycin destroyed mostly actively proliferating cells (8). It is being used experimentally for the treatment of acute leukemia (9,10).

FIGURE 1.

Structure of Daunomycin



a. Inhibition of RNA and DNA synthesis.

These effects are undoubtedly a result of the influences daunomycin has on RNA and DNA synthesis and mitosis. The early work indicated an inhibition of both RNA and DNA synthesis, (1,11) the extent of which was dependent on the concentration of added daunomycin (11). Rusconi and Calendi (12) measured the incorporation of 8-¹⁴C-adenine into the RNA and DNA of HeLa cells. Increased daunomycin concentration led to decreased incorporation of the ¹⁴C-adenine into both RNA and DNA but DNA synthesis was more sensitive. Actinomycin (another widely used antibiotic which will be discussed later) had the opposite effect; RNA synthesis was preferentially inhibited. This selective inhibition was also found by others(13, 14). Kim and co-workers (13) studied the synthesis in HeLa cells and found that daunomycin (1μg/ml) reduced DNA synthesis to 10% of controls after one hour, whereas RNA synthesis was reduced to 25% and protein synthesis was hardly affected. They further observed that daunomycin was most toxic during the S phase of the cell cycle, during which DNA synthesis occurs, while it was least effective during the G₁ phase, a growth period during which RNA and protein are synthesized.

Daunomycin also inhibits RNA dependent DNA polymerase (reverse transcriptase) activity (15,16). Mice infected with Friend leukemia virions (FLV) and chickens infected with Rous Sarcoma virus (RSV) survived when treated with

daunomycin (16). This led DiMarco and co-workers to study the inhibition of reverse transcriptase by daunomycin assuming that daunomycin allowed survival because it affected virus-associated enzyme activity. Daunomycin was very effective in inhibiting reverse transcriptase of FLV and RSV. Interestingly the inhibition was dependent upon the nature of the template. Poly dA·poly dT was sensitive to daunomycin inhibition but if poly dI·poly dC was used as template the enzyme was unaffected (16). Actinomycin had no effect on RNA dependent DNA polymerase activity (15).

b. Antimitotic effect.

The addition of daunomycin to a HeLa cell culture resulted in an immediate reduction in the mitotic index (7,17). An equivalent dose of actinomycin required four hours for a similar effect. Reduction in the mitotic index occurred during the G₂ phase, after DNA synthesis had already been completed and so this antimitotic effect did not seem to be related to the inhibition of DNA synthesis (17). A later study, using rat fibroblasts, indicated that the cytological effects of daunomycin were dependent on the physiological activity of the cells at the time of antibiotic uptake (18). Cells in the G₁ phase experienced inhibition of enzyme synthesis (those enzymes necessary for DNA replication), inhibition of DNA replication occurred if the cells were in the S phase and for cells in G₂ there was inhibition of RNA synthesis. If the cells were in mitosis,

the addition of daunomycin resulted in a blockage of mitosis if given before prophase.

All of the above mentioned effects could be traced to the formation of a complex between daunomycin and DNA (1). The correlation of the cytological effects with the binding capacity of the daunomycin was further indicated by the use of N-acetyl daunomycin. This derivative of daunomycin, which has an acetate group attached to the amino moiety on the sugar, had a reduced capacity to bind to DNA (19) and caused almost none of the cytological effects described above (17,18).

A study of the binding of daunomycin to DNA would, therefore, be expected to elucidate its mechanism of action. Before describing the physicochemical properties of the daunomycin-DNA interaction, it would be instructive to compare the complexes formed between DNA and other representative compounds. Among the many small molecules (small in comparison to DNA) that bind to DNA are mutagens, antibiotics, carcinogens and metal ions. Some aspects of complex formation are similar for many of these interactions and so a description of the information available for some of the above compounds is useful for an understanding of the general process of DNA-small molecule binding.

II. Binding of Dyes to DNA.

Perhaps the first study of this type was carried out by Michaelis in 1947 (20). He examined the binding

of dyes (methylene blue, toluidine blue) to nucleic acids. The spectra of these molecules showed three different bands which were designated α (monomer), β (the dimeric species) and γ (higher aggregates). When these dyes bound to nucleic acid, however, the α and β species were evident dependent on the molar ratio of dye to nucleic acid but no γ spectrum was observed even at very low concentration of nucleic acid. He concluded that the dye molecules which were attached to the negative phosphate groups of the nucleic acid would lie in the space between the planes of the bases and so they would be prevented from forming multiple aggregates (20). This was later shown to be the case with acridines.

III. Acridines.

A. Structure and cytological effects.

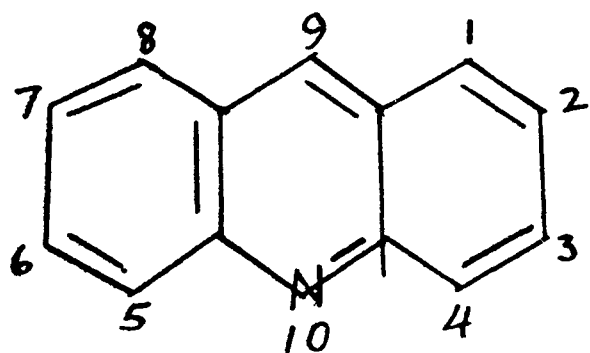
The acridine dyes are perhaps the best studied in terms of their interactions with DNA. These compounds are very potent mutagens, probably by causing the insertion or deletion of a base pair in DNA (21). They were affectively used by Crick, et al.(22) to determine the coding ratio in protein synthesis. The structure of acridine is shown in figure 2. It consists of a three ring aromatic, and therefore, planar system and usually exists as the cation at physiological pH (pH 7.0-7.4).

B. Acridine-DNA interaction.

The pioneering study in acridine-DNA binding was

FIGURE 2.

Structure of Acridine



performed by Peacocke and Skerrett (23) using proflavine (3,6-diaminoacridine). The interaction was studied by spectrophotometric titration and equilibrium dialysis. They observed that purine deoxynucleotides, but not pyrimidine deoxynucleotides, caused changes in the proflavine spectrum similar to those produced by DNA. These alterations were a decrease in absorbance and a shift in the peak to a higher wavelength. Apurinic acid caused a decrease in absorbance but no shift in the peak. They noted that denatured DNA bound just as well as native and so hydrogen bonds were not important for the interaction. The Scatchard plots which they constructed were convex to the x-axis, rather than a straight line (figure 25), which indicated two different modes of binding. A strong binding denoted as type I, was the result of interactions of single proflavine molecules with DNA and the second weaker type of binding, type II, was due to the binding of aggregates. Hydrogenated proflavine and apurinic acid gave less specific interactions and so Peacocke and Skerrett concluded that purine rings and a flat dye molecule were necessary for strong binding. The necessity for overlap suggested that this binding was some type of π interaction. In addition, they proposed that the aggregates bound to the phosphates.

a. Intercalation model.

Lerman (24) studied the effect that proflavine had on the physical properties of DNA and found that it en-

hanced the viscosity of DNA solutions tremendously and also resulted in a decrease in the sedimentation coefficient. These results are best explained by a decrease in the mass per unit length of the DNA molecule. This led Lerman (24) to propose that acridines bound by intercalation, i.e. there was an insertion of the flat acridine molecule between successive base pairs along the DNA. Thus an acridine would occupy the same amount of space as a base pair and therefore the distance along the DNA chain should not change on intercalation. However, since acridines have a lower molecular weight than a base pair, intercalation would also result in a decrease in mass per unit length. Intercalation could be accomplished by extension of the backbone of the DNA molecule and an untwisting of the bases.

This proposal was further supported by Lerman's studies using flow dichroism (25) and X-ray diffraction (24). Flow dichroism is a measure of the perpendicularity of the bases to the helix in DNA. The addition of acridine enhanced the dichroism of DNA which indicated that the helix was straighter and stiffer. The x-ray studies showed that the 3.4 Å spacing usually found with DNA was retained but the regular helical structure was lost.

b. Effect of ionic strength.

Various workers have also studied the effect of ionic strength on the acridine-DNA complex and found that an

increase in ionic strength led to decreased binding (23, 26,27,28). Ichimura, et al.(27) found that increasing the ionic strength from 0.01 to 0.1 resulted in a 10-fold decrease in the association constant for the acridine orange (N,N'-tetramethyl proflavine)-DNA interaction. Increasing the ionic strength, in addition to decreasing the association constant, also led to a decrease in n , the number of binding sites per DNA phosphate. Chambron, et al.(29) attributed this to a decrease in the repulsion of the phosphate groups which left less space between the planes of the bases and so fewer molecules can bind. Blake and Peacocke (30) observed that although both type I and type II binding were diminished, type II was more sensitive to ionic strength.

c. Binding to denatured DNA.

In line with this it was observed that a denatured DNA-acridine complex was not affected as much by ionic strength as was a native DNA complex (27). This was taken as an indication that electrostatic effects were less important for the denatured DNA complex. In fact, Drummond et al.(26) found that denatured DNA always had more binding sites than did native DNA. This is a real increase in sites and not just a difference in association constants. It is also possible that there was less steric hindrance in denatured DNA because it is a more open structure although there is still sufficient helical structure to allow for intercalation (26).

d. Description of two modes of binding.

The hydrogenation of one ring of 9-aminoacridine reduced its ability to bind by half. Poly A, which is a single stranded polynucleotide, markedly depressed the spectrum of proflavine. Poly U, on the other hand, was without apparent effect. This led Blake and Peacocke (30) to propose that conditions for strong binding must be such that interaction could occur either by hydrogen bonding or by base stacking either on one polynucleotide chain or different chains. Thus, a double stranded structure may not be necessary. They further characterized type I, strong binding as: 1) having a binding energy of 6-10 kcal/mole of acridine bound; 2) being favored by three flat aromatic rings which can interact with DNA bases probably via van der Waals forces; 3) producing an increase in the contour length of DNA and a decrease in the mass/unit length; 4) having the plane of acridines parallel to those of the bases; 5) having a maximum binding of $r = 0.25$. In addition, they proposed a modified intercalation model to especially account for denatured DNA binding. Rather than the acridine being between successive base pairs in both chains, there was partial intercalation in which the acridine was inserted between the bases in one polynucleotide chain. In this manner the positively charged nitrogen of acridine can interact strongly with the DNA phosphate. This was a more satisfactory explanation

for how binding can occur with single stranded structures.

They also characterized the weak, type II binding process as (30): 1) involving interaction between bound acridines; 2) being electrostatic in nature and enhanced by decreased ionic strength to a greater extent than type I; 3) being an external binding process since it follows type I; 4) increasing relative to type I binding when the complex was formed with denatured DNA rather than with native DNA. The acridine was bound edgewise to the outside of the helix with the positive nitrogen close to the phosphate. When r was large enough, the dye molecules could stack on one another, parallel to the helix axis.

e. Effect of acridine and DNA structure.

The structures of both the acridine and DNA dictate the type and extent of each mode of binding. Lober (31) found that alkylation of the ring nitrogen of proflavine or acridine orange resulted in increased binding while the opposite was true for acridine. He concluded that no single intercalation model was satisfactory for all acridine dyes. For acridine, the partial intercalation model of Peacocke and co-workers (26,30) was best, while for proflavine, the results were best explained by the full intercalation model of Lerman (24). Similarly, changes in the DNA could affect the complex. Li and Crothers (32) showed that as r increased the isosbestic point of proflavine-DNA shifted indicating a change to a

second type of binding. With T-2 phage DNA, which contains glucose residues in the large groove, this change was not observed. Thus monomer binding to DNA appeared to take place but binding to the outside was precluded by the presence of glucose residues.

f. Effect of acridine binding on T_m

1. Description of T_m

A further consequence of acridine binding was an increase in T_m , the temperature at which the DNA helix-coil transition occurred. When a solution of DNA is heated there is an increase in the absorbance at the 260 nm peak which is usually 25-30% greater than that of the native DNA. This phenomenon is known as hyperchromism. It is a manifestation of the helix-coil transition for DNA, i.e. the destruction of the highly ordered double-stranded helical form in which native DNA exists resulting in two less ordered single-stranded polynucleotide chains.

The simplest explanation for the absorbance increase is that it is due to a destruction of the planar base stacking. Tinoco (33) proposed a theoretical explanation for this phenomenon. Light absorption induces dipoles and Tinoco calculated the degree to which the transition moment, a measure of the amount of light absorbed, is altered by interactions of light-induced dipoles. If the induced dipoles are linked head-to-tail the transition moment increases. However, if they are arranged side by side both the transition moment and the absorbance decrease.

For DNA, the induced dipoles are in the planes of the bases, but because the bases are stacked at right angles to the axis of the helix, the induced dipoles in superposition cause a decrease in absorbance. Likewise, a destruction of the stacking at right angles results in an absorption increase.

If the absorbance at 260 nm is plotted as a function of temperature, a curve such as that shown in figure 32 is obtained. The temperature at the midpoint of the rise (half the difference between the absorbance where the curve begins to rise and the maximum absorbance obtained) is denoted T_m , or melting temperature. This is understood to be the temperature of the helix-coil transition(34).

Doty and co-workers (34) studied the effect of ionic strength on the T_m of various DNA's. As the ionic strength was increased, the T_m increased and a plot of T_m versus $\log [Na^+]$ yielded a straight line. This indicated that the DNA helix had been stabilized since a higher temperature was required for strand separation. This stabilization was due to neutralization of the phosphate repulsion by positively charged Na^+ ions.

Marmur and Doty (35) studied the effect of base composition on T_m . At a given ionic strength, the greater the GC (guanine and cytosine) content, the higher the T_m . A GC base pair has greater stability because it has three hydrogen bonds as opposed to an AT pair which has only two.

These workers were able to set up empirical relationships for calculating the T_m of a particular DNA simply based on its %GC.

Chambron et al. (36) found that at all concentrations of added proflavine, the T_m of the complex was always higher than that of free DNA. As the ionic strength was increased the T_m increased. The difference between the T_m of the complex and that of free DNA (ΔT_m), however, decreased with increased ionic strength. They also observed that at the T_m of the complex the proflavine was released, therefore, the destruction of the DNA helix led to a release of the bound dye. Similar observations were made by other workers (37,38). Jordan and Sansom (37) attributed this behavior to a reduced binding of acridine to single stranded DNA at high temperature while there was still considerable binding to duplex DNA. Kleinwachter, et al. (38) observed that at $r < 0.1$, as the temperature increased r remained constant until the T_m was reached and then there was a release of dye. However, when $r > 0.1$, r varied with temperature which indicated some release of bound dye even below the T_m . When $r < 0.1$, the dye was bound mostly by means of a type I complex, while at higher r values there was binding by type II interactions as well, and it was these weakly bound dye molecules which were released below the T_m . Jordan (39) drew a similar conclusion based on the observation that the T_m for the proflavine-DNA complex increased as a

function of r but reached a plateau at the r value which was the maximum for type I binding. He concluded that the increased stability of the complex was due to dye bound by intercalation rather than those bound by the type II interaction.

g. Effect of organic solvents.

The importance and nature of the intercalation reaction was further illustrated by the effects of organic solvents. The formation of a proflavine-DNA complex was accompanied by a decrease in proflavine fluorescence. However, the addition of organic solvents led to a diminution of the quenching effect (40). An increase in the number of methyl groups of the solvent enhanced this effect (e.g. propanol has a greater effect than methanol) and so hydrophobic forces were implicated in intercalation. Lober, et al. (40) used k/n as their binding parameter (based on fluorescence) and found that an increase in the percent organic solvent gave reduced binding. Organic solvents are known to denature DNA (41) but these studies were performed at concentrations of solvent which did not cause denaturation. Lober, et al. ascribed this to a competition between the solvent and DNA base pairs as a hydrophobic binding site for the dye molecules. Since the complex was destroyed at solvent concentrations which are too low to denature DNA, the hydrophobic forces stabilizing the dye-DNA complex were weaker than those involved

in stabilization of the DNA helix (40).

h . Dependence on DNA base composition.

Some early work by Tubbs et al. (42) had indicated that the binding of acriflavine (10-methyl proflavine) to DNA was dependent on the GC content. More recent studies, however, have indicated that this might not be the case. Kleinwachter, et al. (38) based on their T_m studies, concluded that binding was not GC dependent. Ellerton and Isenberg (43) found that *M. lysodeikticus* DNA (72% GC), calf thymus DNA (43%), T-2 DNA (34%) and poly dAT (0%) all had association constants of the same order of magnitude in their binding with proflavine. Schmechel and Crothers (44) made a similar observation for poly A·poly U and so it appeared that acridine binding did not have any base preference. This would be expected for an intercalation process.

i. Kinetic studies.

Kinetic studies of acridine-DNA binding have also yielded valuable information concerning the intercalation process. Li and Crothers (45) employed a temperature jump technique and observed two relaxation times for the proflavine-DNA interaction. At high ionic strength the slow process accounted for 95% of the total dye bound. Therefore the slow reaction was an intercalation process. It would appear that the dye bound to the outside in a very rapid step, followed by the slower intercalation step. This allowed time for the structural alteration of the DNA molecule

which must accompany intercalation. The time required for insertion of an externally bound proflavine was of the order of one millisecond (45).

IV. Ethidium Bromide

A. Structure and cytological effects.

Ethidium bromide (figure 3) is another example of a compound which binds to DNA almost exclusively by intercalation. Structurally it is similar to the acridines in that it is an aromatic, three ring, planar molecule which exists as the cation at physiological pH. Ethidium bromide is a trypanocide but it can also inhibit DNA polymerase and DNA-dependent RNA polymerase in vitro (46). Presumably this is accomplished by binding to the template DNA and investigations of this interaction have shed further light on the mechanism of intercalation.

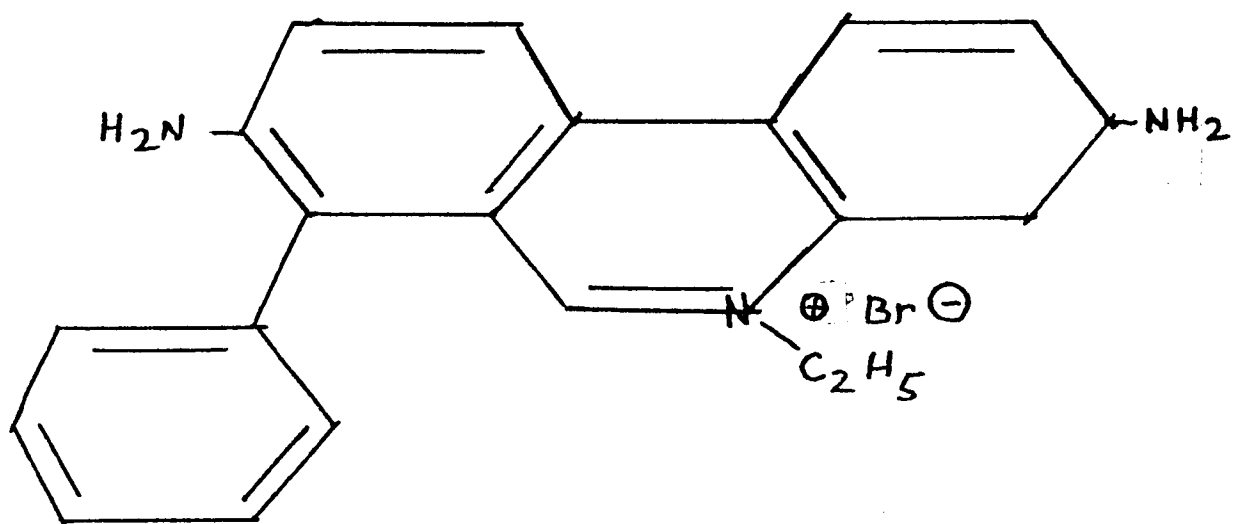
B. Ethidium bromide - DNA interaction

a. Binding to polynucleotides.

Waring (47) studied the interaction by testing the binding of polynucleotides to ethidium bromide. Poly A, poly I and poly U induced shifts in the ethidium bromide spectrum which indicated interaction. Binding isotherms for these, however, showed that there was very little binding until higher concentrations of free ethidium bromide were attained. This indicated a lack of type I binding by these compounds. Similarly, apurinic and apyrimidinic acids, whose structures are less ordered than that of DNA, bound

FIGURE 3.

Structure of Ethidium Bromide



ethidium bromide, but there was less interaction than that found with DNA. On the other hand, with the homopolymer mixtures, poly (A and U), poly (A and I) and poly (I and C), the binding curves were very similar to those found for DNA. This indicated the need for a base-paired helical structure for ethidium bromide binding. Kreishman, et al. (48) used proton magnetic resonance and detected an intercalation complex for the ethidium bromide-poly U interaction, although they stated that this might differ stereochemically for the ethidium bromide complex with DNA.

b. Binding to closed circular DNA.

X-ray studies by Fuller and Waring (49) were compatible with intercalation. They constructed a model for the ethidium bromide-DNA interaction in which the binding of an ethidium bromide molecule resulted in a 12° local unwinding of the helix. Particularly strong support for this model came from studies with closed circular DNA. These circular duplex molecules are super helices, i.e. the helix is twisted with right hand twists because the number of base pairs per turn is lower than that needed to result in an open, unstrained circle. Therefore, any structural change that would increase the number of base pairs per turn would lead to a decrease in the number of right hand twists, the number would go through zero, and the helix would rewind with left hand twists. Since twisted

covalently closed circles have an anomalously high $S_{20,w}$, these changes could be followed in the ultracentrifuge. If intercalation caused local uncoiling of the DNA helix it should result in the changes described above (50). Waring (51) used this technique to study the binding of many compounds to ϕ X174 RF supercoil DNA as a test for intercalation. Ethidium bromide and proflavine behaved just as described above for a molecule assumed to intercalate. Using ethidium bromide as a reference for complete intercalation (12° unwinding), Waring calculated that the fraction of proflavine intercalated was 0.7 ± 0.2 with an unwinding of $8.4^{\circ} \pm 2.4^{\circ}$. Paoletti and LePecq (52) on the basis of fluorescence depolarization, stated that intercalation by ethidium bromide winds, rather than unwinds, the helix by 13° and they built a satisfactory model for this (53).

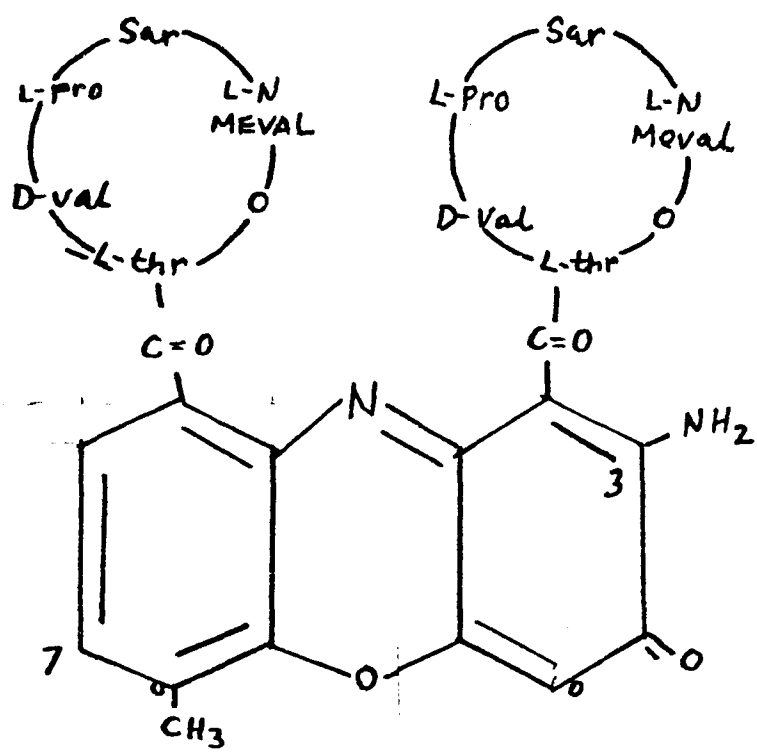
V. Actinomycin

A. Inhibition of RNA synthesis.

Perhaps the best known and most widely used of the antibiotics which bind to DNA is actinomycin (figure 4). Actinomycin added to exponentially growing S. aureus resulted in cessation of RNA synthesis followed by termination of protein synthesis (54). If ϕ X174 DNA, which is single-stranded, was used as a primer for RNA synthesis, there was inhibition by actinomycin. Hurwitz, et al. (54) also observed inhibition when denatured DNA was the primer. This observation was later modified by Kahan, Kahan and

FIGURE 4.

Structure of Actinomycin D



Hurwitz (55) who found that there was less actinomycin inhibition when denatured rather than native DNA was used as the primer. However, no differences were observed in the binding of either native or denatured DNA with actinomycin. On the other hand, Reich and Goldberg (56) noted decreased binding of actinomycin to denatured DNA.

B. Actinomycin - DNA interaction

a. Physicochemical changes induced in DNA

The addition of actinomycin to a solution of DNA induced physicochemical changes generally associated with binding to DNA. The peak in the visible spectrum of actinomycin was shifted from 440 nm to 458 nm and there was a decrease in absorbance at 440 nm (56). The T_m of an actinomycin-DNA solution was higher than that of free DNA (56,57). Actinomycin had an anomalous effect on the viscosity and sedimentation coefficient of DNA. With low concentrations of actinomycin the viscosity decreased and the sedimentation coefficient increased, which indicated a tighter coiling of the DNA molecule (57). This is exactly the reverse of what one would expect for a molecule which intercalates between base pairs. As the actinomycin concentration was increased the viscosity began to increase. It should be mentioned that actinomycin preferentially inhibits RNA synthesis; DNA synthesis is much less sensitive to actinomycin (12,56). This is contrary to what was observed with daunomycin which preferen-

tially inhibited DNA synthesis (12).

b. Requirement for guanine.

Kahan, et al. (55) observed that DNA dependent RNA polymerase reactions which were primed with poly dT, poly dA·poly dT or poly dC were not inhibited by actinomycin. Inhibition occurred only if dG residues were present in the primer. In addition, the amount of actinomycin bound was directly related to the GC content. Reich and Goldberg further noted (56) that apurinic acid, and poly dI·poly dC did not bind to actinomycin but apyrimidinic acid and poly dG·poly dC did bind. Synthetic poly d(AT) did not form a complex but crab poly d(AT), which contains 2-3% guanine, did interact with actinomycin.

Kersten, et al. (57) observed a decrease in the buoyant density of DNA in the presence of actinomycin. The density shift was clearly dependent upon the GC content of DNA. Noting that the only difference between poly dG·poly dC and poly dI·poly dC is the 2-amino group of guanine, Cerami, et al. (58,59) synthesized a double stranded polymer consisting of one strand of diamino purine (DAP). This compound had chemical properties similar to those of adenine and similar base pairing behavior. The only property it had in common with guanine was the amino group on the 2 position of the purine ring. Poly dDAP·poly dT formed a complex with actinomycin just as did DNA whereas poly d(AT) did not. The presence of the 2-amino group was thus sufficient to promote actinomycin

binding.

c. Covalent binding model.

Reich and co-workers proposed a model for the binding of actinomycin to DNA (56,60). The interaction required a double stranded helix (to account for the differences between native and denatured DNA) and the presence of guanine. According to this model, actinomycin bound in the minor groove of DNA and hydrogen bonds were formed between the quinoidal oxygen of actinomycin and the guanine 2-amino group, the actinomycin amino group and N-3 of guanine, and the actinomycin amino group and the ring oxygen of deoxyribose. Four additional hydrogen bonds could be formed between the peptide residues of actinomycin and the DNA phosphates. They excluded the possibility that binding occurred by intercalation because this cannot explain the need for guanine.

d. Intercalation model

Wells (61,62) subsequently demonstrated that the presence of guanine did not insure binding nor did the absence of guanine preclude it. Poly d(ATC)·poly d(GAT) which is a double stranded, high molecular weight polymer exhibited no binding to actinomycin as judged by spectroscopy, equilibrium dialysis, buoyant density, T_m , and in vitro inhibition of DNA dependent RNA polymerase. The presence of guanine residues (33% GC for this polymer) was thus not sufficient for complex formation (61). In addition,

even though it lacked a 2-amino group, poly dI, showed definite complex formation with actinomycin (62).

Muller and Crothers (63) made an extensive study of the actinomycin-DNA interaction. Contrary to earlier results, they observed that the binding was very dependent upon the ionic strength and that elevated ionic strength resulted in decreased binding capacity. As previously noted, addition of actinomycin caused an initial decrease in the viscosity of DNA followed by an increase. Viscosity increases could be due either to an increase in length or increase in the rigidity of the DNA molecules. Using low molecular weight DNA, Muller and Crothers observed an increase in viscosity with increasing r and a decrease in the sedimentation coefficient. Low molecular weight DNA is already a rigid rod so with this DNA viscosity changes can be due only to a length increase. These results would be expected for a molecule which binds by intercalation. In an interesting experiment, they tested the binding of actinomycin to aryl sulfonates and found that it was bound by means of a " π -complex" which was stabilized by hydrophobic forces. Aryl sulfonates provided an environment similar to that offered by the base pairs of DNA. Similarly, proflavine formed complexes with aryl sulfonates. Thus hydrophobic interactions appear to be more important than hydrogen bonding. Actinomycin substituted at the 7-position with a bulky group, e.g. 7-trimethylacetamino, exhibited

very slow association kinetics. According to the model of Hamilton, et al. (60), the 7-position is on the side of the molecule which would project away from the DNA. These three pieces of evidence point strongly to intercalation as the mode of binding of actinomycin to DNA (63). Some additional stabilization was obtained by interaction of the peptides with the DNA backbone.

The intercalation model was also favored by some work done with closed circular DNA. Waring (51) calculated that the DNA was unwound by $11.4^{\circ} \pm 3.0^{\circ}$. This corresponded to $95\% \pm 25\%$ of the actinomycin which bound was complexed by means of intercalation. Wang (64) used closed circles of DNA and observed that actinomycin unwound the helix by an angle identical to that for ethidium bromide. These two results were in close agreement and were strong evidence that actinomycin did indeed bind to DNA by means of intercalation.

VI. Ion-DNA Interactions.

A. General description.

Completely different types of complexes are formed between DNA and metal ions. These interactions are important because: 1) metal ions are ubiquitous in the cell and they have profound effects on nucleic acid structure and 2) many reactions of nucleic acids are mediated in the cell by metal ions, e.g. the need for Mg^{++} in protein synthesis. In general, metal ions fall into three classes in relation to their interaction with

nucleic acids: 1) those which interact exclusively with the bases, 2) those which interact with both base and phosphate, and 3) those which interact solely with the phosphate (65). It has been generally established that interaction with the phosphate groups resulted in stabilization whereas reaction with the bases destabilized the nucleic acid (66). This observation was made by Eichhorn (66) who found that Mg^{++} increased the T_m of DNA while Cu^{++} decreased the T_m . Since most of the relevant work was carried out with either Mg^{++} or Cu^{++} , these will be discussed in greater detail. However, it would be instructive to describe briefly the effects of other metal ions.

B. Binding of alkali metal ions and transition metal ions.

Alkali metal ions, e.g. Na^+ , stabilize the secondary structure of DNA by neutralizing the phosphate repulsive forces. It is generally agreed that these ions bind to phosphate and not to the bases (65). Interestingly, Na^+ ions are bound more strongly by native DNA than by denatured DNA (67,68). Transition metal ions vary greatly in their interactions with nucleic acids. Cr^{3+} and Mn^{++} were found to bind to the phosphates as did Fe^{++} (69). Fe^{3+} , on the other hand, could bind to either the phosphates or the bases (69) and Eichhorn (66) concluded that Fe^{3+} was first bound to the phosphate and as the temperature was raised it began to bind to the bases. Hg^{++} , on the

basis of the UV spectra (70) and viscosity studies (71), was found to bind to the bases. There was no evidence that it bound to the phosphates (71). Ag^+ was also found to bind to the bases (72,73) and the interaction was stronger with denatured DNA than with native DNA (73).

C. Effect of ion binding on T_m .

Eichhorn and Shin (74) studied the effects of a number of metal ions upon the melting behavior of DNA. Increasing concentrations of Mg^{++} resulted in increases in the T_m . In addition, if the solution was slowly cooled (renaturation) and then reheated the renaturation and reheating curves were superimposable. This was the stabilization expected if the ions were bound to the phosphates. The decrease in absorbance upon renaturation was due to randomly formed base stacks which could be easily disrupted upon heating, thus the superimposability of the two curves. Co^{++} and Ni^{++} had effects similar to Mg^{++} on the T_m , i.e. as concentrations were increased so were the T_m 's. The reheating curves, however, were no longer superimposable and exhibited a two-step process with the second T_m almost equivalent to the T_m of the initial heating. This indicated that some of the metal was able to hold complementary bases in register during heating so that rewinding could occur upon cooling. This base binding affected only a small portion of the DNA since most of the DNA is melted out in the first reheating step, that for the random stacks. Low

concentrations of Mn^{++} resulted in an increased T_m but at higher concentration the stabilizing effect reversed itself so that the T_m began to decrease. This indicated a change in the binding site from the phosphates to the bases. The same was evident for Zn^{++} . With increasing concentration, Cd^{++} caused a decrease in T_m ; no renaturation took place. Binding took place with the bases preventing them from regenerating the helix. The results for Cu^{++} were similar to those for Cd^{++} except that binding to the bases was stronger for Cu^{++} . Apparently, ion binding is not an all-or-none process in terms of binding to the base or phosphate. Rather, there was a gradual shift from those which bind solely to the phosphate (e.g. Mg^{++}), to those which bind to both moieties (Co^{++} , Ni^{++} , Mn^{++} , Zn^{++}) and finally, to those which bind exclusively (or nearly so) to the bases (Cd^{++} and Cu^{++}).

Eichhorn, et al., (75) found that addition of Cu^{++} either before or after denaturation caused spectral shifts as would be expected for ions which complex with the bases. This behavior was not expected for Mg^{++} . Interestingly, Fishman et al., (76) observed that addition of Mg^{++} to already denatured DNA did not induce any spectral changes. However, if the DNA was denatured in the presence of Mg^{++} , there was a spectral shift and a reduction in absorbance. Thus binding of Mg^{++} to the nitrogen bases seems to be facilitated by denaturation in the presence of the ion. Most evidence, however, points to binding

of Mg^{++} to the phosphates exclusively, The same is true for interactions with polynucleotides. Mg^{++} complexed with poly A and poly U through the phosphate and this resulted in a more ordered secondary structure, by screening the negative charge (77).

D. Base specificity of Cu^{++} binding.

Cu^{++} could form a chelate with either C_6-NH_2---- N_7 or $N_3-----N_9$ in purines. Pyrimidines would probably have an affinity lower than purines. Eichhorn, et al. (74) used ^{31}P -NMR to study Cu^{++} binding and detected a complex with purine N-7. There was also an indication of binding to the phosphates. Hiai (78) observed that low concentrations of Cu^{++} caused a T_m increase indicating binding to the phosphate. He suggested the possibility that Cu^{++} preferentially attacks GC pairs in DNA because there was greater destabilization for DNA rich in GC base pairs than for those rich in AT pairs. This view was supported by experiments which showed that methylation of the N-7 of guanine lessened the destabilization effect (79). A possible explanation was indicated by X-ray studies which showed the preferential binding site for Cu^{++} in cytosine to be at N-3. This position is usually involved in the hydrogen bond between guanine and cytosine and could account for the extra destabilization (80).

Berger and Eichhorn used NMR to study Cu^{++} binding (81,82). Cu^{++} was bound to adenosine at N-7 and either

N-3 or N-1. The addition of a phosphate group to adenosine to make AMP changed the binding preference to N-7 almost exclusively. This was true for 3'- and 5'-AMP but 2'- or cyclic AMP had equal binding at N-7 and N-3 or N-1. Thus the phosphate, although presumably not involved in the Cu^{++} binding had an affect as to which type of complex was formed (81). The N-7 was preferred in poly A, probably because this position was most available and less involved in stacking interactions. Poly I was also attacked preferentially at N-7 while poly C and poly U formed complexes at N-3 (82). They studied the complex with poly A-poly U as well and found that poly A was preferentially attacked (82).

E. Effect of ions on antibiotic-DNA complexes.

The complexing ability of the ions has been used as a probe of antibiotic-DNA complexes. Thus, Fishman and Rosenwasser (83) observed a shift in the actinomycin spectrum with the addition of both native and denatured DNA. When Cu^{++} was added, the denatured DNA-actinomycin spectrum returned to that observed with the actinomycin. Cu^{++} had no effect on the native DNA complex. Thus Cu^{++} was able to displace actinomycin from its complex with DNA but only if the DNA was denatured. This confirms that Cu^{++} binds to the bases and indicates that the sites for actinomycin and Cu^{++} may be the same or close to each other on the DNA molecule.

Rusconi (84) studied the effect of Ag^+ and Hg^{++} on the complexes of actinomycin and daunomycin with DNA. Ag^+ caused a release of the antibiotics from their complexes. Hg^{++} produced a similar effect on the actinomycin-DNA complex. Daunomycin, however, was not released even at higher Hg^{++} concentrations. If the actinomycin-DNA complex was added to daunomycin, the spectral shift was the same as occurred with the addition of DNA alone and both actinomycin and daunomycin are bound. When Hg^{++} was added to the ternary complex only actinomycin was released. The conclusions to be drawn from this were two-fold. The binding of Ag^+ and Hg^{++} , although believed to take place at the bases, are not exactly the same. Secondly, the binding sites for actinomycin and daunomycin appeared to be different because they could both be bound at once to the DNA.

VII. Physicochemical Effect Caused by Daunomycin Binding to DNA.

A. Effect on absorption spectra.

When DNA was added to a solution of daunomycin the absorbance at 475 nm peak decreased and the peak shifted to 505 nm (19). This red shift is characteristic of base-dye molecule interactions (39). Increasing the concentration of DNA resulted in a more profound effect which leveled off at a DNA/daunomycin ratio of 7:1. Ward, et al. (85) reported that purine mononucleotides also induced spectral changes but pyrimidine mononucleotides did

not. Calendi, et al, (19) observed this as well but 400-fold higher concentrations of mononucleotide were necessary to achieve an effect equivalent to that found with DNA.

B. Effect on fluorescence spectra.

Daunomycin exhibited a fluorescence emission spectrum when excited at 485 nm with a peak at 580 nm. The addition of DNA resulted in a decrease in fluorescence intensity. This quenching was concentration dependent but leveled off at a molar ratio of 8.7:1 DNA/daunomycin. Interestingly, the fluorescence of the chromophore alone was not quenched on addition of DNA (19). With N-acetyl daunomycin the visible and fluorescence spectral changes were similar to those with DNA but required higher DNA/daunomycin ratios (19:1) (19).

C. Effect on T_m

Daunomycin induced stabilization of DNA as evidenced by an increase in the T_m on daunomycin addition. Kersten, et al. (57) observed that anthracyclines (the group of antibiotics to which daunomycin belongs) were more effective in raising the T_m of DNA than was actinomycin. Daunomycin exhibited a double wave pattern, i.e. a slight increase in absorbance at low temperature, followed by the larger absorbance increase characteristic of the helix-coil transition. The slight absorbance increase was probably due to release of daunomycin from the DNA even at temperatures below the T_m . This double wave pattern was not observed with

actinomycin (57). Any alteration of the sugar amino group resulted in a lower T_m (86) which indicated a reduced stabilization effect.

D. Effect on viscosity and sedimentation.

Various studies have demonstrated that the addition of daunomycin resulted in an increase in DNA viscosity and a decrease in the sedimentation coefficient (19,57,87, 88). Calendi, et al. (19) observed that these effects were absent when denatured DNA was used and were less drastic with N-acetyl daunomycin (6). The viscosity increased as a function of r until an r value of 0.2 was reached (88). This corresponded to the number of strong binding sites as calculated from a Scatchard plot. Thus, just as with the acridines (28), the binding of daunomycin caused a stiffening and elongation of the molecule which could best be explained by intercalation (24). Kersten, et al. (57) however, concluded that there was no evidence for intercalation by anthracyclines.

E. Hydrogen bonding model of daunomycin binding.

Calendi, et al. (19) proposed a model for daunomycin binding involving a bond between the chromophore hydroxyl groups and DNA, probably via hydrogen bonding. An additional bond could be formed between the sugar amino group and this bond was proposed as being the stronger one since an unaltered group was necessary for strong binding.

F. Requirement for unaltered daunomycin sugar amino group.

A series of studies by DiMarco, Zunino and co-workers (86,89) also indicated the importance of an unaltered sugar amino group for maximum interaction with DNA. Alterations of the chromophore had little effect on the decrease in absorbance at 475 nm. Changes in the sugar residue, however, resulted in virtually no decrease in absorbance with the addition of DNA (89). A similar observation was made for the increase in viscosity, i.e. daunomycin with an altered sugar moiety had little effect on the viscosity of DNA (89). The cytological effects of daunomycin were also influenced by alteration of the sugar moiety. These daunomycin molecules exhibited little or no anti-mitotic activity as opposed to daunomycin or daunomycin with alterations in the chromophore (89). The association constant for daunomycin with a glucosamine residue, instead of daunosamine, was 40 times smaller than for daunomycin. Acetylation of the amino group of daunomycin reduced the binding capacity 250-fold (86). This led DiMarco, et al. (89) to propose three classes of daunomycin compounds (86): 1) those with an unaltered sugar and intact chromophore acetyl group are capable of strong binding with DNA, inhibit mitotic activity, and DNA synthesis; 2) those with changes in the chromophore acetyl moiety could still allow strong DNA binding and have anti-mitotic activity but DNA synthesis is not affected; 3) those with alterations of the sugar amino group possess a weak DNA binding capacity and a lack of biological activity.

G. Evidence for two binding modes.

Zunino (88) studied the behavior of daunomycin on a DNA-cellulose column. Daunomycin yielded two peaks, one which was eluted at 0.2-0.4 M NaCl and another which required 2.5-3.0 M urea. This corresponded to two binding types, a weak binding which could be broken by NaCl and was, therefore, probably electrostatic in nature. The other was strong and was broken only by urea. This was in agreement with the experiments of Zunino, et al. (86) who found that Scatchard plots for the daunomycin-DNA interaction were convex to the X-axis, another indication of two binding modes.

H. X ray diffraction studies.

X-ray analysis of a daunomycin-DNA complex was consistent only with an intercalation model (90). The base pairs were separated by an additional 3.4 Å and there was a 12° untwisting of the helix at the point of intercalation. A model was proposed in which the planar rings of the daunomycin chromophore overlap with the bases and the sugar sits in the large groove of the DNA molecule. The amino group is close to the phosphates, allowing interaction. This model was supported by Waring's work with closed circular DNA (51). He observed, however, that daunomycin would unwind the helix by only 5.2° and thus only about 50% of the molecules would be intercalated.

VIII. Purpose of Present Study.

Daunomycin thus affords an opportunity for studying the interaction between an antibiotic molecule and DNA. Much as the situation was with actinomycin, there are two proposed mechanisms for binding with the bulk of the evidence supporting the intercalation model. However, some questions remain. If Waring (51) is correct, and only half of the daunomycin which is bound is intercalated, what is the nature of the other binding process? Is there a base preference in daunomycin binding to DNA? If, indeed, acridine dyes, ethidium bromide, actinomycin, and daunomycin all do bind by intercalation why do they have different cytological effects? In order to answer some of these questions and further characterize the daunomycin-DNA complex the present study was undertaken.

It was noted earlier than ions can form complexes with nucleic acids and this binding can result in profound changes in the properties of the nucleic acid. Therefore, it seemed of interest to study the effects ions might have on the DNA-daunomycin complex. Two divalent cations were chosen, Cu^{++} , as representative of those ions which bind to the nitrogen bases in DNA, and Mg^{++} , which binds to the phosphate groups. Such a study could help elucidate which of the various groups on the daunomycin and nucleic acid molecules are necessary for complex formation.

In order to ascertain the minimum nucleic acid size

necessary for complex formation to occur between daunomycin and a nucleic acid, the binding of daunomycin with nucleic acid bases, nucleosides, nucleoside monophosphates, and nucleoside triphosphates will be studied.

The effect of daunomycin on the T_m behavior of DNA's of varying base ratio will be investigated. This would provide information on the base specificity for the daunomycin-DNA interaction, if such a preference indeed exists. In addition, the T_m studies, if performed at various ionic strengths, would allow an evaluation of the effect which electrostatic interactions have on the DNA-daunomycin complex.

Base preference and electrostatic effects were also to be studied by spectral titrations and equilibrium dialysis. Quantitative binding data could be determined by these methods for DNA's of varying GC content and various polynucleotides at three ionic strengths. In addition, such data could be obtained for single-vs. double-stranded polynucleotides and ribo- vs. deoxyribo-polynucleotides thus permitting an evaluation of the effect which the sugar moiety and the number of polynucleotide chains may have on the daunomycin nucleic acid interaction.

Materials and Methods

I. Materials:

A. DNA:

Calf thymus DNA was purchased from Worthington Biochemicals, Freehold, New Jersey. Cl. perfringens DNA used for the T_m studies was obtained from both Sigma Biochemicals, St. Louis, and Nutritional Biochemical Co., Cleveland. The Cl. perfringens DNA used for the spectral titrations was purchased from Calbiochem. San Diego, California and Micrococcus lysodeikticus DNA was purchased from Sigma Biochemical Co.

B. Daunomycin:

Daunomycin was kindly supplied by Farmitalia, Milan, Italy and by Dr. Harry Wood of the Cancer Chemotherapy Research group at the National Institutes of Health, Bethesda, Maryland.

C. Polynucleotides:

Poly A, poly C, poly G, poly I, poly U, poly dA, poly dT, poly dG·poly dC, and poly rA·poly dT were purchased from Miles Laboratories, Research Products Division, Elkhart, Ind.

Poly (dA-dT)·poly (dA-dT) and a second preparation of poly dA were obtained from Calbiochem.

Poly dG and poly dA·poly dT were obtained from P-L Biochemicals, Milwaukee, Wis. and poly A·poly U was purchased from Sigma Biochemicals.

Data was supplied by each company giving most of the pertinent physical characteristics such as λ_{\max} , minimum molecular weight, S_{20} (sedimentation coefficient), and molar extinction coefficient for the homopolymers and polynucleotide duplexes.

II. Methods:

A. Preparation of Nucleic Acid Solutions:

DNA stock solutions were prepared by suspending approximately 10 mg of DNA in 5 ml of $5 \times 10^{-3}M$ NaCl. A drop of chloroform was added to prevent bacterial growth. The solution was allowed to stand at $4^{\circ}C$ with occasional rotation, for a period of four days after which it was diluted to 100 ml with $5 \times 10^{-3}M$ NaCl and stored at $4^{\circ}C$.

The homopolynucleotide and polynucleotide duplex solutions were prepared by dissolving 10-20 mg of polynucleotide in $5 \times 10^{-3}M$ NaCl. Most polynucleotides readily dissolved. For those which did not, such as poly G and poly C, some shaking was necessary in order to facilitate solution.

B. Denaturation of DNA:

DNA was denatured by heating the stock solution in a closed screw cap test tube in a boiling water bath for 15 minutes followed by rapid cooling in ice. The amount of DNA so treated varied between 1.0-10.0 ml, depending on the amount needed for a particular experiment.

C. Preparation of Daunomycin Solutions:

Daunomycin stock solutions were prepared by dissolving 14.05 mg in 25 ml of 5×10^{-3} M NaCl. The resultant solution was 10^{-3} M (using 563.9 as the molecular weight for daunomycin). These solutions were stored in the dark at 4° C.

D. Characterization of Solutions:

Before use, a UV spectrum of each stock solution was taken. This was done for the purpose of checking its spectral properties (λ_{\max} , A_{260}/A_{280} , A_{330}/A_{260}) and also determining its concentration based on its molar extinction coefficient. The following molar extinction coefficients were used:

<u>compounds</u>	<u>ϵ_{260} (expressed as $E(P)_{260}$ unless other indicated)</u>
Calf Thymus DNA	6800
<u>Cl. perfringens</u> DNA	7320
<u>M. lysodeikticus</u> DNA	7250
Poly A	10000
Poly C	5190
Poly G	9480
Poly I	5280
Poly U	10720
Poly dA (Miles)	8900
Poly dA (Calbiochem)	9600
Poly dG	9800 ($E(P)_{252}$)
Poly dT	8900

Poly dA·poly dT	6000
Poly (dA-dT)·poly (dA-dT)	6600 (E(P) ₂₆₂)
Poly dG·poly dC	7360
Poly dT·poly rA	6700
Poly A·poly U	7000 (E(P) ₂₅₇)
Daunomycin	36209 (E ₂₃₃)
	9700 (E ₄₇₅)

E. Spectral Studies:

a. Absorbance:

Absorbance measurements were made with either a Cary model 14 or 15 recording spectrophotometer. Preliminary measurements for the nucleic acid components were made with a Perkin-Elmer model 402 recording spectrophotometer.

b. Fluorescence:

Fluorescence measurements were made with a Perkin-Elmer MPF-2A fluorescence spectrophotometer equipped with a Hitachi QPD-33 recorder. Solutions containing daunomycin were excited at 466 nm and emission spectra were recorded from 540-590 nm. The fluorescence spectrophotometer was calibrated to read a specific fluorescence intensity using a 2.5×10^{-5} M daunomycin solution (0.1 ml of the 10^{-3} M stock solution in 3.9 ml of 5×10^{-3} M NaCl) as a standard. This was done in order to minimize day-to-day instrumental variations.

c. Titration:

1. Spectrophotometric Titrations - Spectrophotometric titrations were performed on a Zeiss PMQ II

spectrophotometer. Readings were taken at 475 nm, the visible peak for daunomycin. The concentration of daunomycin was held constant at $2.5 \times 10^{-5} \text{M}$ and the concentration of nucleic acid was varied from $5 \times 10^{-6} \text{M}$ to $3 \times 10^{-4} \text{M}$.

2. Spectrofluorimetric Titrations - Spectrofluorimetric titrations were carried out with a Perkin-Elmer MPF-2A fluorescence spectrophotometer. Whenever possible, all repetitive runs of a particular experiment were performed on the same day. As indicated above, this was done to avoid day-to-day instrumental deviations. For these experiments, the concentration of daunomycin was held constant at $1 \times 10^{-6} \text{M}$. The concentration of nucleic acid was varied from $1 \times 10^{-6} \text{M}$ to $3 \times 10^{-5} \text{M}$. The instrument was set to read approximately 90 on the fluorescence intensity scale with a $1 \times 10^{-6} \text{M}$ daunomycin solution (which was sample #1 for each experiment). This setting on the instrument was used for all runs of a particular experiment.

F. Determination of Binding Equilibria:

Data from the spectral titrations were used to calculate binding data for the daunomycin-DNA or daunomycin-polynucleotide interaction. For a small molecule, D, interacting with a large macromolecule, P, we can write



The association constant (K) can be represented as,

$$K = \frac{[PD]}{[P][D]} \quad (2)$$

and r , the number of moles of D bound, for total molecules of P present,

$$r = \frac{[PD]}{[PD] + [P]} \quad (3)$$

If P contains n sites capable of binding D we can still denote K as in equation (2). If

$$r = \sum_{i=1}^n r_i = nr_i$$

is the total average number of occupied sites per molecule of P, then the probability that any site, chosen at random from any molecule in the solution, is occupied by D, is given by:

$$r/n = \frac{K[D]}{1 + K[D]} \quad (4)$$

Equation (4) can be rearranged to give

$$r = \frac{nK[D]}{1 + K[D]} \quad (5)$$

and finally, (91-93)

$$r/[D] = Kn - Kr \quad (6)$$

This is the usual form of the equation for multiple binding equilibria for a macromolecule and is the form of the equation most often used. Sometimes C is substituted for D, as it will be for the purposes of the rest of this discussion.

Data of this type is usually plotted as r/c versus r . This is commonly referred to as a Scatchard plot (94). If such a plot is constructed (figure 25), the curve should be a straight line, the slope of which is $-K$, the intrinsic association constant. The intercept on the r axis is n , which is the number of binding sites on the molecule P.

The plot yields a straight line only if the binding sites are equivalent and non-interacting. For any other case, the plot will deviate from a straight line, and for two classes of interacting binding sites, will be convex to the r axis, as was the case in this study (figure 25).

Peacocke and Skerrett (23) formulated a method whereby data for a Scatchard plot could be derived from spectral titrations. This method made use of the fact that there was a change in the absorption spectrum of the small molecule on being bound to the macromolecule. A single wavelength was chosen at which the difference in absorbance is most pronounced (for daunomycin this was 475 nm, its peak).

If T_D is the total concentration of daunomycin and T_P is the total concentration of nucleic acid, then α , the fraction of total ligand bound is

$$\alpha = \frac{rT_P}{T_D} = \frac{D_1 - D}{D_1 - D_2} \quad (7)$$

where,

D_1 = absorbance of free daunomycin, $r=0$; $[D] = T_D$

D_2 = absorbance of completely bound daunomycin, $rT_P=T_D$;
 $[D] = 0$.

D = absorbance of a particular daunomycin - nucleic acid complex.

In practice it is necessary to obtain absorbance values for pure daunomycin (D_1), the complex (D), and completely

bound daunomycin (D_2). From this one can calculate:

$$r = T_D/T_P$$

and

$$c = [D] = T_D (1 - \alpha)$$

With values for r and c it is possible to construct Scatchard plots.

It is difficult to determine the absorbance of completely bound daunomycin. To this end, a plot of $1/\text{absorbance}$ versus $1/c$ was made and extrapolation to infinite c gave the absorbance of completely bound daunomycin.

The addition of nucleic acid to a solution of daunomycin resulted in a decrease in the fluorescence intensity of daunomycin. This decrease was dependent on the concentration of added nucleic acid, as was true for absorbance. Therefore, Peacocke and Skerrett's treatment could be applied to spectrofluorimetric titrations. As described by Löber, et al (40) (based on a prior treatment by Förster (95)) the fluorescence intensity is directly related to dye concentration if the product of $\epsilon \cdot b \cdot c \ll 1$. For the work reported here, $\epsilon = 9.7 \times 10^3$ liter/mole cm, $b = 1.0$ cm, and $c = 10^{-6}$ M and so this condition was fulfilled. The wavelength of interest was 555 nm which was the emission peak for daunomycin ($\lambda_{\text{ex}} = 466$ nm). A test experiment was performed using identical samples for both spectrophotometric and spectrofluorimetric titrations. The results for the two techniques were comparable within experimental

error.

G. Equilibrium Dialysis:

Special cells were used for the equilibrium dialysis experiments. These consisted of two polymethacrylate blocks with a cavity in each block. These could be tightened by means of screws so that the two cavities faced each other. A dialysis membrane of regenerated cellulose was placed over the cavities and acted as both a membrane boundary and a gasket. Each cavity was capable of holding 5 ml of solution. 4 ml of daunomycin solution (usually $2.5 \times 10^{-5}M$) were added to one side and 4 ml of $5 \times 10^{-3}M$ NaCl (for blank runs) or DNA or polynucleotide solution were added to the other side. The dialysis cell was then placed on a Burrell wrist-action shaker in the dark at $4^{\circ}C$ for 24 hours. It was determined that 24 hours was sufficient to establish equilibrium. The concentrations of the daunomycin solutions on either side of the membrane were determined by measuring their absorbances at 475 nm.

Daunomycin adsorbs to the membrane and in order to correct for this blanks were run of daunomycin solutions versus $5 \times 10^{-3}M$ NaCl. The difference between the concentration of the initial daunomycin solution and the concentrations of the solutions on both sides of the membrane was assumed to be equal to the concentration of daunomycin adsorbed. This value was used as a correction factor in all calculations.

The concentration of free daunomycin (C_f), bound

daunomycin (C_b), total daunomycin (C_t) and daunomycin bound to the membrane (C_{bm}) were determined by one of three methods:

1. At equilibrium, C_f is equal on either side of the membrane. Therefore, C_f was determined directly by measuring the absorbance of the solution on the one side to which daunomycin was initially added. Therefore, $C_t - (2C_f + C_{bm}) = C_b$.
2. Free daunomycin (C_f) and the spectra of its complexes with various nucleic acids exhibited isosbestic points. Since the extinction coefficient for free daunomycin and the complex is the same at any given isosbestic point these can be used to determine C_b directly.
3. The addition of 0.1 ml of 1.0 M HCl to a nucleic acid - daunomycin complex dissociates the complex as indicated by the spectra (i.e. the spectrum of the acid-treated complex was identical to that of free daunomycin). This was used to determine C_b . This value was adjusted by a factor of 3.1/3.0 to account for the added acid.

All the above methods yielded values for C_f and C_b which were used for determining quantitative binding data according to Scatchard as described previously.

H. pH Studies:

For the pH studies, pH was controlled by the use of

0.1M Tris-HCl buffer. Both the buffer and 5×10^{-3} M NaCl were used to make the appropriate dilutions. In the lower pH ranges (i.e. below pH 5), where Tris was not an effective buffer, an attempt was made to use 0.2M acetate buffer. It was found, however, that acetate caused changes in the free daunomycin spectrum and was, therefore, not used. The solutions were thus essentially unbuffered but 0.1M Tris was present in order to cancel any effect which may have resulted from the presence of Tris.

The pH was measured using either a Corning model 5, model 7 or model 12 pH meter.

I. T_m Studies:

DNA melting studies were carried out with a Gilford model 2400 spectrophotometer equipped with a fifth channel to record temperature automatically. The temperature was controlled by a Neslab TP-2 temperature programmer connected to a Lauda K-2R circulating bath. The bath was a water-ethylene glycol mixture (1:2). For each experiment the melting profiles were recorded for both a free DNA and a daunomycin-DNA complex. This cancelled out any day to day instrumental differences.

RESULTS

I. Spectral Studies

A. Ultraviolet and Visible Studies

Daunomycin had a characteristic absorbance spectrum in both the ultraviolet and visible regions. In the UV the spectrum consisted of two intense peaks at 233 nm and 255 nm and one of lesser intensity at 292 nm (figure 5). In the visible region daunomycin displayed a broad peak with maximum absorbance at 475 nm (figure 6).

As can be seen in figures 5 and 6, the addition of DNA to a solution of daunomycin resulted in alterations of the daunomycin spectrum. Concentrations as low as $10^{-5}M$ DNA were sufficient to cause the disappearance of the peak at 292 nm. The peak at 255 nm was enhanced but this could be due to the absorbance of the DNA. The 233 nm peak was diminished and at higher DNA concentrations ($1.0 \times 10^{-4}M$) was slightly shifted toward higher wavelengths. The absorbance values at the peaks were not additive (i.e. they were not equal to the sum of the individual absorbances of free DNA and free daunomycin). In the visible region the effects caused by DNA addition were not complicated by a DNA spectrum because it did not absorb in the visible. The absorbance at 475 nm was diminished and the peak was shifted to 505 nm.

B. Fluorescence.

When a solution of daunomycin was excited at 466 nm it gave a characteristic emission spectrum consisting of a

FIGURE 5.

Effect of addition of DNA on ultraviolet spectrum •
of daunomycin. —————, Daunomycin ($2.5 \times 10^{-5}M$);
-----, Daunomycin plus DNA ($6.25 \times 10^{-5}M$).

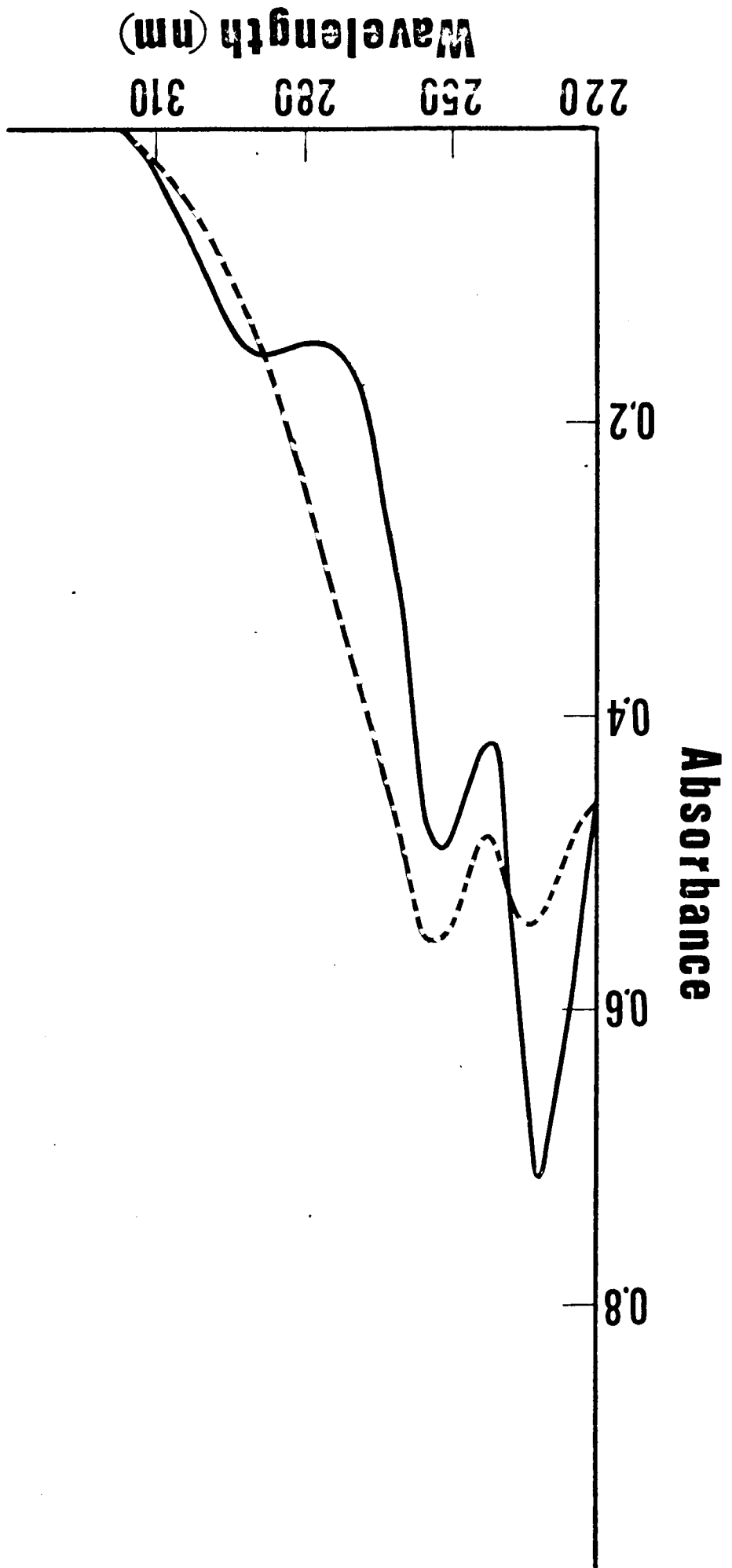
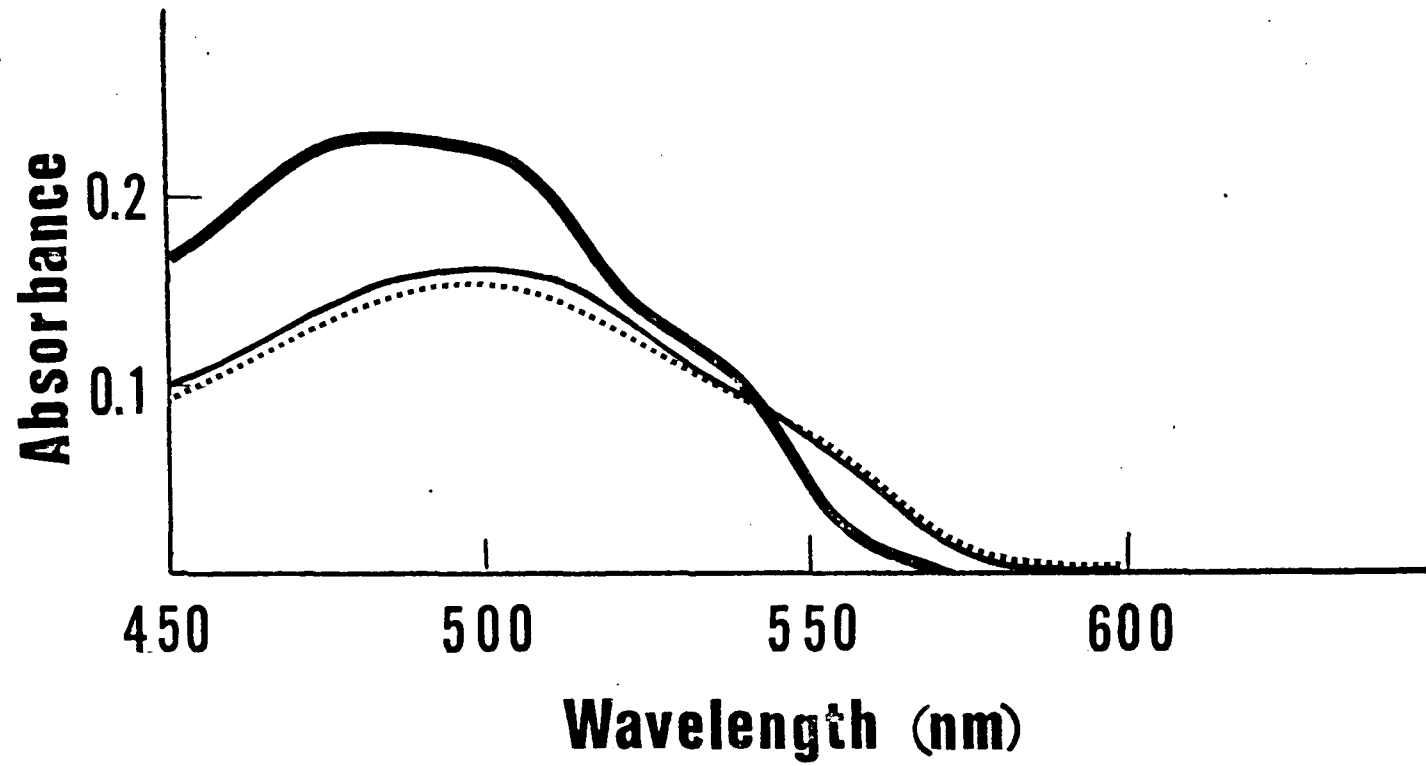


FIGURE 6.

Addition of DNA to Daunomycin ($2.5 \times 10^{-5} \text{M}$).

————, Daunomycin; ————, Daunomycin plus native DNA ($1.0 \times 10^{-4} \text{M}$); ······, Daunomycin plus denatured DNA ($1.0 \times 10^{-4} \text{M}$).



peak at 555 nm and a shoulder at 580 nm (figure 7). The fluorescence intensity of free daunomycin remained relatively unchanged as the pH was varied from 1.5 to 7.8 (table 1).

The addition of DNA to daunomycin (4:1 molar ratio) resulted in a drastic reduction in fluorescence intensity. When the concentration ratios were comparable, denatured DNA had a greater quenching effect than native DNA. At pH's below 2.5, the quenching effect of DNA was diminished and the fluorescence intensities were the same in the presence and absence of DNA. This indicated the possibility that the complex was being split at the low pH (table 1).

C. Concentration dependence.

The alterations of the UV and visible spectra which occurred when daunomycin and DNA were mixed and the quenching of daunomycin fluorescence with the addition of DNA clearly indicated the formation of a complex. These spectral effects in both the absorption and fluorescence studies were concentration dependent, being greater as the concentration of added DNA was increased (figures 7 and 8). The absorption decrease leveled off between 7.5:1 and 10:1 molar ratio of DNA/Dm. This confirmed the work of Calendi, et al. (19) which had shown that the decrease in absorbance at 475 nm and the quenching of fluorescence continued until a molar ratio of DNA/Dm = 8.7:1 was reached.

II. Effect of Cu⁺⁺ on the Daunomycin-DNA Complex

A. Absorption Studies

The addition of Cu⁺⁺ (at least 10⁻⁴M) to a solution

TABLE 1

FLUORESCENCE INTENSITY OF DAUNOMYCIN-DNA COMPLEXES

Excitation at 466 nm
Emission at 555 nm

[DNA] = $1.0 \times 10^{-4} M$
[Daunomycin] = $2.5 \times 10^{-5} M$

pH	Dm	Dm -nDNA	Dm -dDNA	Effect of Cu^{++} $1.0 \times 10^{-4} M$			Effect of Mg^{++} $1.0 \times 10^{-1} M$		
				Dm	Dm -nDNA	Dm -dDNA	Dm	Dm -nDNA	Dm -dDNA
7.8	68.6	28.3	29.9				16.2	14.4	14.4
7.5				35.1	6.5	3.7			
7.1	72.0	21.2	6.2	33.0	5.2	1.1	46.6	31.0	24.7
6.8	69.5	17.8	6.7	25.3	4.0	0.8	51.2	34.8	31.0
6.5	68.0	13.2	11.7	25.5	4.0	0.7	54.0	40.2	34.0
6.1	70.4	21.8	16.5	36.8	8.3	1.9	58.9	44.2	39.0
5.8	71.3	22.0	16.5	66.0	21.0	8.0	70.1	47.5	47.5
5.5	77.4	26.3	15.2	70.3	22.5	12.0	70.1	48.0	46.5
4.6	72.1	22.2	17.1				72.1	49.6	
4.3				73.6	28.9	19.5			
3.5	73.4	29.9	29.5				69.9	48.4	54.0
2.3	74.3	53.7	63.7	74.3	65.8	72.0	70.0	63.1	68.0
1.5	74.3	69.1	68.0				68.4	67.3	66.0

FIGURE 7.

Effect of DNA addition on the visible spectrum of daunomycin ($5 \times 10^{-5}M$). ———, no DNA; -----, $5 \times 10^{-6}M$ DNA; ······, $2.5 \times 10^{-5}M$ DNA; ooooo, $5 \times 10^{-5}M$ DNA; - - - - - , $7.5 \times 10^{-5}M$ DNA.

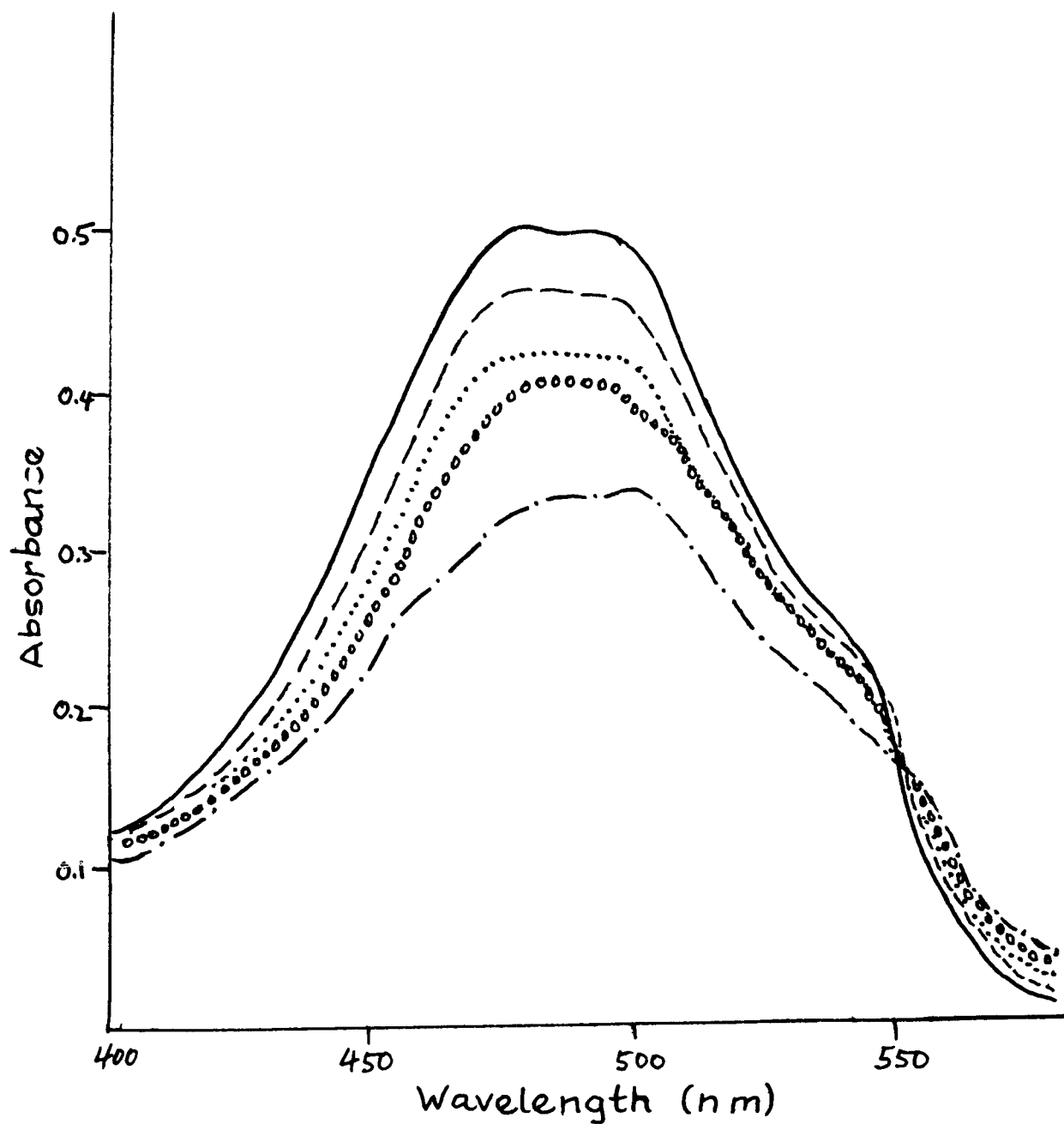
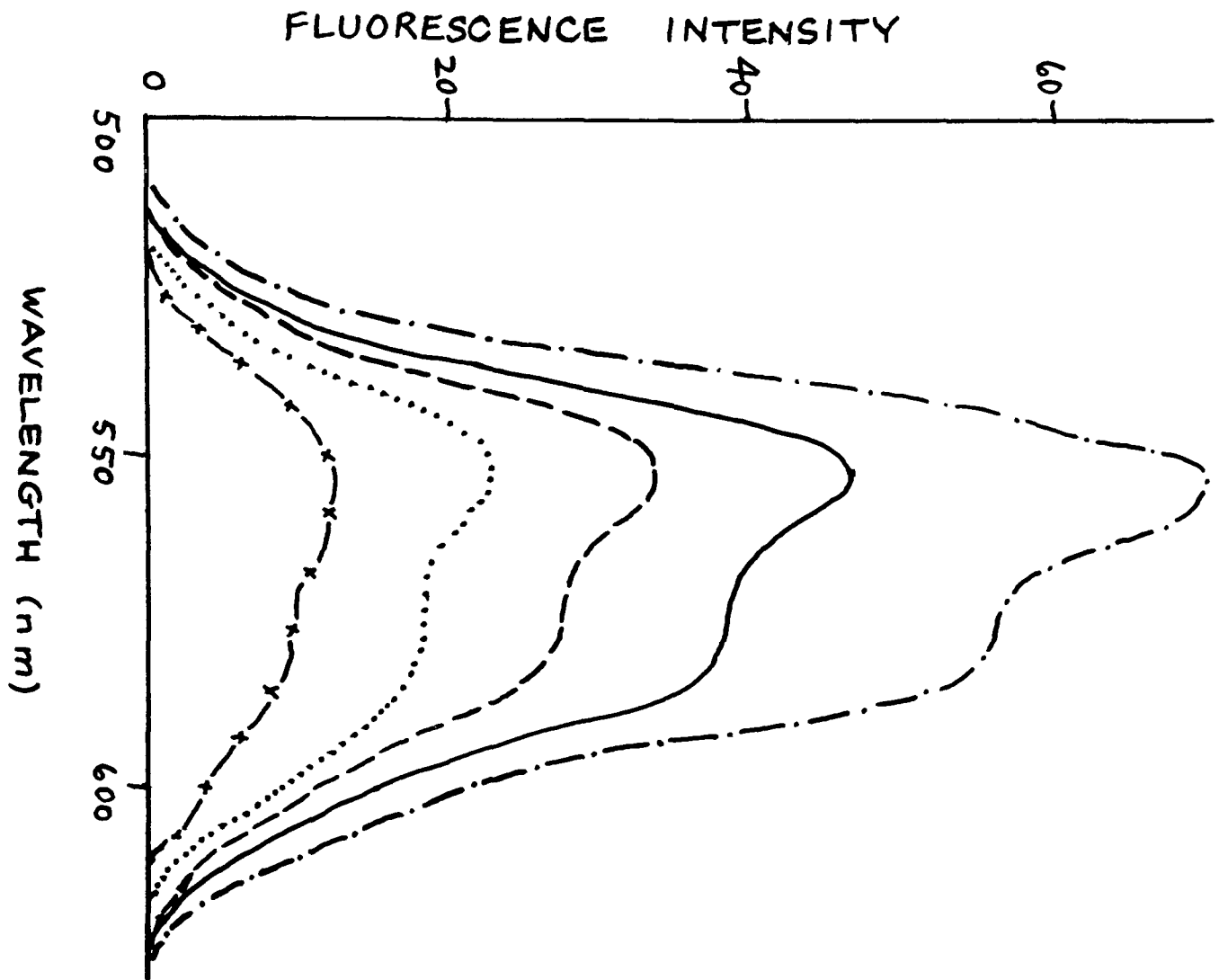


FIGURE 8.

Effect of addition of DNA on fluorescence emission spectrum of daunomycin ($2.5 \times 10^{-5} \text{M}$). - - - - -, daunomycin; _____, Dm + native DNA ($2.5 \times 10^{-5} \text{M}$); - - - - -, Dm + native DNA ($5 \times 10^{-5} \text{M}$); ······, Dm + denatured DNA ($5 \times 10^{-5} \text{M}$); -x-x-x, Dm + native DNA ($1.0 \times 10^{-4} \text{M}$).



of daunomycin resulted in an altered spectrum. The peak at 475 nm was shifted to 495 nm and two shoulders appeared at 535 nm and 565 nm (figure 9). This indicated that Cu^{++} , in the absence of DNA was bound to daunomycin. If DNA ($1.0 \times 10^{-4}\text{M}$) was then added further changes in the visible spectra occurred (figure 9). With native DNA, there was a broadening of the spectrum with loss of the peaks. On the other hand, with heat-denatured DNA, the peak at 505 nm disappeared and two new peaks appeared one at 540 nm and the other at 582 nm.

These effects were dependent on the concentration of both Cu^{++} and DNA. With a lower Cu^{++} /daunomycin ratio (2:1), there was little difference in the spectra as the dDNA/Dm ratio was increased from 2:1 to 6:1 (figure 10). When the Cu^{++} /Dm ratio was held constant at 6:1 (figure 11), as the dDNA/Dm ratio was increased, the 540 nm and 582 nm peaks were intensified.

A concentration dependence of Cu^{++} was also observed when the DNA/Dm ratio was kept constant and the Cu^{++} /Dm ratio was varied. Figures 12 and 13 illustrate this dependence. These results showed that there was a minimum concentration ratio in relation to daunomycin for both denatured DNA and Cu^{++} necessary to elicit the spectral changes characteristic of the daunomycin-denatured DNA- Cu^{++} complex. These ratios were 4:1 for both Cu^{++} /Dm and denatured DNA/Dm.

FIGURE 9.

Addition of Cu^{++} to daunomycin or daunomycin-DNA complex. **————**, daunomycin ($5 \times 10^{-5}\text{M}$) + Cu^{++} ($3 \times 10^{-4}\text{M}$); **·····**, Dm ($5 \times 10^{-5}\text{M}$) + Cu^{++} ($3 \times 10^{-4}\text{M}$) + native DNA ($2 \times 10^{-4}\text{M}$); **———**, Dm ($5 \times 10^{-5}\text{M}$) + Cu^{++} ($3 \times 10^{-4}\text{M}$) + denatured DNA ($2 \times 10^{-4}\text{M}$).

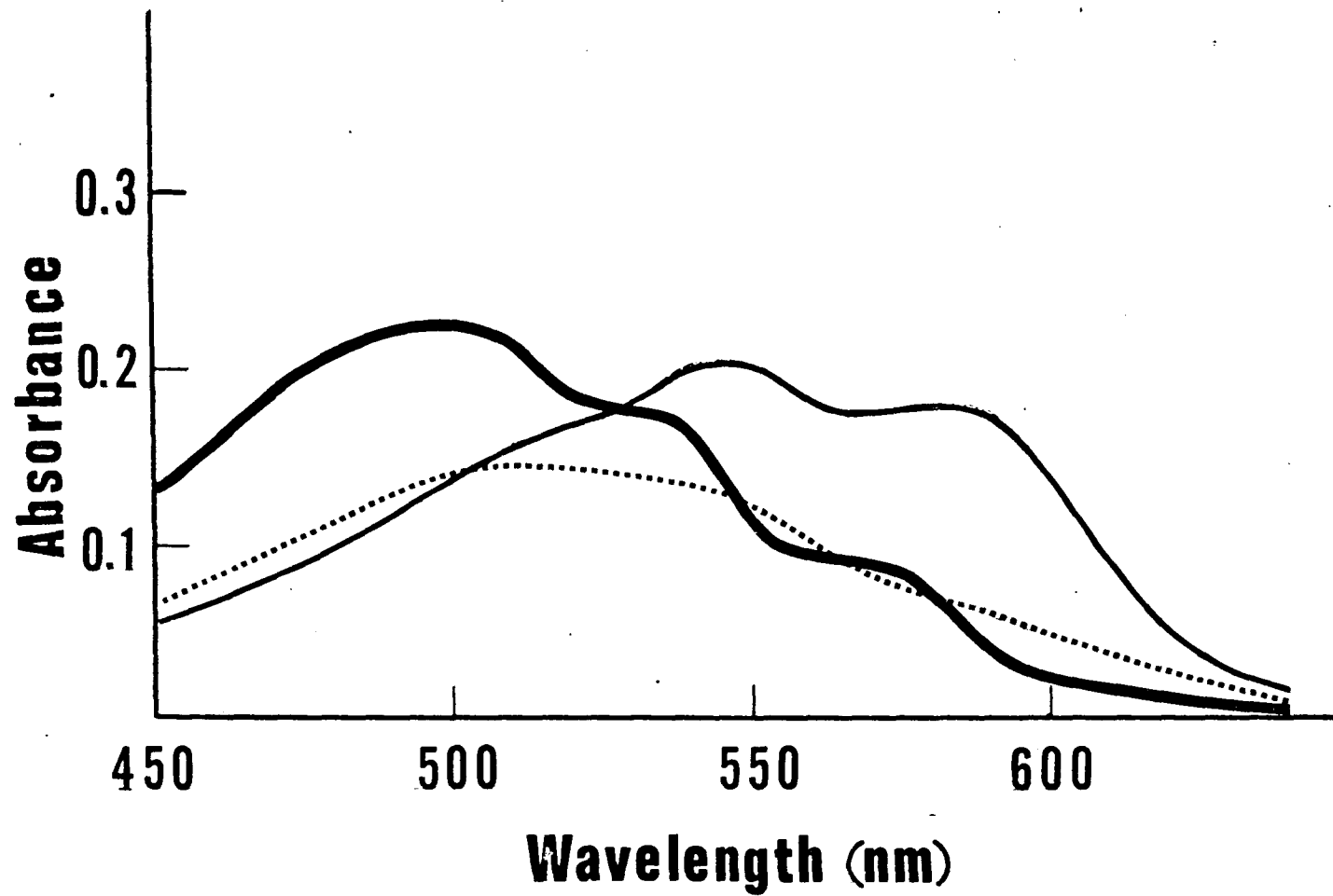


FIGURE 10.

Effect of denatured DNA concentration on the visible spectrum of the denatured DNA-daunomycin-Cu⁺⁺ complex. Concentration of daunomycin is constant at 2.5×10^{-5} M. Concentration of Cu⁺⁺ is constant at 5×10^{-5} M. -----, 5×10^{-5} M DNA; ———, 1.5×10^{-4} M DNA.

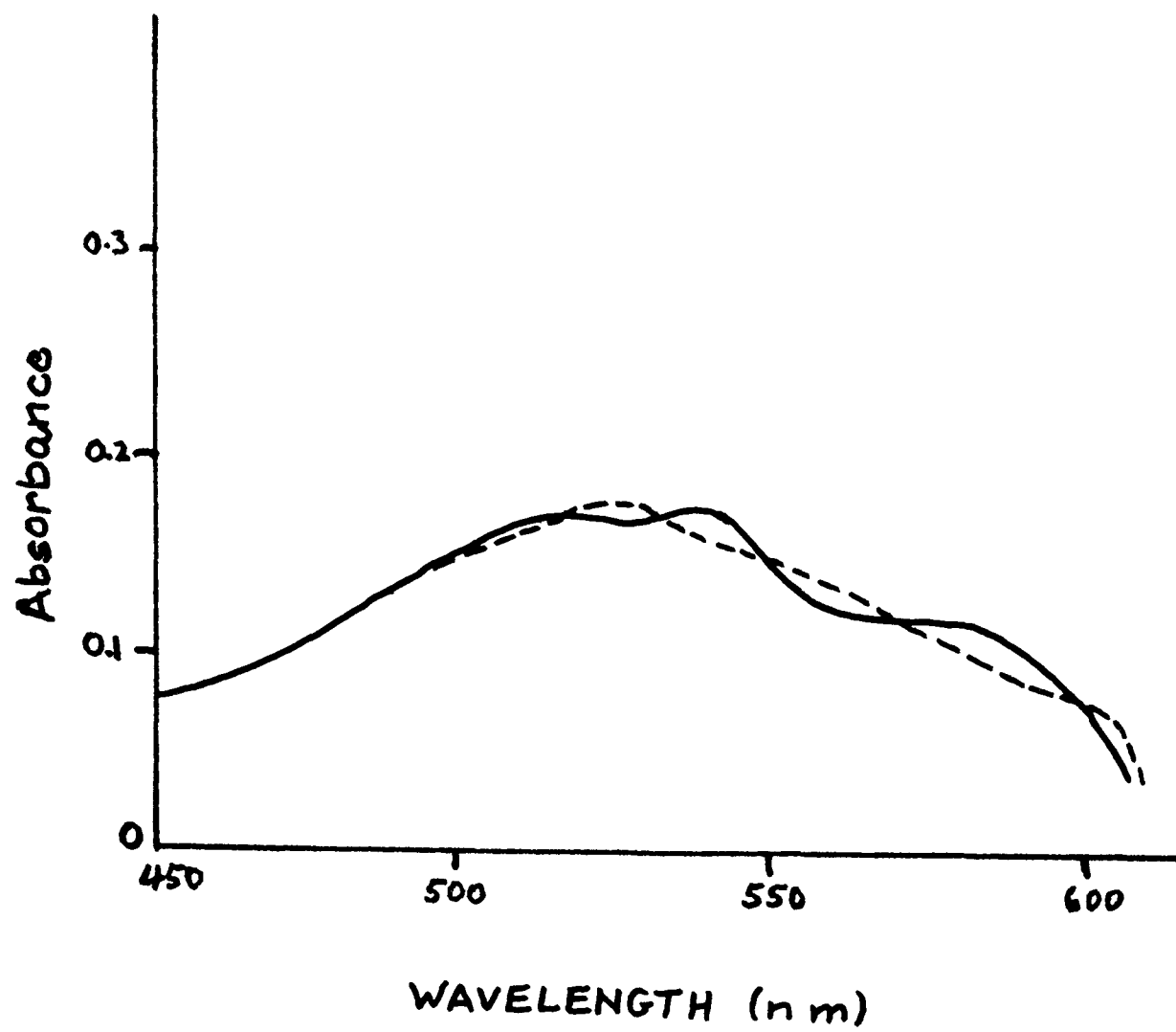


FIGURE 11.

Effect of concentration of denatured DNA on the visible spectra of the daunomycin-Cu⁺⁺ complex. Concentration of Dm is constant at $2.5 \times 10^{-5}M$ and the concentration of Cu⁺⁺ is constant at $1.5 \times 10^{-4}M$. -----, denatured DNA ($5 \times 10^{-5}M$); ———, denatured DNA ($1.0 \times 10^{-4}M$); -·-·-·, denatured DNA ($1.5 \times 10^{-4}M$).

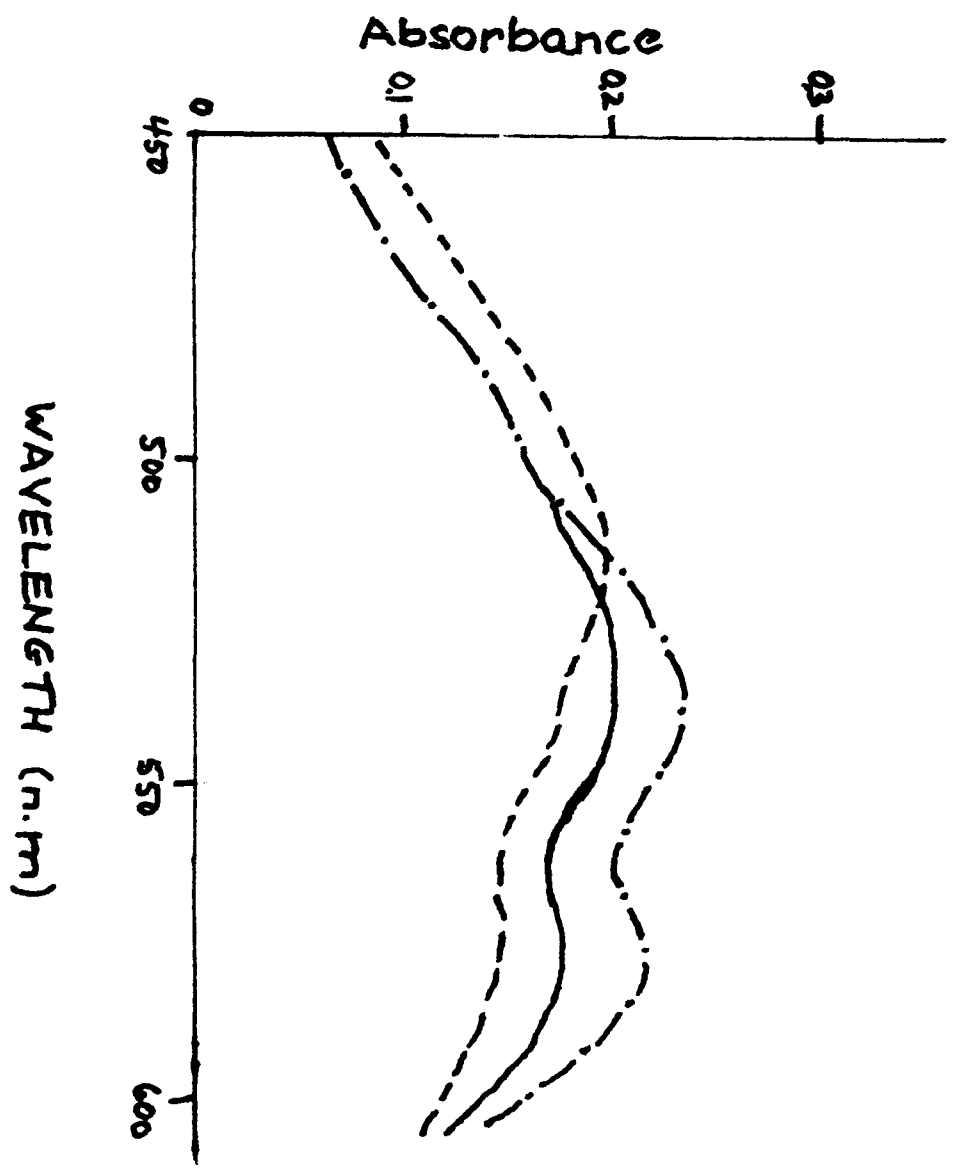


FIGURE 12.

Effect of concentration of Cu^{++} on the visible spectra of the daunomycin-denatured DNA complex. Concentration of daunomycin is constant at $2.5 \times 10^{-5}\text{M}$. Concentration of denatured DNA is constant at $5 \times 10^{-5}\text{M}$. -x-x-x, daunomycin + denatured DNA; - - - -, Dm-dDNA + Cu^{++} ($5 \times 10^{-5}\text{M}$); ———, Dm-dDNA + Cu^{++} ($1.0 \times 10^{-4}\text{M}$).

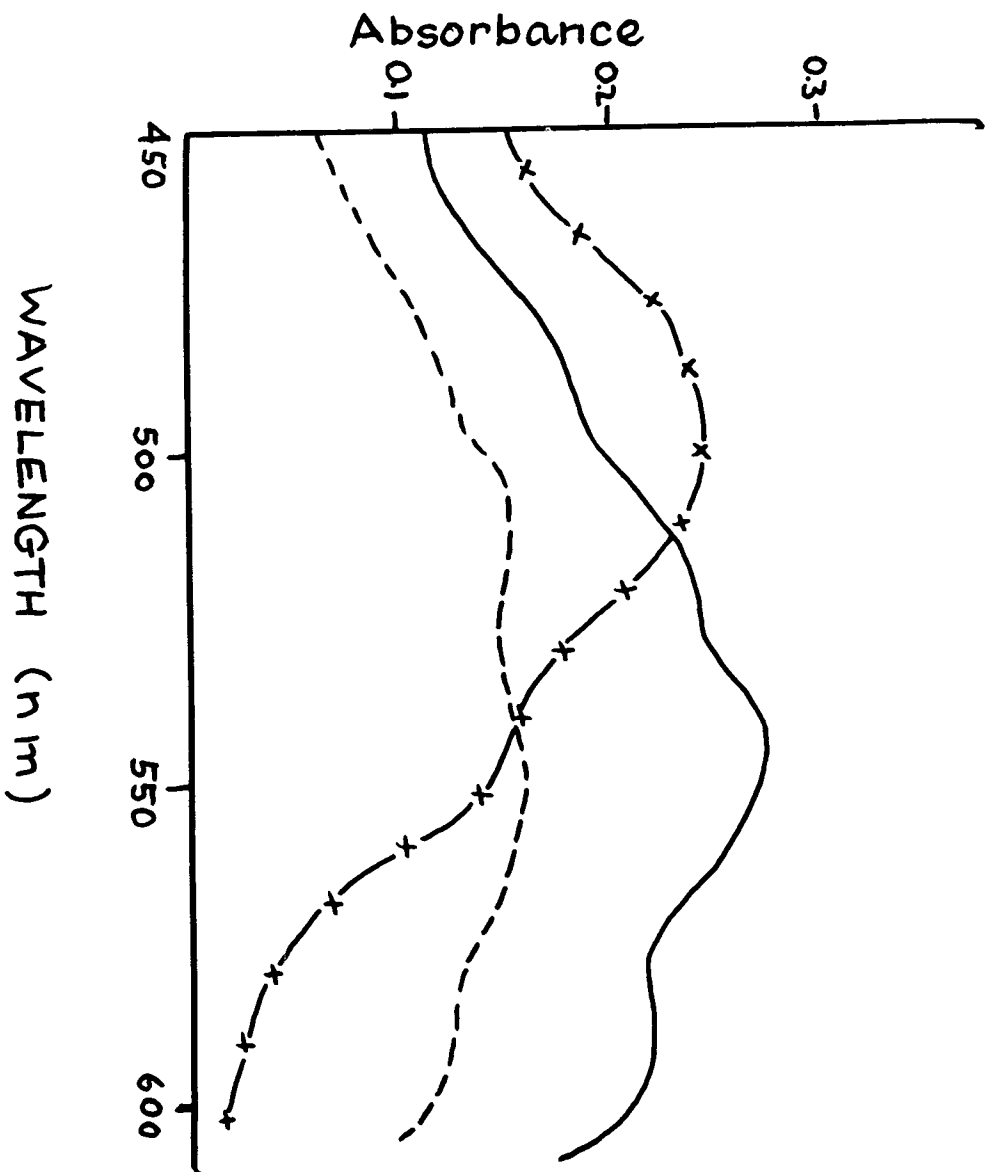
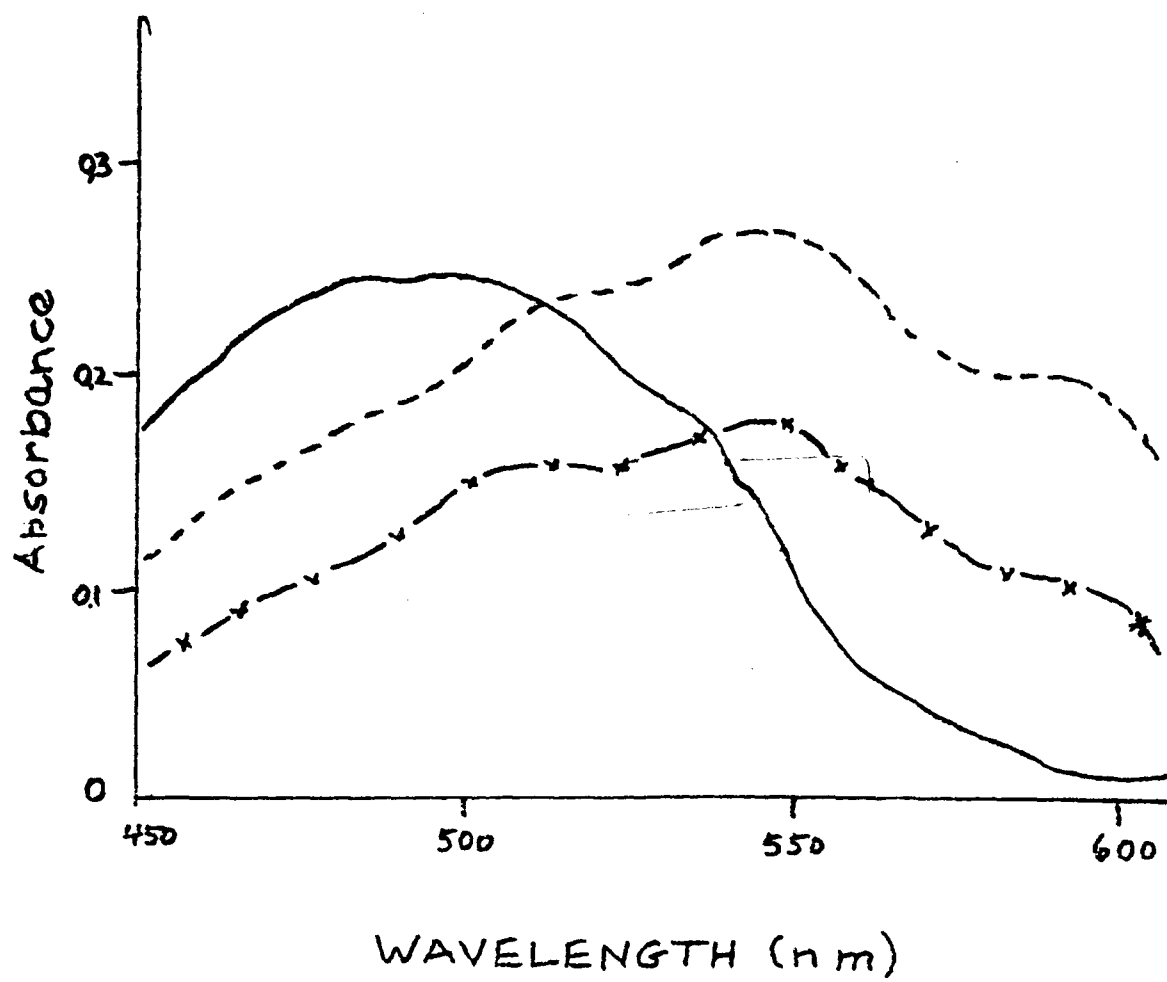


FIGURE 13.

Effect of concentration of Cu^{++} on the visible spectra of the daunomycin-denatured DNA complex. Concentration of daunomycin is constant at $2.5 \times 10^{-5}\text{M}$. Concentration of denatured DNA is constant at $1.5 \times 10^{-4}\text{M}$. ———, daunomycin + denatured DNA; -x-x-x, Dm-dDNA + Cu^{++} ($5 \times 10^{-5}\text{M}$); - - - -, Dm-dDNA + Cu^{++} ($1.0 \times 10^{-4}\text{M}$).



B. Effect of pH,

The effect of pH on complex formation was studied. When the pH was varied (figure 14) either above or below pH 5.6, the spectrum of nDNA-Dm-Cu⁺⁺ complex changed. Above pH 5.6 the spectra appeared to be those of the DNA-Dm complex. Below pH 5.6 the spectra indicated a shift to that of free daunomycin. At pH 5.6 the increased absorbance in the 560-580 nm region was probably indicative of Cu⁺⁺ binding to the complex. It thus appeared that complex formation for native DNA was favored by pH 5.6.

A pH effect was also apparent with denatured DNA as indicated in figure 15. The spectrum characteristic of the dDNA-Dm-Cu⁺⁺ complex was evident at pH 5.1. As the pH was altered above or below 5.1 the peaks indicative of the ternary complex gradually disappeared. At pH 3.6 the spectrum was that of free daunomycin and at pH 7.4 it resembled the spectrum of the dDNA-Dm complex.

C. Fluorescence studies.

The addition of Cu⁺⁺ to a solution of free daunomycin caused a reduction in the fluorescence intensity which was also pH dependent (table 1). This did not occur when the Cu⁺⁺/Dm ratio was 2:1. It was necessary to increase the ratio to 4:1 before the quenching was evident. As can be seen in table 1, the quenching was at a maximum between pH 6.5-6.8. Below pH 6.0, Cu⁺⁺ appeared to be without effect.

FIGURE 14.

Effect of pH on the daunomycin ($2.5 \times 10^{-5} \text{M}$)-
native DNA ($1.0 \times 10^{-4} \text{M}$)- Cu^{++} ($1.0 \times 10^{-4} \text{M}$)
complex. -x-x-x, pH 2.6; - - -, pH 3.7;
xxxx, pH 5.6; ······, pH 6.9; ———, pH 7.8.

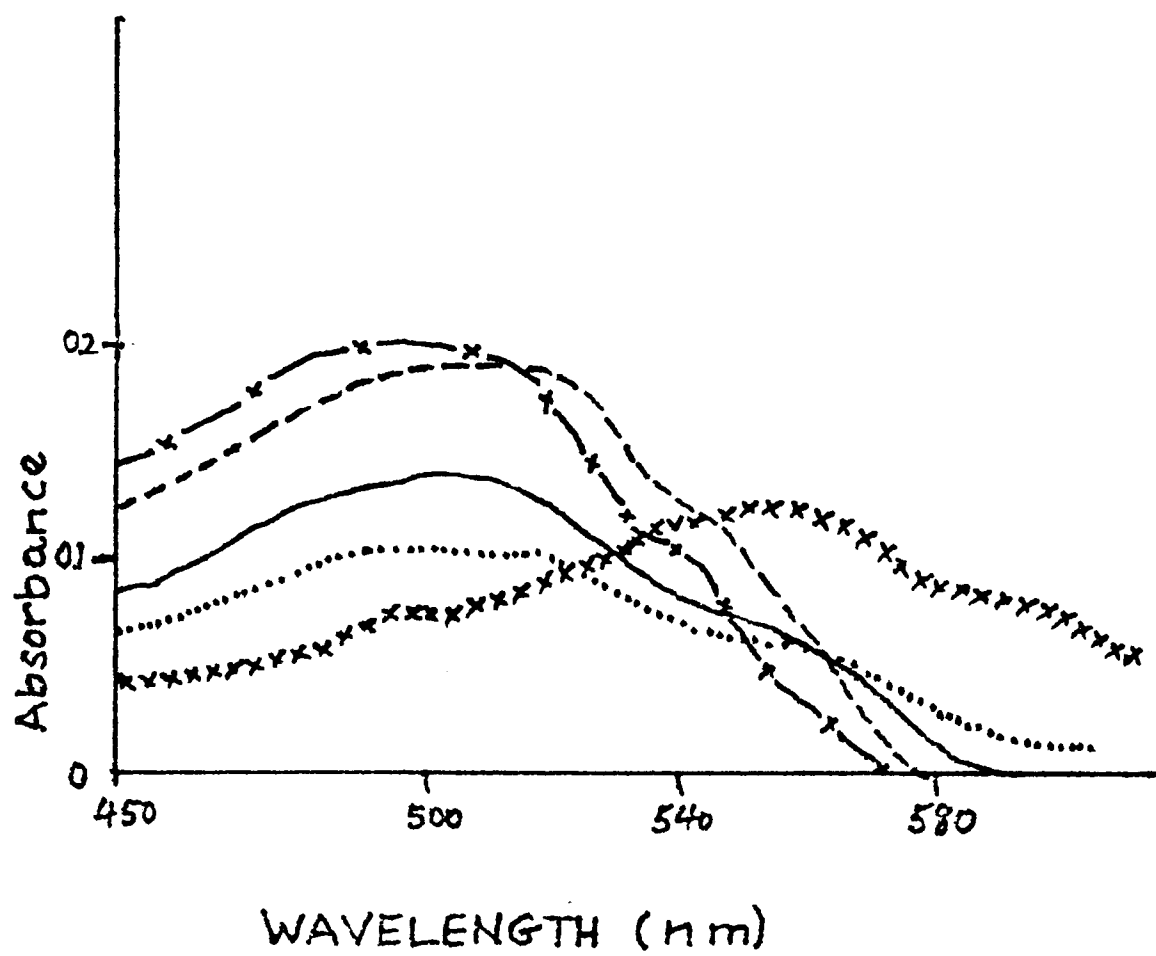
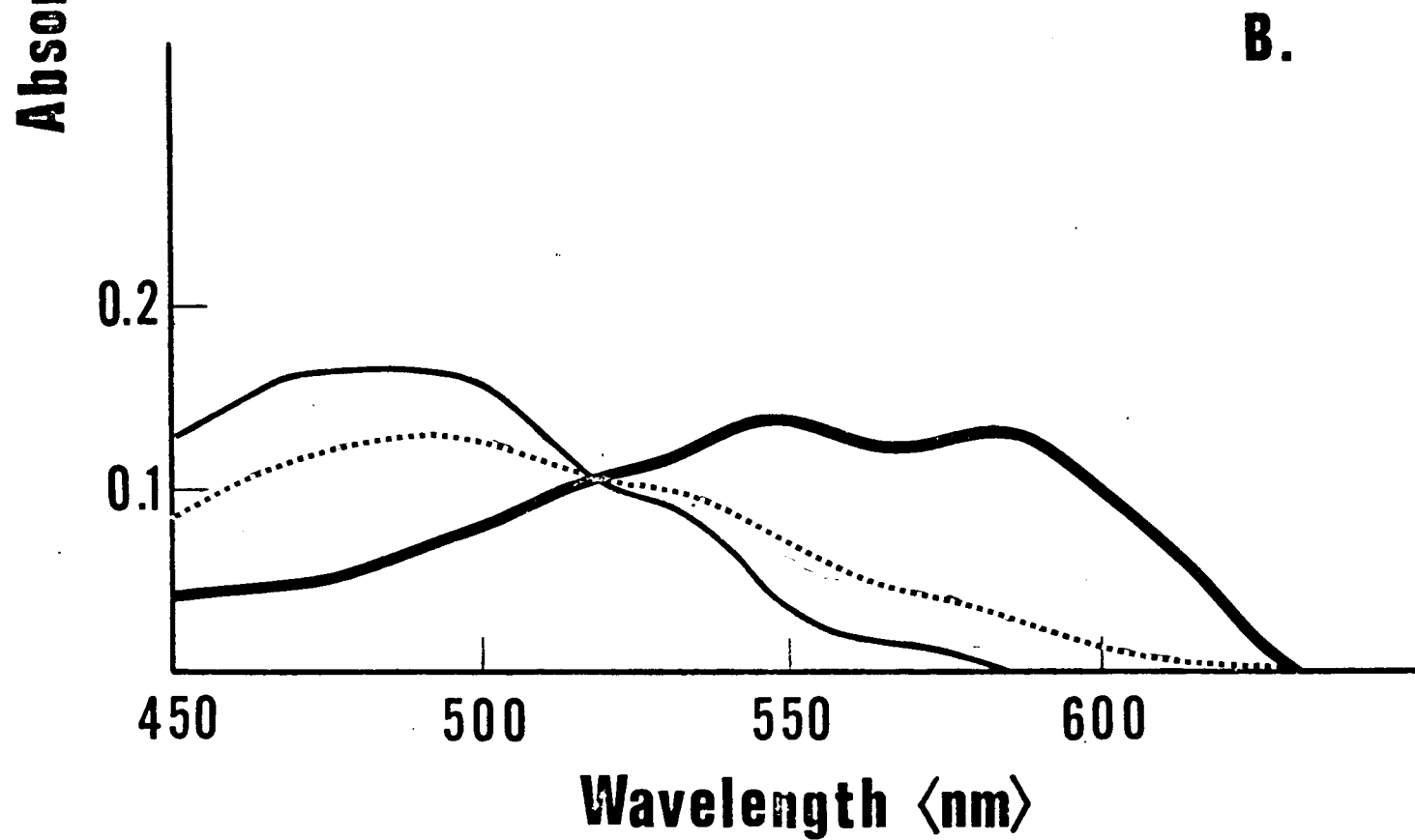
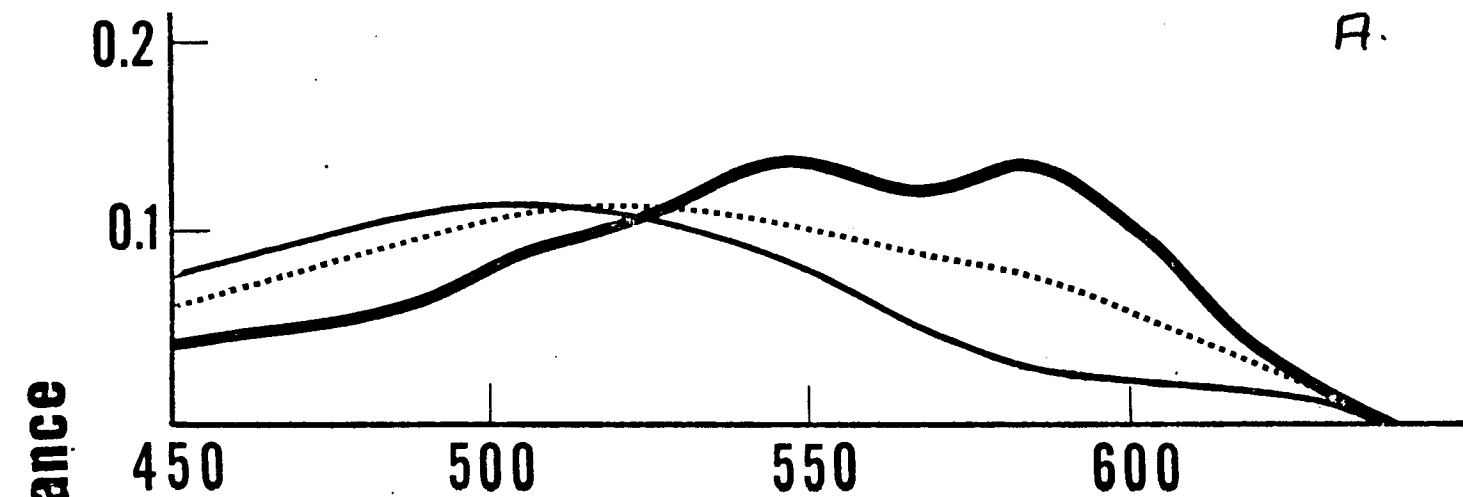


FIGURE 15.

Effect of pH on the daunomycin ($2.5 \times 10^{-5} \text{M}$)-denatured DNA ($1.0 \times 10^{-4} \text{M}$)- Cu^{++} ($1.0 \times 10^{-4} \text{M}$) complex. A. **————**, pH 5.1; **·····**, pH 6.4; **———**, pH 7.4. B. **————**, pH 5.1; **·····**, pH 4.5; **———**, pH 3.6.



Cu^{++} had a similar effect on the DNA-daunomycin complexes. The maximum quenching occurred between pH 6.5-6.8, however, considerable quenching was apparent down to pH 2.3 (table 1). Both DNA and Cu^{++} contributed to the decrease in fluorescence of daunomycin, since the fluorescence intensity of the ternary complex was significantly lower than that of either Cu^{++} -Dm or DNA-Dm complexes (table 1).

III. Effect of Mg^{++} on the Daunomycin-DNA Complex.

A. Effect of pH.

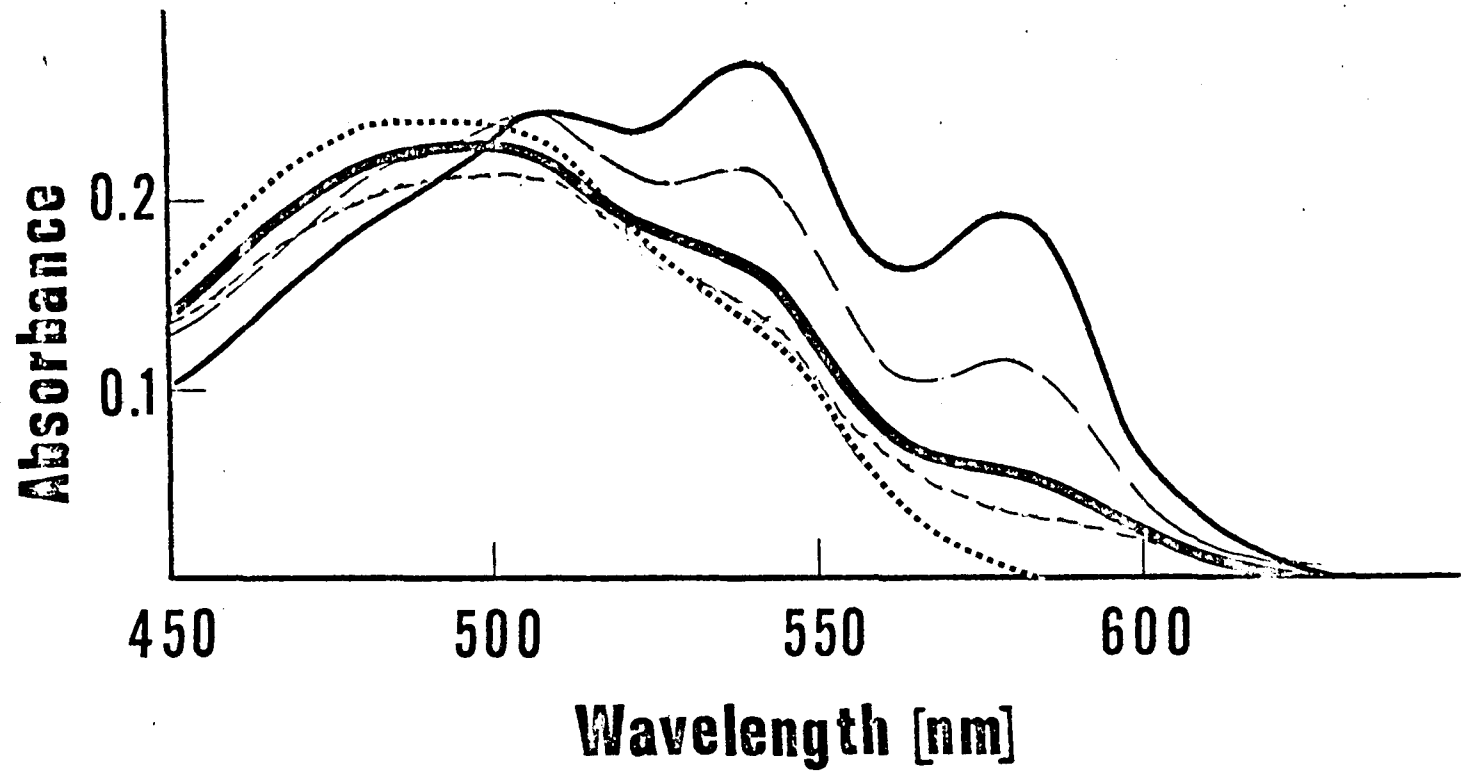
The addition of Mg^{++} to a DNA-daunomycin complex resulted in changes in the visible spectra which were pH dependent (figure 16). The concentration of Mg^{++} necessary to elicit these changes was 0.1M. 0.01M Mg^{++} was not sufficient to induce these shifts.

The changes in the spectra were gradual. At pH 6.1 the spectrum was that of DNA-daunomycin which indicated that Mg^{++} was not binding at this pH. As the pH was increased a gradual change in the spectra occurred until, at pH 7.8, the spectrum was very similar to that observed for the dDNA-Dm- Cu^{++} complex at pH 5.1 (figure 15). It consisted of intense peaks at 540 nm and 582 nm with a shoulder at 505 nm.

The spectra in figure 16 were obtained with native DNA but when denatured DNA was used the same spectra were observed. However, it should be noted that these spectral changes were evident in the absence of DNA. It seems,

FIGURE 16.

Effect of pH on the daunomycin ($2.5 \times 10^{-5}M$)-
DNA ($2 \times 10^{-4}M$)- Mg^{++} (0.1M) complex. ······,
pH 5.75; ----, pH 6.1; **————**, pH 6.9; — — —,
pH 7.4; —————, pH 7.8



therefore, that the spectral effects might be due to the formation of an Mg^{++} -Dm complex.

At pH 2.4, the addition of Mg^{++} to the daunomycin-DNA complex gave rise to spectra in both the visible and UV which closely resembled free daunomycin (figures 17 and 18). The visible spectrum showed a broad peak with a maximum at 475 nm. In this case there was significant turbidity which could be corrected (by subtracting the absorbance at 650 nm from the absorbance values at all other wavelengths) but, in spite of this, the spectrum can be identified as that of free daunomycin (figure 17).

The UV spectra (figure 18) support the above conclusion. Free daunomycin and Mg^{++} -daunomycin gave identical spectra at pH 2.4. The addition of Mg^{++} to the daunomycin-DNA complex resulted in the reappearance of the 290 nm peak and the spectrum resembling free daunomycin. In view of the fact that at this pH the daunomycin-DNA complex alone remained intact, it seemed that Mg^{++} induced the splitting of the daunomycin-DNA complex.

B. Fluorescence studies.

Mg^{++} also affected the fluorescence emission of daunomycin. This effect was concentration dependent as can be seen in figure 19. As the concentration of Mg^{++} was increased, the quenching increased. Since a significant effect occurred at a concentration of 0.1M, this was the concentration of Mg^{++} employed in the remainder of the

FIGURE 17.

Addition of Mg^{++} to the daunomycin-DNA complex
at pH 2.4. **————**, daunomycin ($2.5 \times 10^{-5} M$);
————, plus DNA ($1.0 \times 10^{-4} M$) and Mg^{++} (0.1M).

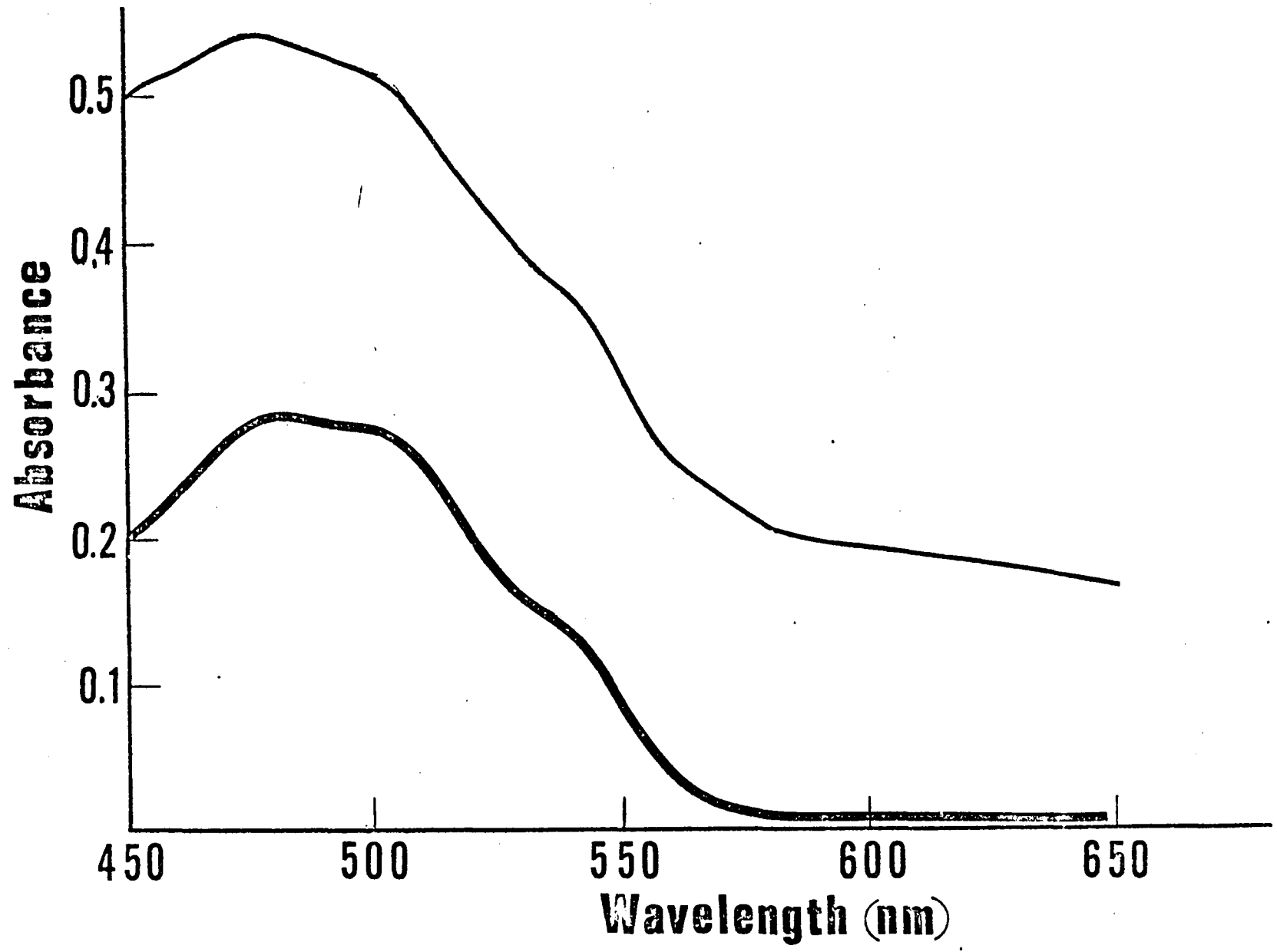


FIGURE 18.

Addition of Mg^{++} (0.1M) to daunomycin or daunomycin-DNA complex at pH 2.4. -----, daunomycin ($2.5 \times 10^{-5}M$); **—————**, daunomycin plus Mg^{++} ; — — —, daunomycin plus DNA ($1.0 \times 10^{-4}M$); —————, daunomycin plus DNA plus Mg^{++} .

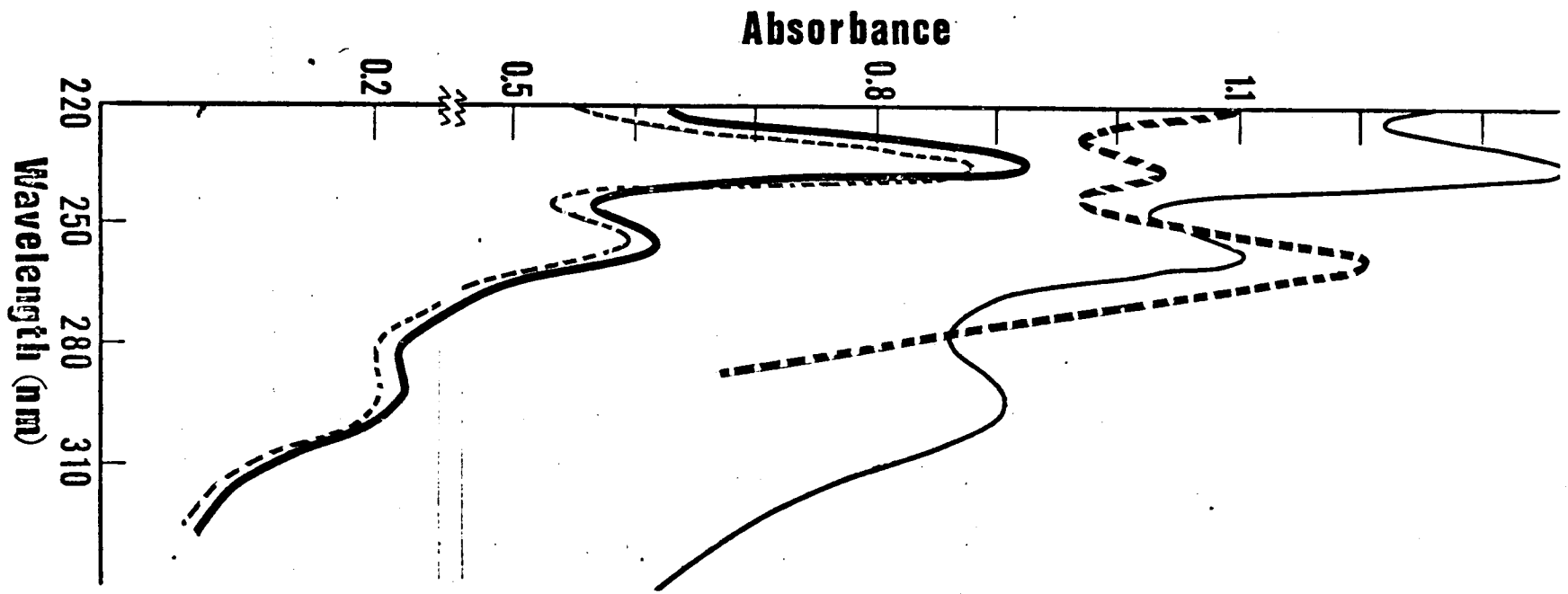
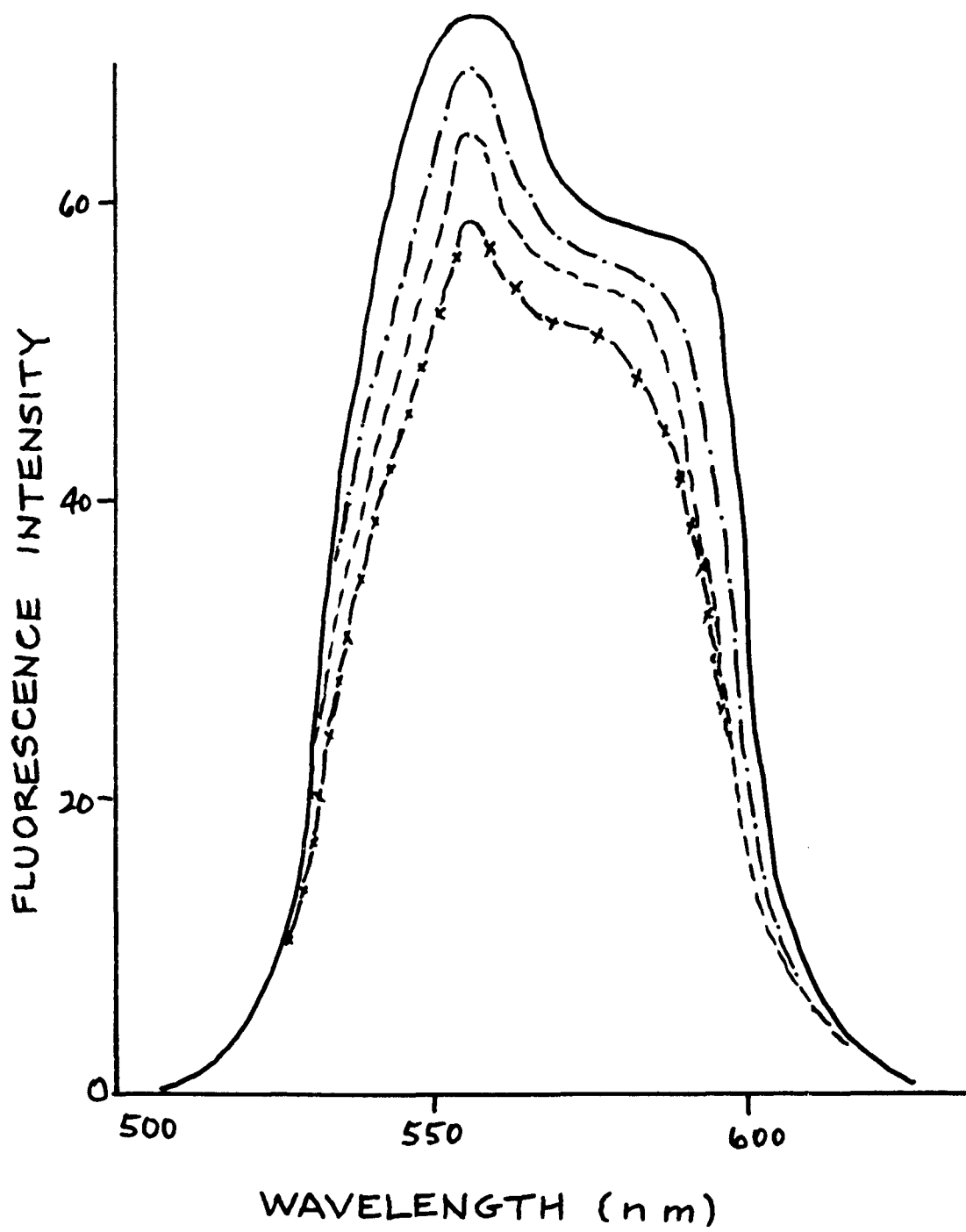


FIGURE 19.

Effect of the addition of Mg^{++} on the fluorescence emission spectrum of daunomycin. ———, daunomycin ($2.5 \times 10^{-5} M$); -·-·-, Dm + Mg^{++} ($1.0 \times 10^{-2} M$); ---, Dm + Mg^{++} ($5 \times 10^{-2} M$); -x-x-x, Dm + Mg^{++} (0.1M).



fluorescence studies involving Mg^{++} ,

Figure 20 illustrates that Mg^{++} induced alterations in the daunomycin emission spectrum. This effect was, once again, pH dependent. As with the visible studies, the maximum effect occurred at pH 7.8. The shoulder at 580 nm became a peak and the peak at 555 nm became a shoulder. This was a gradual change. At pH 7.5 there were two peaks of equal intensity at 555 nm and 580 nm. The Mg^{++} effect decreased sharply as the pH was lowered and completely disappeared below pH 6.0 (table 1).

The addition of Mg^{++} ($10^{-1}M$) also caused changes in the fluorescence exhibited by the daunomycin-DNA complex. In the presence of Mg^{++} the maximum quenching effect with DNA which occurred between pH 6.5-6.7 disappeared (table 1). As the pH was lowered, the quenching continually decreased until, at pH 2, the fluorescence intensities in the presence and absence of Mg^{++} were equal. It should be noted that the effects were comparable with both native and denatured DNA.

IV. Binding of Daunomycin to Nucleic Acid Units.

A. Absorbance studies.

The binding of daunomycin to nucleic acid bases, nucleosides, nucleoside monophosphates, and nucleoside triphosphates was also studied. The compounds tested are listed in table 2.

The UV and visible spectra were monitored for any

FIGURE 20.

Effect of pH on the fluorescence emission spectrum of the daunomycin- Mg^{++} complex. ———, daunomycin ($2.5 \times 10^{-5}M$); pH 7.9; ----, daunomycin + Mg^{++} (0.1M), pH 6.8; -·-·-, Dm + Mg^{++} (0.1M), pH 7.5; — — —, Dm + Mg^{++} (0.1M), pH 8.0.

FLUORESCENCE INTENSITY

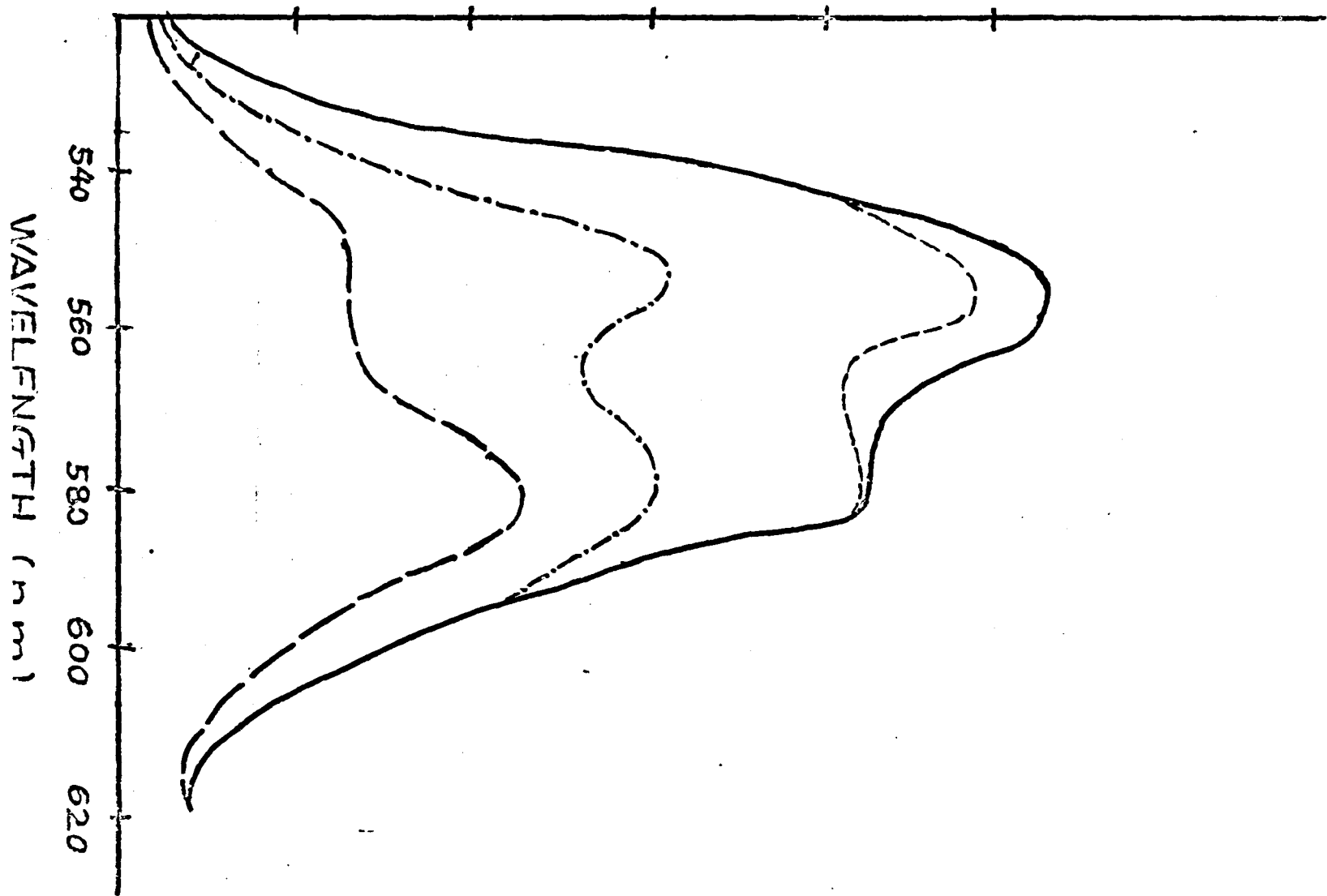


TABLE 2COMPOUNDS TESTED FOR BINDING TO DAUNOMYCIN

BASES	NUCLEOSIDES	NUCLEOSIDE MONOPHOSPHATES	NUCLEOSIDE TRIPHOSPHATES
Adenine	deoxy Adenosine	dAMP	dATP
Cytosine	deoxy Cytidine	dCMP	dGTP
Guanine	deoxy Guanosine	dGMP	UTP
Thymine	Thymidine	TMP	
Uracil	deoxy Uridine	dUMP	
	ribo Uridine	rUMP	

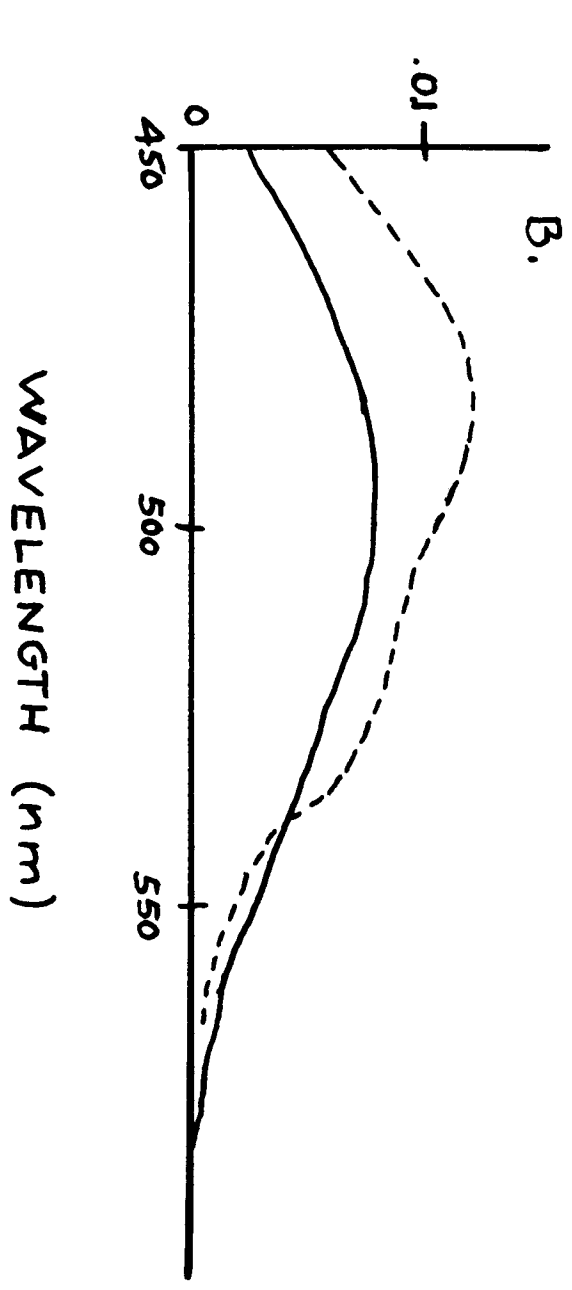
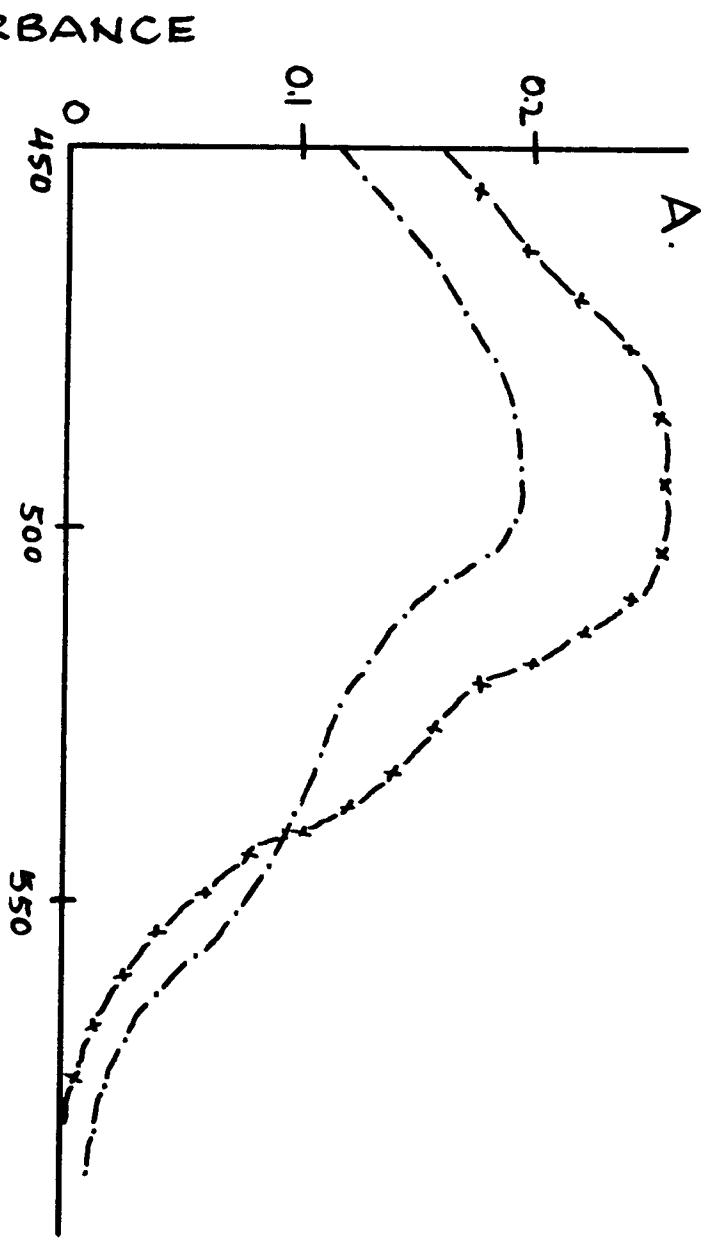
changes which addition of these compounds might cause. As was indicated previously (section I,A, results), changes in UV spectra are difficult to interpret because both daunomycin and nucleic acid absorb in this region. In an effort to simplify the analysis a split cell was used. This is an absorption cell which has a quartz partition in the center. Daunomycin is added to one side of the partition and the particular nucleic acid unit is added to the other side. A spectrum is recorded, which is simply the additive spectra of both components. The cell is then inverted several times to allow mixing and a second spectrum is recorded. In the absence of complex formation the spectra before and after mixing should be identical. If, however, there is an interaction the two spectra will differ.

None of the compounds listed in table 2 induced spectral changes in either the UV or visible regions and it was thus concluded that no interaction occurred between these compounds and daunomycin. For these studies the concentration of daunomycin was $2.5 \times 10^{-5} \text{M}$ and the concentrations of the nucleic acid components were $5 \times 10^{-5} \text{M}$.

The interaction of polynucleotides with daunomycin was also tested. The polyhomoribonucleotides poly A, poly C, poly G, poly I, and poly U were the ones tested. In the visible region all these polynucleotides induced spectral changes which were very similar to those caused by DNA. Figure 21 shows the effect of poly G on the daunomycin spectrum. The results with the other polynucleotides

FIGURE 21.

Effect of poly G on the visible spectrum of daunomycin. A. -x-x-x, daunomycin; -·-·-, daunomycin + poly G; B. - - - -, daunomycin + poly G before mixing in a split cell; ———, daunomycin + poly G after mixing in a split cell. Daunomycin concentration was $2.5 \times 10^{-5} \text{M}$ and that of poly G was $5 \times 10^{-5} \text{M}$.



were identical. As is evident, there was a reduction in absorbance at 475 nm with a shift in the peak to 505 nm, just as was found with the DNA-daunomycin interaction.

B. Fluorescence studies.

The effect of polynucleotides on the fluorescence of daunomycin was also examined. Again, the results were similar to those found with DNA, with a decrease in fluorescence intensity occurring when polynucleotide was added (figure 22). It is of interest to note that there was greater quenching of fluorescence when poly A, poly G, or poly I was added. The effect was less pronounced in the presence of poly C or poly U. The fluorescence intensities of the complexes relative to that of free daunomycin are listed in table 3.

V. Spectrophotometric Titrations.

Spectrophotometric titration studies were carried out in order to determine the binding data for the DNA or polynucleotide-daunomycin complex. These were also determined as a function of ionic strength.

A. Calf thymus DNA

Figure 23 shows the binding isotherms for the binding of native calf thymus DNA at three ionic strengths (0.005, 0.05, 0.5) to daunomycin. The shape of the curves clearly indicated the existence of two binding modes, especially the one at $\mu = 0.005$. There were two portions of the curve, one at low c and the other at high c , at which r increased very rapidly. These were separated by a

FIGURE 22.

Effect of polynucleotides on the fluorescence emission spectrum of daunomycin. x-x-x-, daunomycin ($2.5 \times 10^{-5} \text{M}$); xxxx, Dm + poly C; -·-·-·-, Dm + poly U; ······, Dm + poly A; -·-·-·-, Dm + poly I; ———, Dm + poly G. The polynucleotide concentrations were $5 \times 10^{-5} \text{M}$.

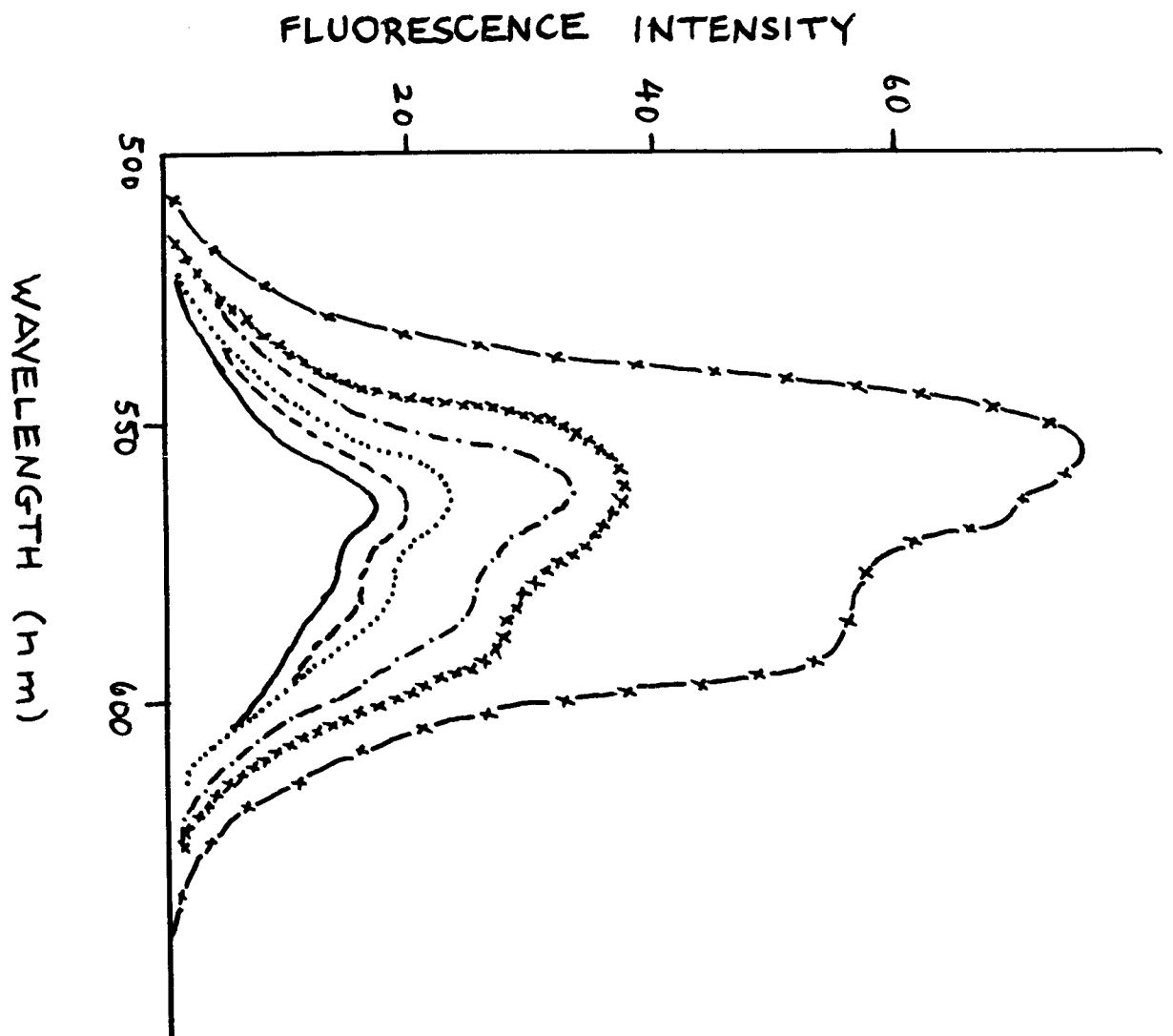


TABLE 3FLUORESCENCE INTENSITY OF POLYNUCLEOTIDE-DAUNOMYCIN COMPLEXES

POLYNUCLEOTIDE ADDED	*F.I. (at 555 nm)
poly A	31.1
poly C	48.3
poly G	27.2
poly I	28.5
poly U	42.7

[polynucleotide] = $5 \times 10^{-5}M$

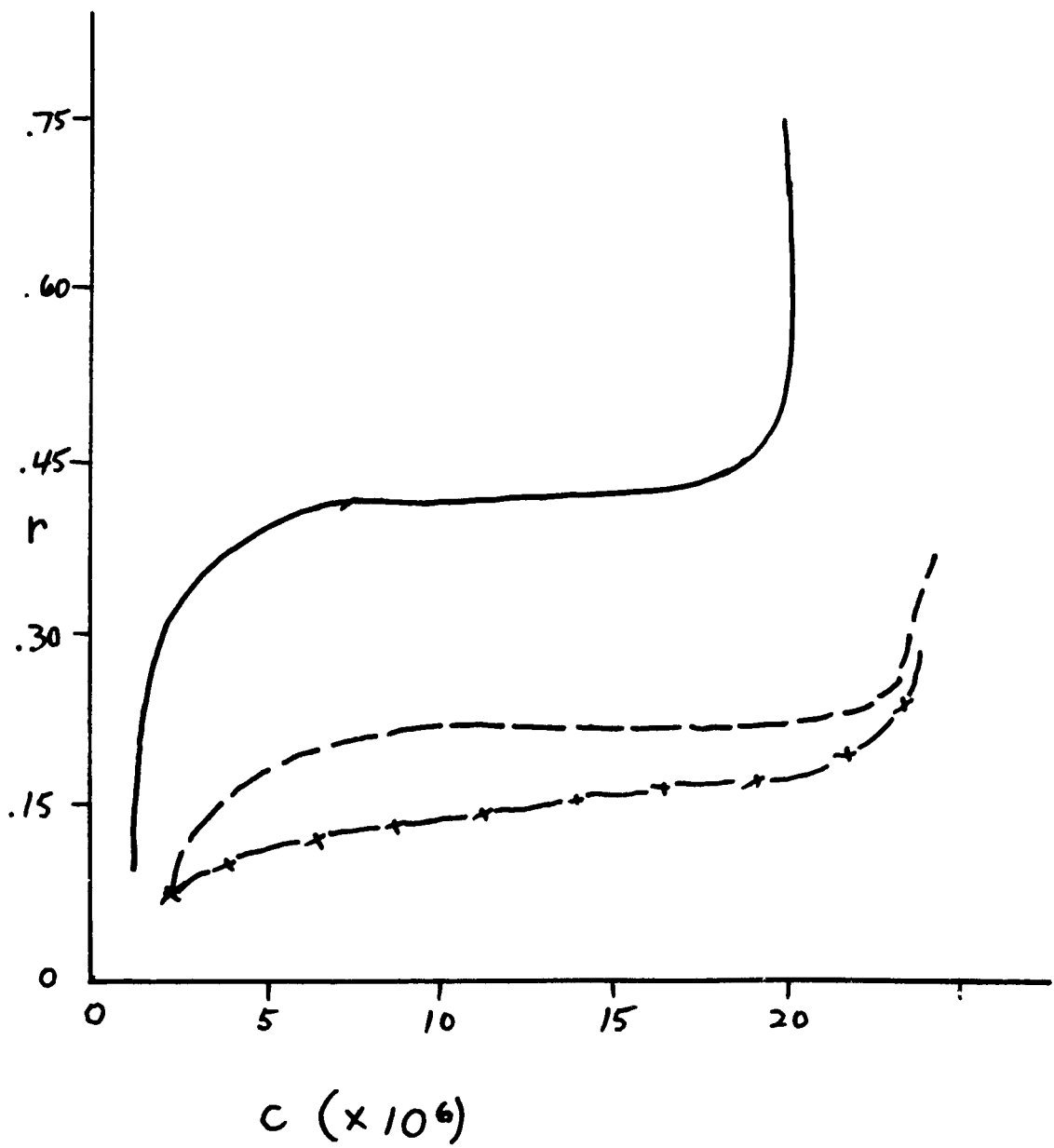
[daunomycin] = $2.5 \times 10^{-5}M$

*Relative to that of free daunomycin, which is set equal to 100.

FIGURE 23.

Binding isotherms for the calf thymus native
DNA-daunomycin complex. Effect of varying ionic
strength.

—————, $\mu = 0.005$; - - - - - , $\mu = 0.05$; -x-x-x, $\mu = 0.5$.



plateau region which was indicative of two modes of binding. The r value in the plateau region yielded an estimate of the maximum number of strong binding sites. As the ionic strength increased, r at the plateau decreased.

The binding plots for heat-denatured calf thymus DNA are shown in figure 24. These curves also showed two distinct binding regions but the plateau, or transition between the two modes, was more gradual. As with native DNA, when the ionic strength was increased the plateau shifted towards a lower r value.

Accurate binding constants are difficult to calculate from the binding isotherms alone and, therefore, Scatchard plots were constructed in order to obtain association constants for the interaction. Figure 25 is a Scatchard plot for native calf thymus DNA at $\mu = 0.005$. The plot is convex to the X-axis which, as noted previously (see Methods section) is expected for systems with heterogeneous binding sites, i.e. more than one binding mode. The values for k , the intrinsic association constant, and n , the number of binding sites/phosphate, for native and denatured calf thymus DNA, at three ionic strengths, are given in table 4. The association constant for native DNA is three-fold greater than that for denatured DNA at $\mu = 0.005$. An increase in ionic strength resulted in a decreased k for native DNA while it had virtually no effect on k for denatured DNA.

FIGURE 24.

Binding isotherms for the denatured calf thymus DNA-daunomycin complex. Effect of varying ionic strength.

——, $\mu = 0.005$; - - - - -, $\mu = 0.05$; -x-x-x, $\mu = 0.5$.

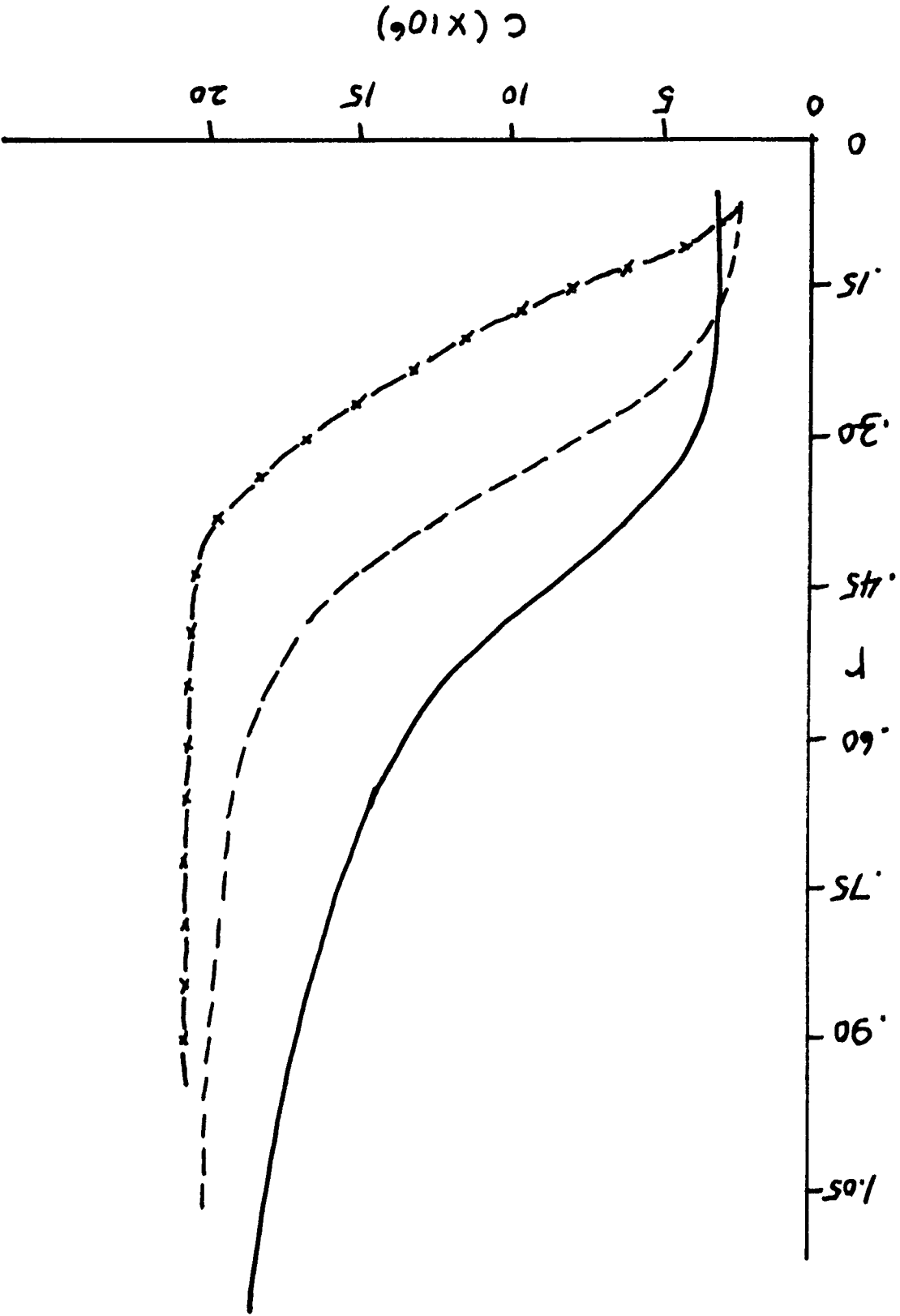
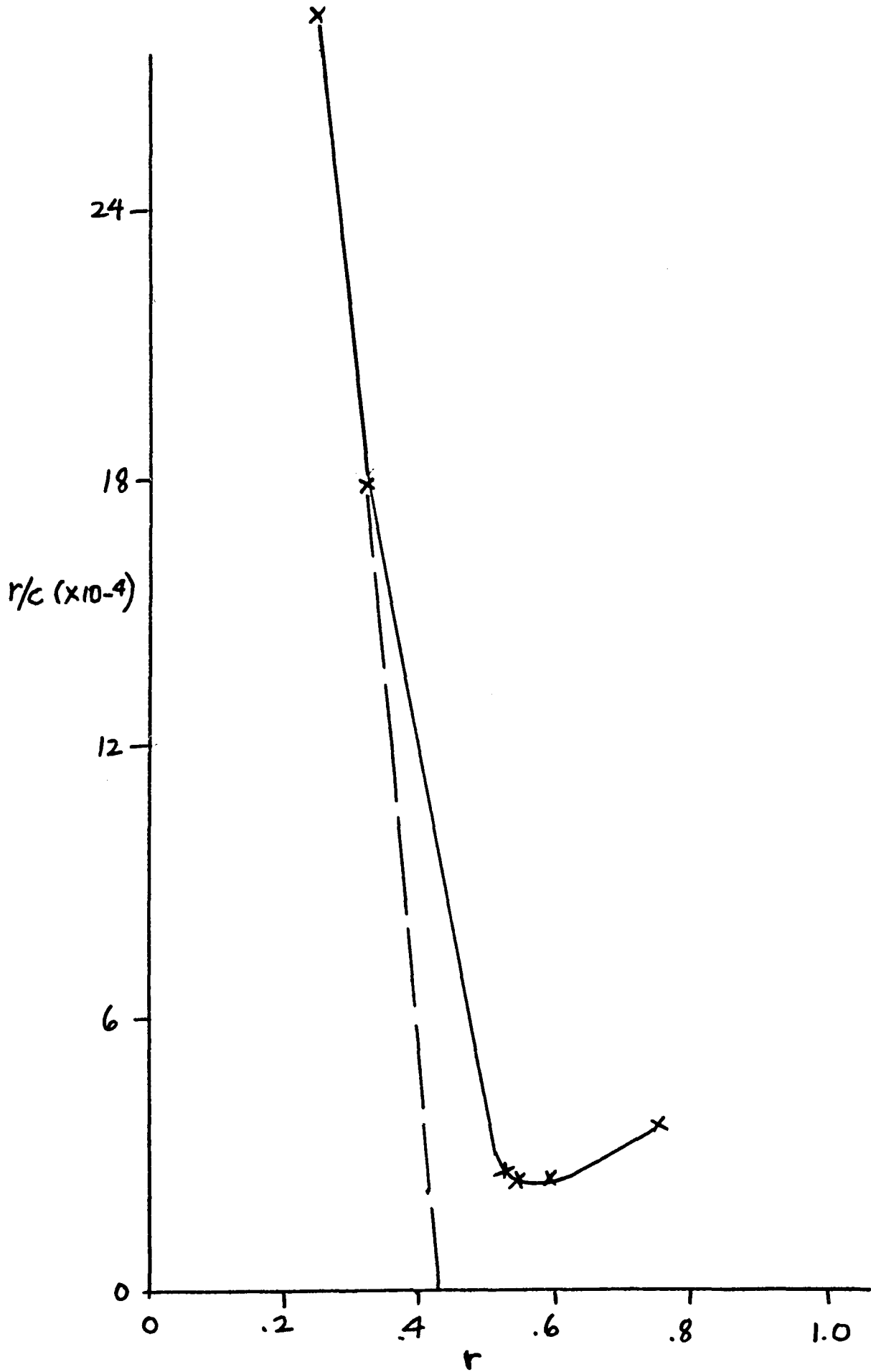


FIGURE 25.

Scatchard plot for the calf thymus native DNA-daunomycin complex at $\mu = 0.005$. Dashed line is extrapolation of the linear portion of the curve in order to obtain type I binding data as described in Methods.



However, the number of binding sites, n , was greater for denatured DNA except at $\mu = 0,5$. Increasing the ionic strength caused a decrease in n for both types of DNA. It should be noted that the convex shape for the Scatchard plots were obtained with both native and denatured DNA at all ionic strengths tested.

B. Ribo-homopolynucleotides.

Binding isotherms for the homopolynucleotides with daunomycin at various ionic strengths are shown in Figure 26. At $\mu = 0.005$, the curves for all the polynucleotides lacked the second slope at high c and this differed markedly from DNA. In addition, as ionic strength was increased, binding to poly U and poly C disappeared or became more difficult to detect. The change in the binding isotherms for poly A and poly G in going from $\mu = 0.005$ to 0.5 indicated the drastic effect of ionic strength on the polynucleotide-daunomycin interaction.

This was also evident from data in table 4. At all ionic strengths the values for the association constants for all polynucleotides were lower than those for DNA. There did not appear to be significant differences amongst the association constants for the polynucleotides nor did the values vary with changes of ionic strength. There were many more binding sites available with the polynucleotides than with DNA at $\mu = 0.005$. Increased ionic strength resulted in a marked reduction in n . Poly I showed somewhat different behavior in that its k increased as the ionic

FIGURE 26.

Binding isotherms for various polynucleotide-daunomycin complexes.

·····, poly A, o-o-o-, poly A, $\mu =$
0.5; ———, poly G; xxxx, poly G, $\mu = 0.5$; - - - - ,
poly C; x-x-x, poly I; - - - - - , poly U. Unless
otherwise indicated, the ionic strength was 0.005.

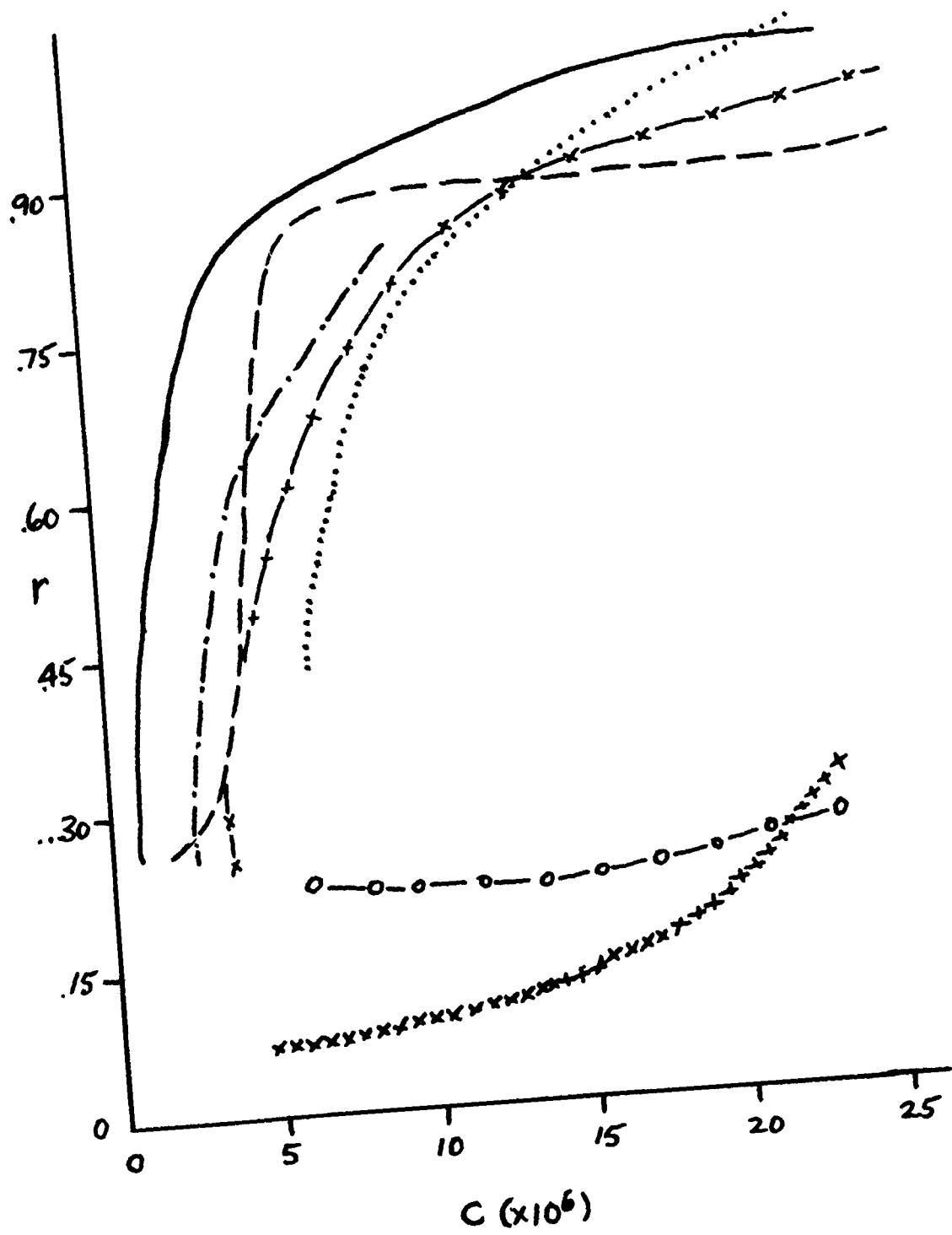


TABLE 4

BINDING DATA FOR DAUNOMYCIN COMPLEXES

IONIC STRENGTH (μ)	0.005		0.05		0.5	
	$k \times 10^5$	n	$k \times 10^5$	n	$k \times 10^5$	n
Calf Thymus DNA, native	15.5	.43	1.85	.30	3.5	.24
Calf Thymus DNA, denatured	5.8	.51	5.8	.35	4.2	.19
poly A	2.7	.88	2.9	.25	3.5	.25
poly G	4.8	1.0	3.2	.15	1.8	.13
poly C	2.1	1.1	3.4	.11		
poly U	5.5	.95				
poly I	1.9	1.1	10.1	.10	no binding	

k = intrinsic association constant

n = no. of binding sites/phosphate

Based on spectrophotometric titration studies.

strength increased. At $\mu = 0.5$, however, binding was completely abolished.

A number of points should be noted in regard to table 4. The Scatchard plots of the polynucleotide-daunomycin interactions were convex to the x-axis as were those for DNA. A distinction should be made between those spaces left blank on table 4 and the entry of "no binding" for poly I. Poly U at $\mu = 0.05$ and 0.5 and poly C at $\mu = 0.5$ caused decreases in the absorbance values for daunomycin at 475 nm . On this basis it could be stated that some binding did occur. It was, however, not possible to construct plots from which reliable binding data could be evaluated. On the other hand, the addition of poly I did not result in a decrease in absorbance at 475 nm and it was assumed, therefore, that no binding to daunomycin occurred at $\mu = 0.5$.

VI. Spectrofluorimetric Titrations.

A. Deoxy-homopolynucleotides

Binding equilibria for the polynucleotide-daunomycin interaction were also studied by means of fluorescence. This was necessary for studies with the homodeoxypolynucleotides and polynucleotide duplexes because these compounds were available only in very small amounts. Since changes in fluorescence could be detected even at very low concentrations of daunomycin this technique was employed.

The polydeoxynucleotides, poly dA, poly dG, and poly dT

were studied for their interaction with daunomycin and those binding curves are shown in figure 27. Poly dT was the only one which exhibited two clear slopes with a plateau between them, thus indicating two phases in its binding to daunomycin. Although it was less clear with poly dG, a plateau region was apparent. The Scatchard plots for these compounds were convex to the x-axis which confirmed that there was heterogeneous binding. At higher ionic strength, it was not possible to obtain sufficient data for poly dA and poly dT and, therefore, no binding curves were plotted. However, there was some quenching of daunomycin fluorescence at 555 nm. Therefore, it cannot be stated that no binding occurred at these ionic strengths.

Binding data for the polydeoxynucleotides are listed in table 5. The association constants for poly dA and poly dT were similar to each other and at $\mu = 0.005$ were $2\frac{1}{2}$ to 3-fold greater than those for poly dG.

B. Polynucleotide duplexes.

The binding of the following polynucleotide duplexes to daunomycin was also studied by spectrofluorimetric titration: 1) poly rA·poly rU, a duplex consisting of one strand poly A and the other poly U; 2) poly dA·poly dT, a duplex of one strand poly dA and one strand poly dT; 3) poly (dA-dT)·poly (dA-dT), a double stranded polymer of which each strand is an alternating copolymer of dA

FIGURE 27.

Binding isotherms for various polynucleotide-
daunomycin complexes.

————, poly dT; -----, poly dA; -----, poly dG.

Ionic strength was 0.005.

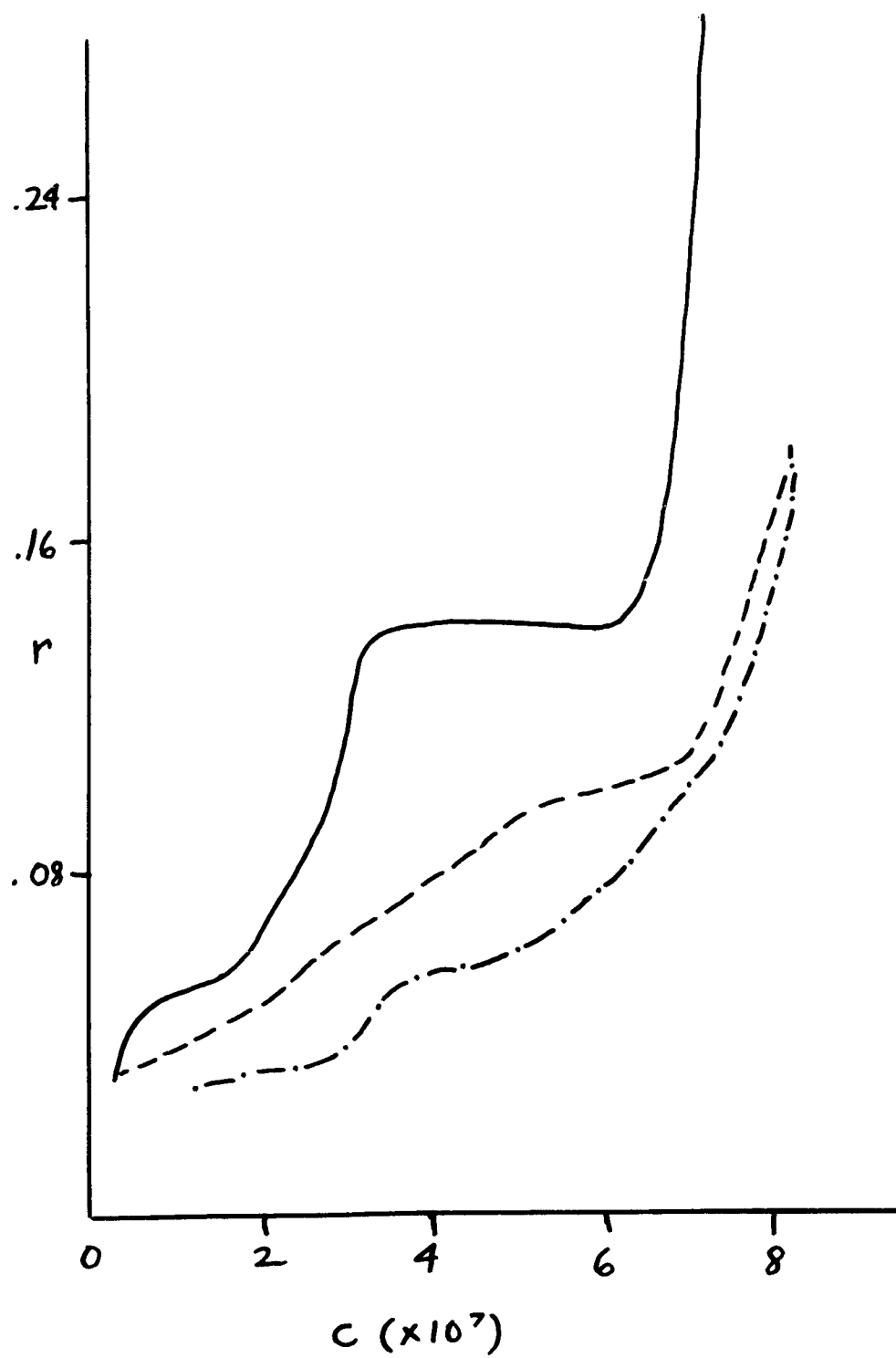


TABLE 5

BINDING DATA FOR DAUNOMYCIN COMPLEXES

IONIC STRENGTH (μ)	0.005		0.05		0.5	
	$k \times 10^6$	n	$k \times 10^6$	n	$k \times 10^6$	n
Cl. perfringens DNA	9.1	.24	6.9	.099	3.7	.074
poly dA	38.0	.058				
poly dG	12.6	.048	22.2	.034	13.6	.025
poly dT	33.0	.072				
poly rA·poly rU	15.5	.043	11.8	.034		
poly dA·poly dT	6.5	.053	13.9	.035	7.9	.025
poly rA·poly dT	4.8	.094	6.8	.056		
poly (dA-dT)· poly (dA-dT)			13.7	.155	3.3	.100
poly dG·poly dC	29.2	.061	12.5	.053	11.6	.050

k = intrinsic association constant

n = no. of binding sites/phosphate

Based on spectrofluorimetric titration studies.

and dT; 4) poly rA·poly dT, a hybrid duplex with one strand of poly A and the other of poly dT; 5) poly dG·poly dC, a double stranded polymer consisting of one strand poly dG and the other poly dC. Both poly (dA-dT)·poly (dA-dT) and poly dG·poly dC can be synthesized by DNA polymerase and both have secondary structures similar to that of DNA.

Binding isotherms for these compounds at $\mu = 0.05$ are shown in figure 28. The two compounds with the most biphasic character were poly (dA-dT)·poly (dA-dT) and poly dG·poly dC. Poly dA·poly dT and poly rA·poly dT exhibited plots similar to one another. Poly rA·poly rU showed curvature only at higher daunomycin concentrations.

Figure 29 shows the binding curves for poly dG·poly dC as a function of ionic strength. The different binding regions were clearly separated by a plateau and these plots were similar to those found with calf thymus DNA. The plateaus were smooth transitions between the sloped regions as occurred with denatured DNA rather than the flat plateaus found with native calf thymus DNA.

The binding data for the polynucleotide duplexes are listed in table 5. At all ionic strengths, poly dG·poly dC had the highest association constant. At $\mu = 0.05$, poly dA·poly dT and poly (dA-dT)·poly (dA-dT) had k values comparable to those for poly dG·poly dC. As with poly dG, increasing the ionic strength did not have an appreciable effect on the k or n values for poly dG·poly dC especially at $\mu > 0.05$.

FIGURE 28.

Binding isotherms for various polynucleotide duplex-daunomycin complexes.

————, poly (dA-dT)·poly (dA-dT); -----, poly dG·poly dC; x-x-x, poly rA·poly dT; -----, poly dA·poly dT; o-o-o, poly rA·poly rU.

Ionic strength was 0.05.

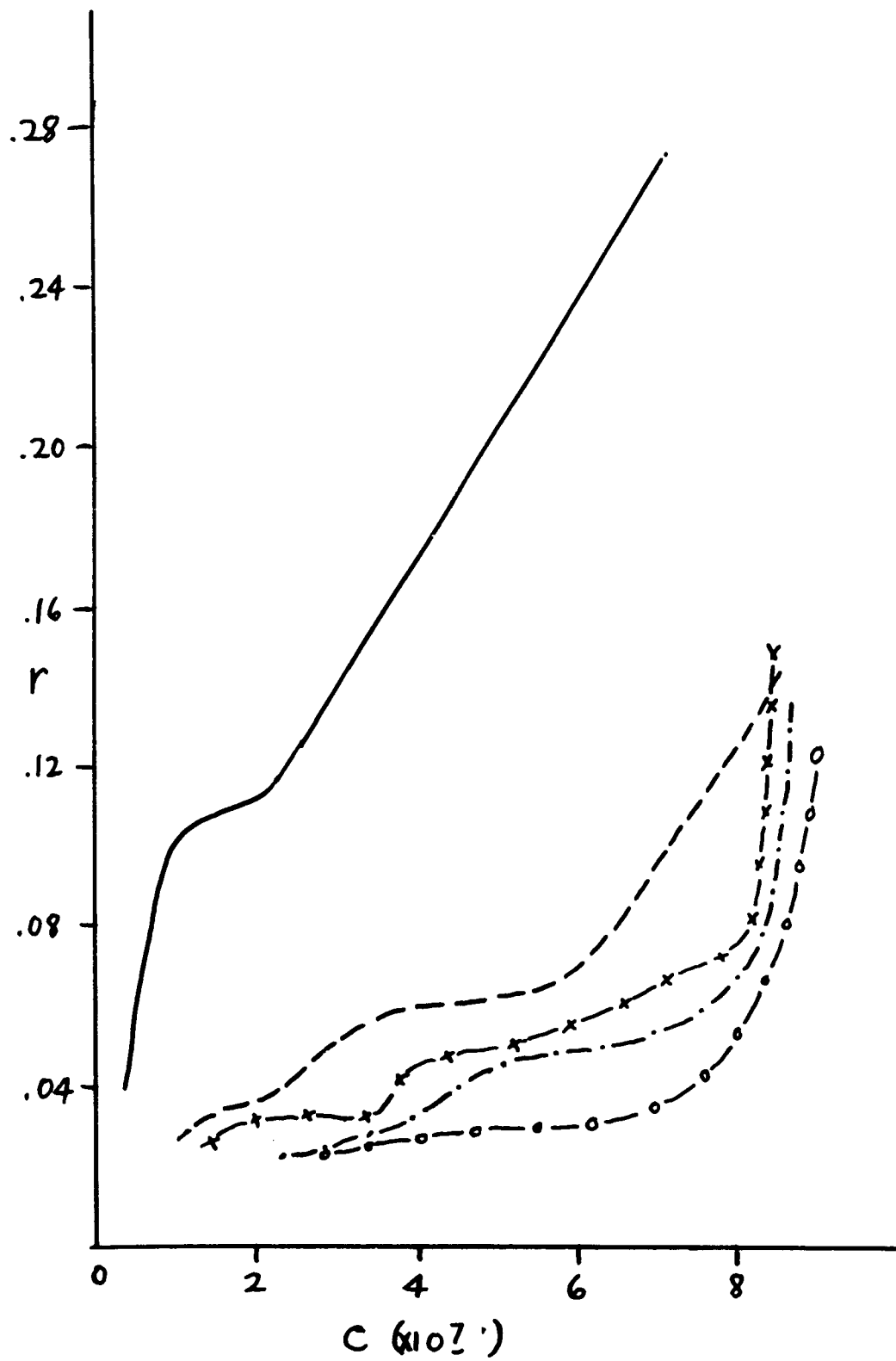
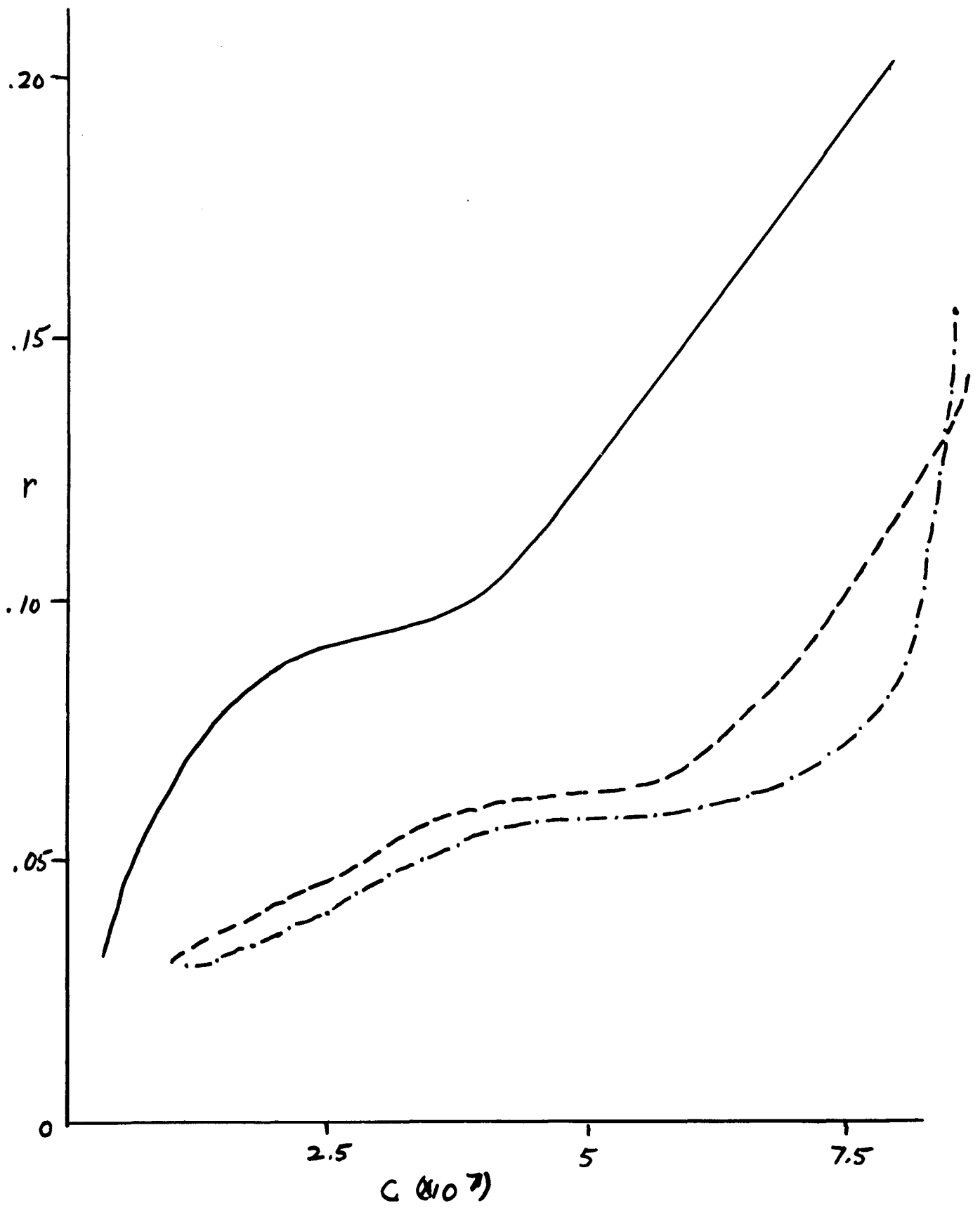


FIGURE 29.

Binding isotherms for the poly dG·poly dC-
daunomycin complex.

——, $\mu = 0.005$; -----, $\mu = 0.05$; -.-.-, $\mu = 0.5$.



The association constants for poly rA·poly dT were lower than those for either poly rA·poly rU or poly dA·poly dT at comparable ionic strengths. There were more binding sites available with poly rA·poly dT than with the other two polynucleotide duplexes.

Poly (dA-dT)·poly (dA-dT) resembled DNA more closely than the other polynucleotides in its behavior with respect to ionic strength. When the ionic strength was raised from $\mu = 0.05$ to $\mu = 0.5$, there was a four-fold decrease in k . In addition, the n values were more similar to those found with native DNA.

At comparable ionic strengths, the homopolymers, poly dA, poly dT, and poly dG had higher association constants than the polymer duplexes (table 5). In most cases, the duplexes had higher n values than the deoxyhomopolymers. In all cases, an increase in ionic strength caused a decrease in the n value. This was found to be true for the ribohomopolymer series as well.

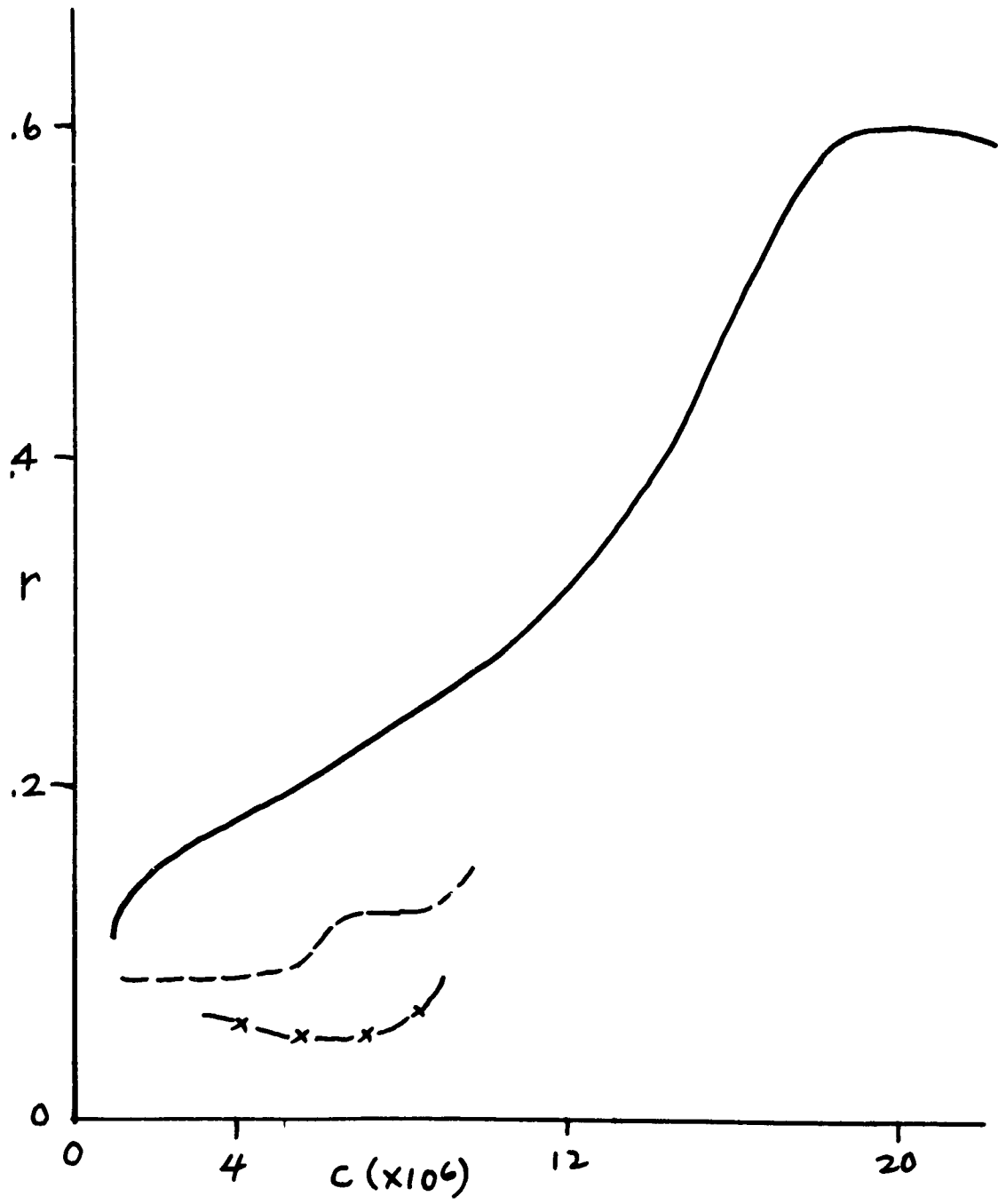
VII. Cl. perfringens DNA.

The interaction of Cl. perfringens DNA with daunomycin was also studied by this fluorescence method. The binding isotherms are shown in figure 30. At low ionic strength, the curve had the biphasic character indicative of two binding modes but it was unlike those obtained with calf thymus DNA. At the higher ionic strengths (i.e. $\mu = 0.05$ and 0.5) the plots did not show this behavior.

FIGURE 30.

Binding isotherms for the C1. perfringens DNA-
daunomycin complexes.

————, $\mu = 0.005$; -----, $\mu = 0.05$; -x-x-x, $\mu = 0.5$.



From the Scatchard plots (figure 31), it did appear that at $\mu = 0.005$ and 0.05 , there was heterogeneous binding because of the curvature in the plot. Table 5 lists the k and n values for C1. perfringens DNA evaluated from these Scatchard plots. They differed from those obtained for calf thymus DNA in that the association constants increased when the ionic strength was raised from $\mu = 0.005$ to $\mu = 0.05$ and then decreased when ionic strength was further increased to $\mu = 0.5$. Like calf thymus DNA, n decreased with increased ionic strength.

VIII. T_m Studies.

A. Absorbance vs. temperature profiles

A typical T_m plot for DNA ($1.0 \times 10^{-4}M$) is shown in figure 32. The addition of daunomycin ($1.0 \times 10^{-5}M$) resulted in an increase of approximately 20° in the T_m of the solution, as well as an increase in the hyperchromicity. The experiment shown in figure 33 was run with a 10-fold increase in the daunomycin concentration. The T_m in this case was increased by 32.6° . Prior to the temperature at which the helix-coil transition commenced there was a steady increase in absorbance. This occurred only at the higher daunomycin concentrations ($5 \times 10^{-5}M$ or higher). Although figures 32 and 33 were obtained with calf thymus DNA (%GC = 43), similar plots were observed when either C1. perfringens DNA (%GC = 32) or M. lysodeikticus DNA (%GC = 72) was used.

FIGURE 31.

Scatchard plots for the C1. perfringens DNA-daunomycin complex.

————, $\mu = 0.005$; o-o-o, $\mu = 0.05$; x-x-x, $\mu = 0.5$.

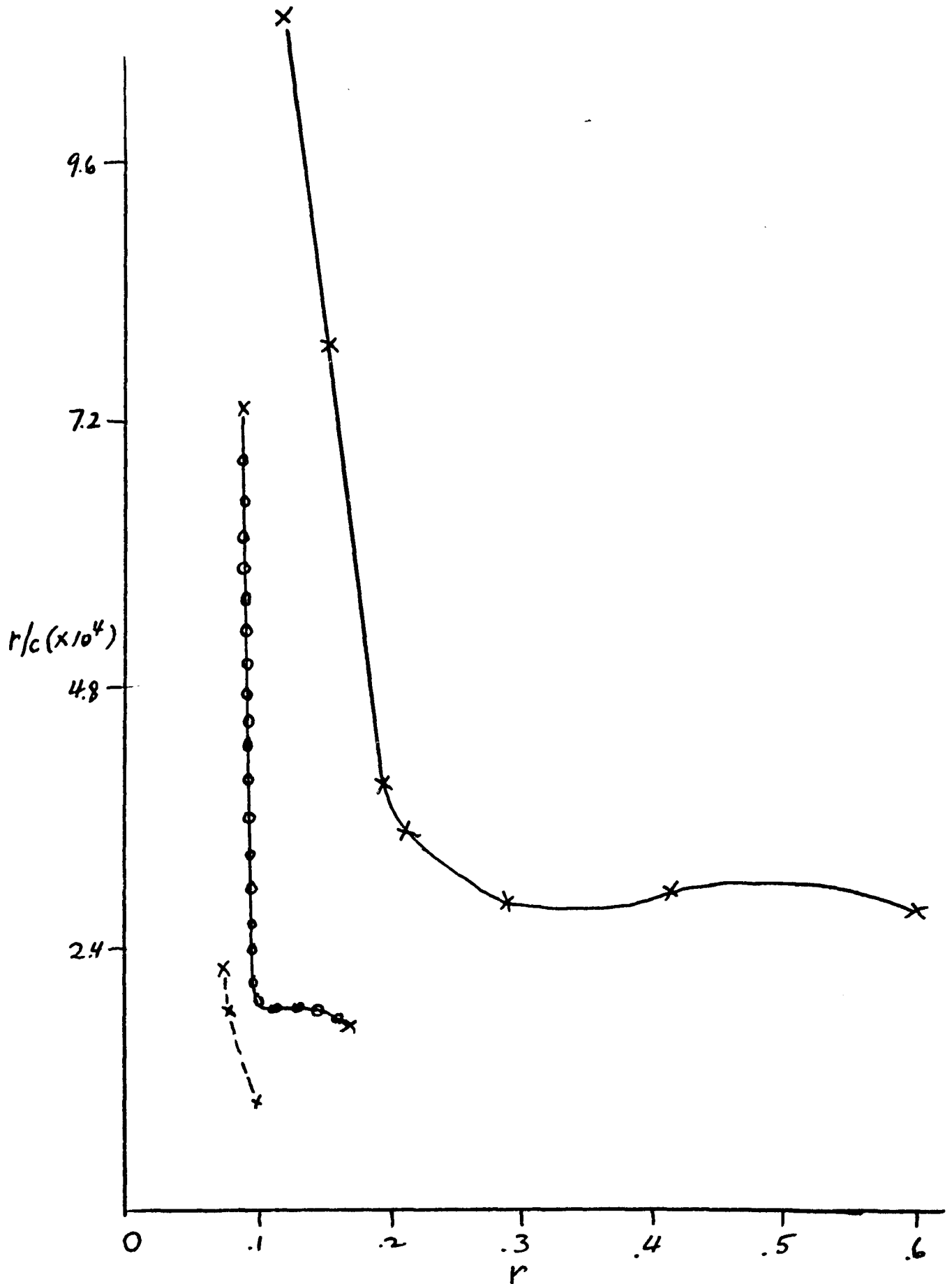


FIGURE 32.

Effect of daunomycin on the melting curve (T_m)
of calf thymus DNA.

——, DNA ($1.0 \times 10^{-4}M$); ----, DNA ($1.0 \times 10^{-4}M$)
+ daunomycin ($1.0 \times 10^{-5}M$).

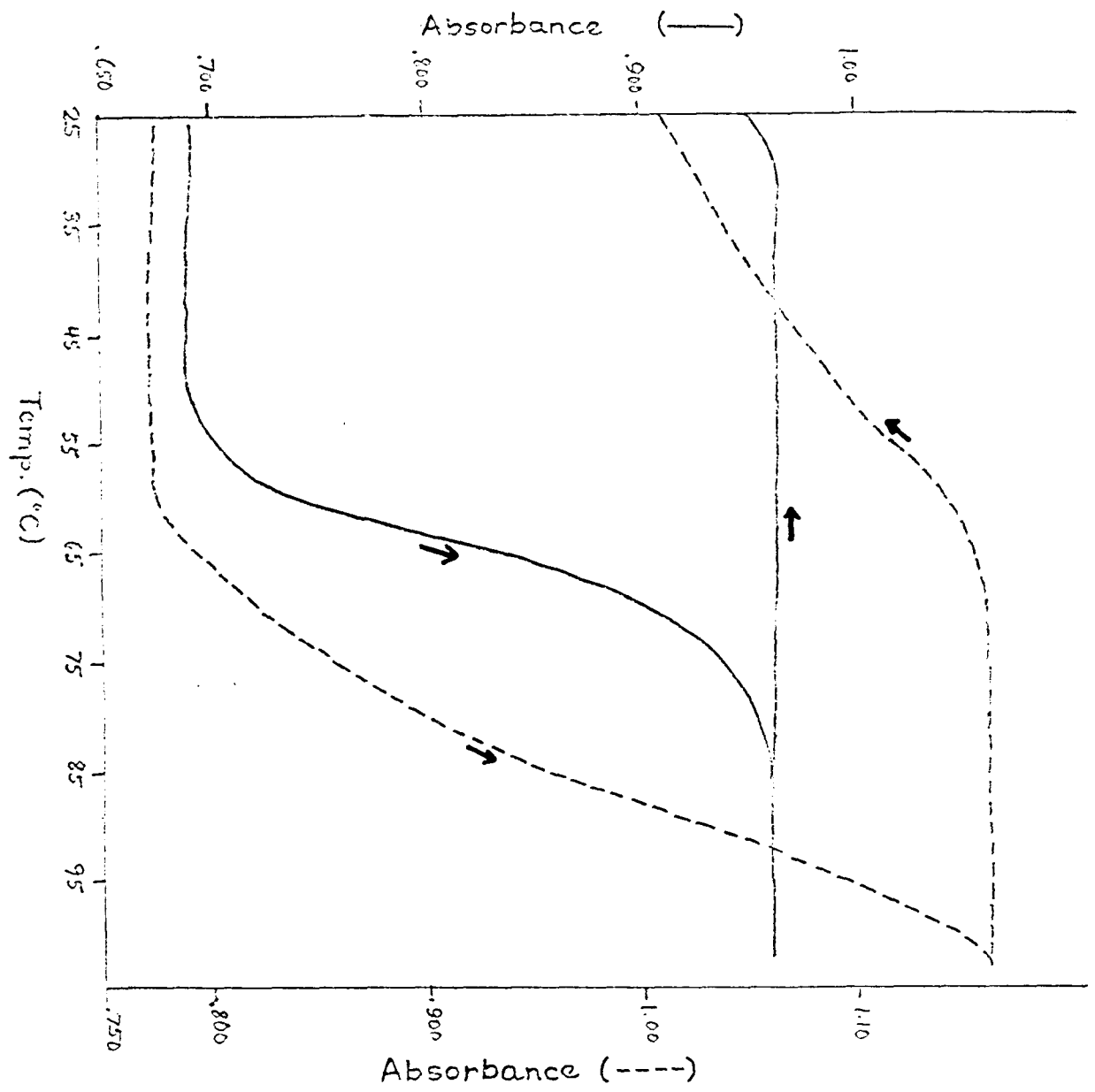
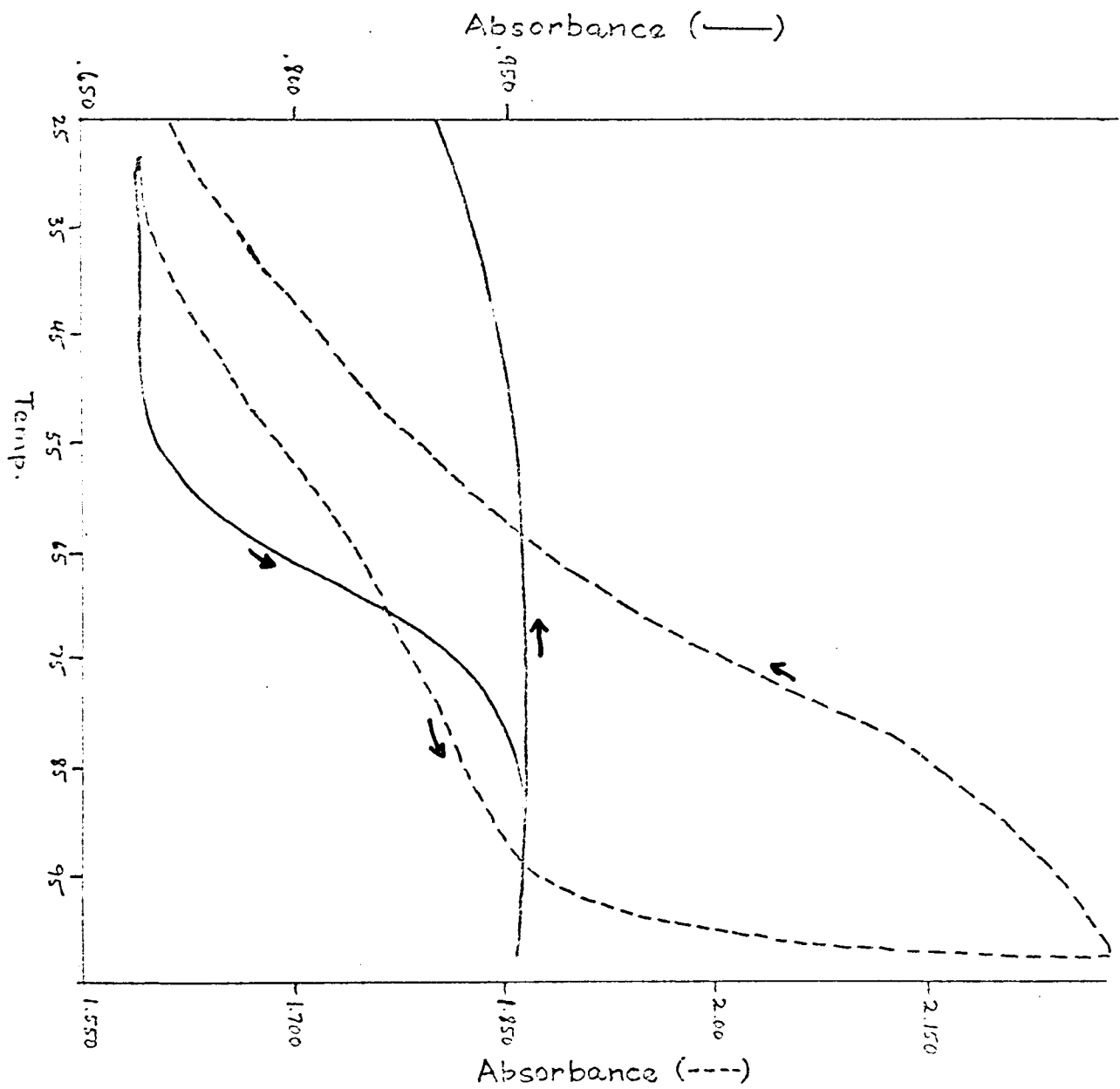


FIGURE 33.

Effect of daunomycin on the melting curve (T_m)
of calf thymus DNA.

————, DNA ($1.0 \times 10^{-4}M$); -----, DNA ($1.0 \times 10^{-4}M$)
+ daunomycin ($1.0 \times 10^{-4}M$).



B. Effects of daunomycin concentration

a. Calf thymus DNA.

Table 6 lists the T_m data for the daunomycin-calf thymus DNA complex. These are given at three different ionic strengths. Figures 34 and 35 illustrate some of the results graphically. Figure 34 shows the T_m of the complex (denoted as T_m') as a function of T_D/T_P , the ratio of the daunomycin concentration to that of calf thymus DNA and figure 35 is a plot of ΔT_m vs. T_D/T_P . As increasing amounts of daunomycin were added (over a ten-fold range of concentration) both the T_m' and ΔT_m increased.

b. C1. perfringens DNA

Table 7 lists the T_m data for the C1. perfringens DNA-daunomycin complex and figures 36 and 37 are plots of T_m' and ΔT_m versus T_D/T_P for C1. perfringens DNA. They were similar to those obtained when calf thymus DNA was used, i.e. there was an increase in both T_m' and ΔT_m with increasing daunomycin concentration. It should be noted that the T_m for free C1. perfringens DNA was lower than that of calf thymus DNA at comparable ionic strengths. This could be attributed to differences in GC content.

c. M. lysodeikticus DNA

Table 8 lists the T_m data for the M. lysodeikticus-DNA-daunomycin complex and figure 38 shows the T_m' and ΔT_m vs. T_D/T_P plots. As with the other DNA's tested, there was an increase in both the T_m' and ΔT_m as the concentration of

TABLE 6

T_m DATA FOR CALF THYMUS DNA-DAUNOMYCIN COMPLEXConcentration of DNA = 1.0 x 10⁻⁴M

DAUNOMYCIN CONC.	[DNA]/[Dm]	°C	T _m Δ°C	DENATURATION		RENATURATION		
				%	Δ%	%	Δ%	
<u>μ = 0.005</u>								
NONE	0	65.3	-	38.1	-	16.7	-	
10 ⁻⁵ M	10:1	83.8	18.5	44.1	6.0	46.8	30.1	
2.5 x 10 ⁻⁵ M	4:1	90.1	24.8	43.5	5.4	82.6	65.9	
5 x 10 ⁻⁵ M	2:1	94.6	29.3	43.6	5.5	89.0	72.3	
10 ⁻⁴ M	1:1	96.8	31.5	40.1	2.0	94.0	77.3	
<u>μ = 0.05</u>								
NONE	0	80.1	-	38.3	-	46.8	-	
10 ⁻⁵ M	10:1	88.5	8.4	43.2	4.9	65.7	18.9	
2.5 x 10 ⁻⁵ M	4:1	91.8	11.7	45.7	7.4	87.8	41.0	
5 x 10 ⁻⁵ M	2:1	97.9	17.8	37.5	-0.8	92.9	46.1	
10 ⁻⁴ M	1:1	T _m > 100 ⁰ ; not measurable						
<u>μ = 0.5</u>								
NONE	0	94.9	-	37.4	-	70.1	-	
10 ⁻⁵ M	10:1	95.7	0.8	42.4	5.0	72.2	2.1	
2.5 x 10 ⁻⁵ M	4:1	95.5	0.6	40.0	2.6	86.9	16.8	
5 x 10 ⁻⁵ M	2:1	98.9	4.0	35.1	-2.3	95.7	25.6	
10 ⁻⁴ M	1:1	T _m > 100 ⁰ ; not measurable						

All values are averages of three separate runs.

FIGURE 34.

Melting temperature (T_m') of the daunomycin-calf thymus DNA complexes as a function of daunomycin/DNA ratio (T_D/T_P). o-o-o, $\mu = 0.005$; \otimes - \otimes - \otimes , $\mu = 0.05$; \bullet - \bullet - \bullet -, $\mu = 0.5$.

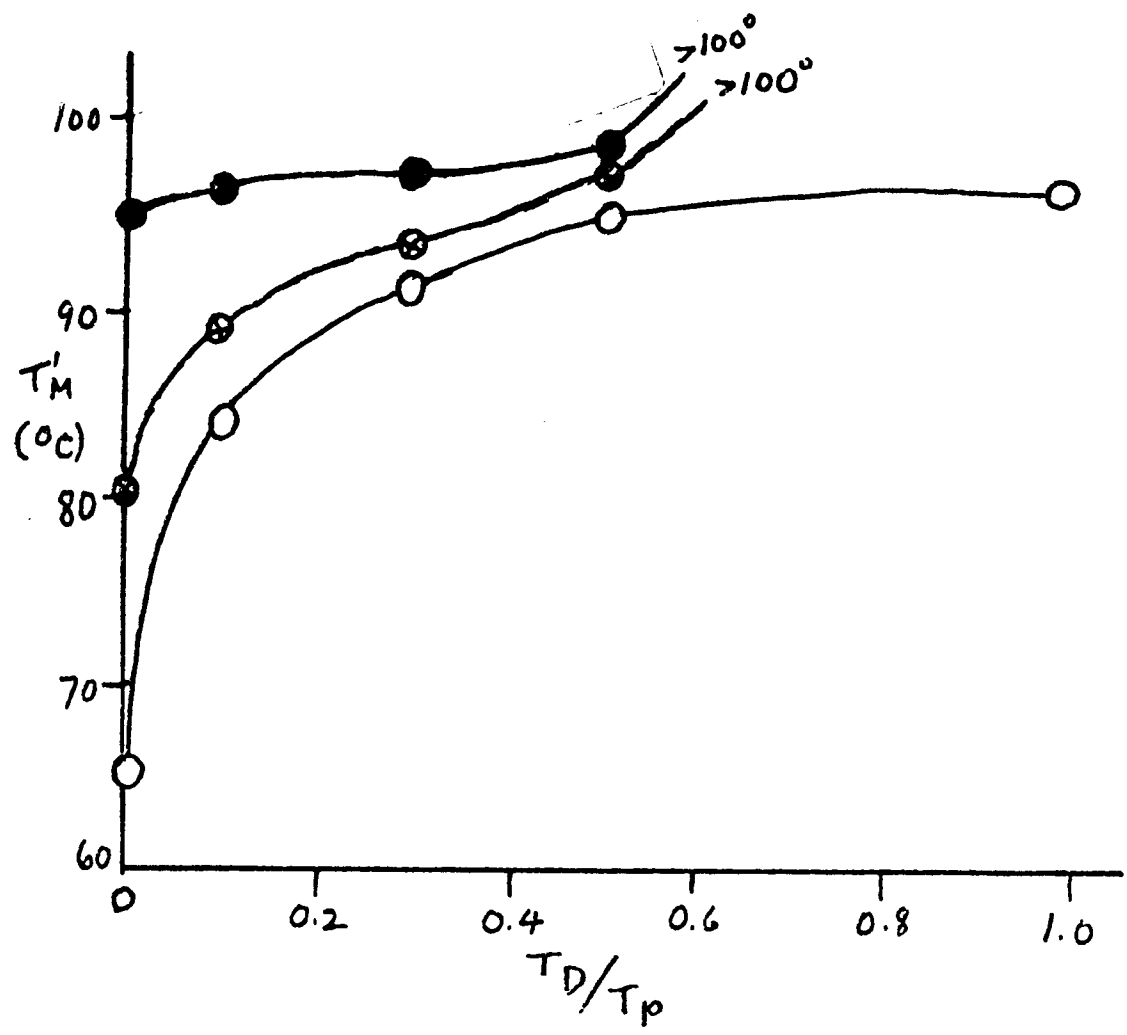


FIGURE 35.

Change in the melting temperature of (ΔT_m) of calf thymus DNA due to complex formation with daunomycin as a function of daunomycin/DNA ratio (T_D/T_p).
o-o-o, $\mu = 0.005$; \otimes - \otimes - \otimes , $\mu = 0.05$; \bullet - \bullet - \bullet , $\mu = 0.5$.

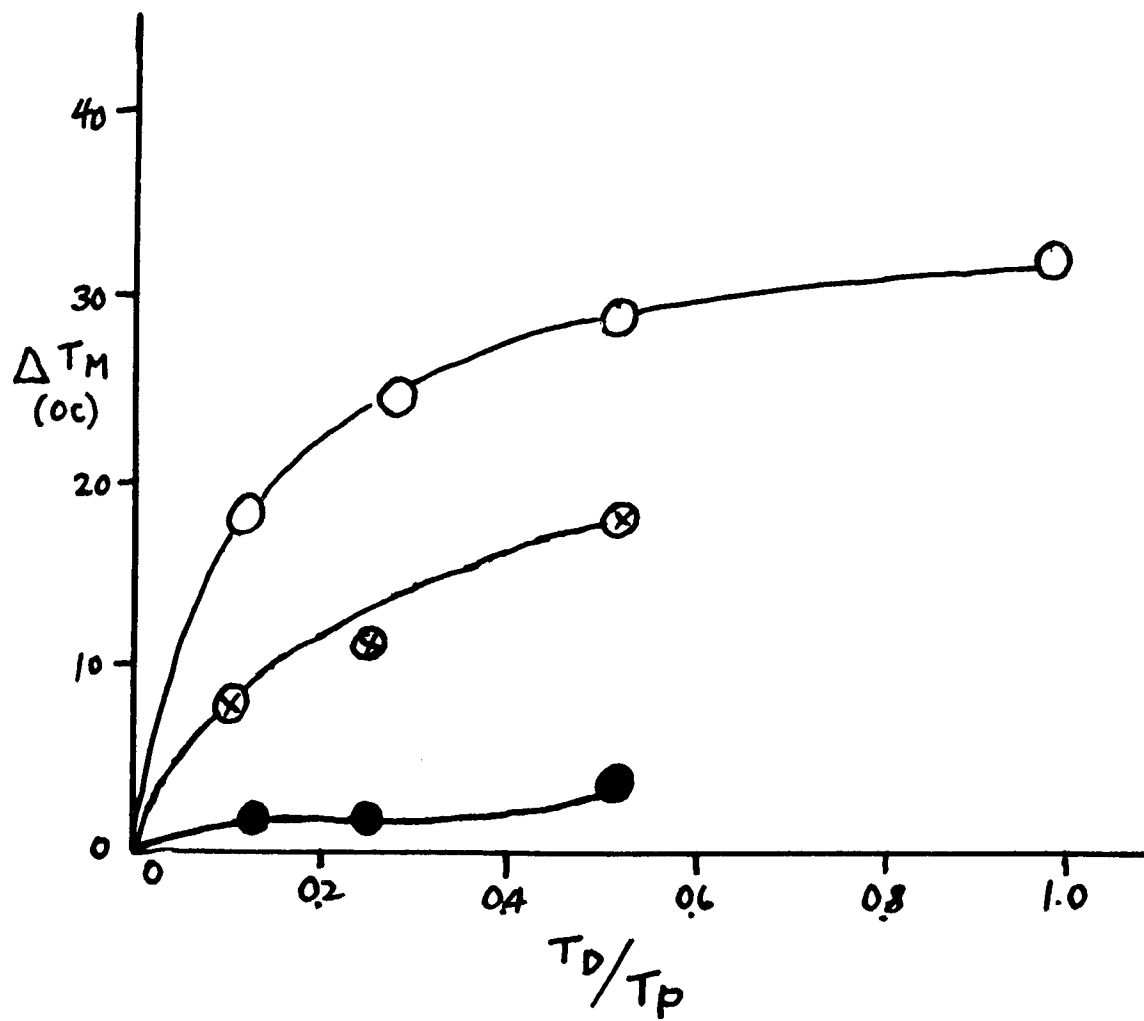


TABLE 7

T_m DATA FOR CL. PERFRINGENS DNA-DAUNOMYCIN COMPLEXConcentration of DNA = $1.0 \times 10^{-4}M$

DAUNOMYCIN CONC.	[DNA]/[Dm]	^o C T _m	$\Delta^{\circ}C$	DENATURATION %	$\Delta\%$	RENATURATION %	$\Delta\%$
<u>$\mu = 0.005$</u>							
NONE	0	61.0	-	30.5	-	15.8	-
$10^{-5}M$	10:1	81.9	20.9	39.9	9.4	58.5	42.7
$2.5 \times 10^{-5}M$	4:1	90.3	29.3	42.7	12.2	87.1	71.3
$5 \times 10^{-5}M$	2:1	92.6	31.6	42.1	11.6	82.1	66.3
$10^{-4}M$	1:1	96.8	35.8	33.7	3.2	92.0	76.2
<u>$\mu = 0.05$</u>							
NONE	0	72.2	-	29.3	-	26.9	-
$10^{-5}M$	10:1	83.9	11.7	36.5	7.2	67.6	40.7
$2.5 \times 10^{-5}M$	4:1	88.8	16.6	36.7	7.4	91.9	65.0
$5 \times 10^{-5}M$	2:1	91.6	19.4	32.1	2.8	92.2	65.3
$10^{-4}M$	1:1	95.6	23.4	30.6	1.3	90.8	63.9
<u>$\mu = 0.5$</u>							
NONE	0	88.7	-	30.0	-	73.2	-
$10^{-5}M$	10:1	88.4	-0.3	32.0	2.0	85.4	12.2
$2.5 \times 10^{-5}M$	4:1	89.7	1.0	32.3	2.3	92.1	18.9
$5 \times 10^{-5}M$	2:1	93.2	4.5	29.8	-0.2	96.5	23.3
$10^{-4}M$	1:1	95.4	6.7	28.3	-1.7	99.0	25.8

All values are averages of three separate runs.

FIGURE 36.

Melting temperature (T_m') of the daunomycin-C1.
perfringens DNA complexes as a function of
daunomycin/DNA ratio(T_D/T_P).

o-o-o, $\mu = 0.005$; \otimes - \otimes - \otimes , $\mu = 0.05$; \bullet - \bullet - \bullet , $\mu = 0.5$.

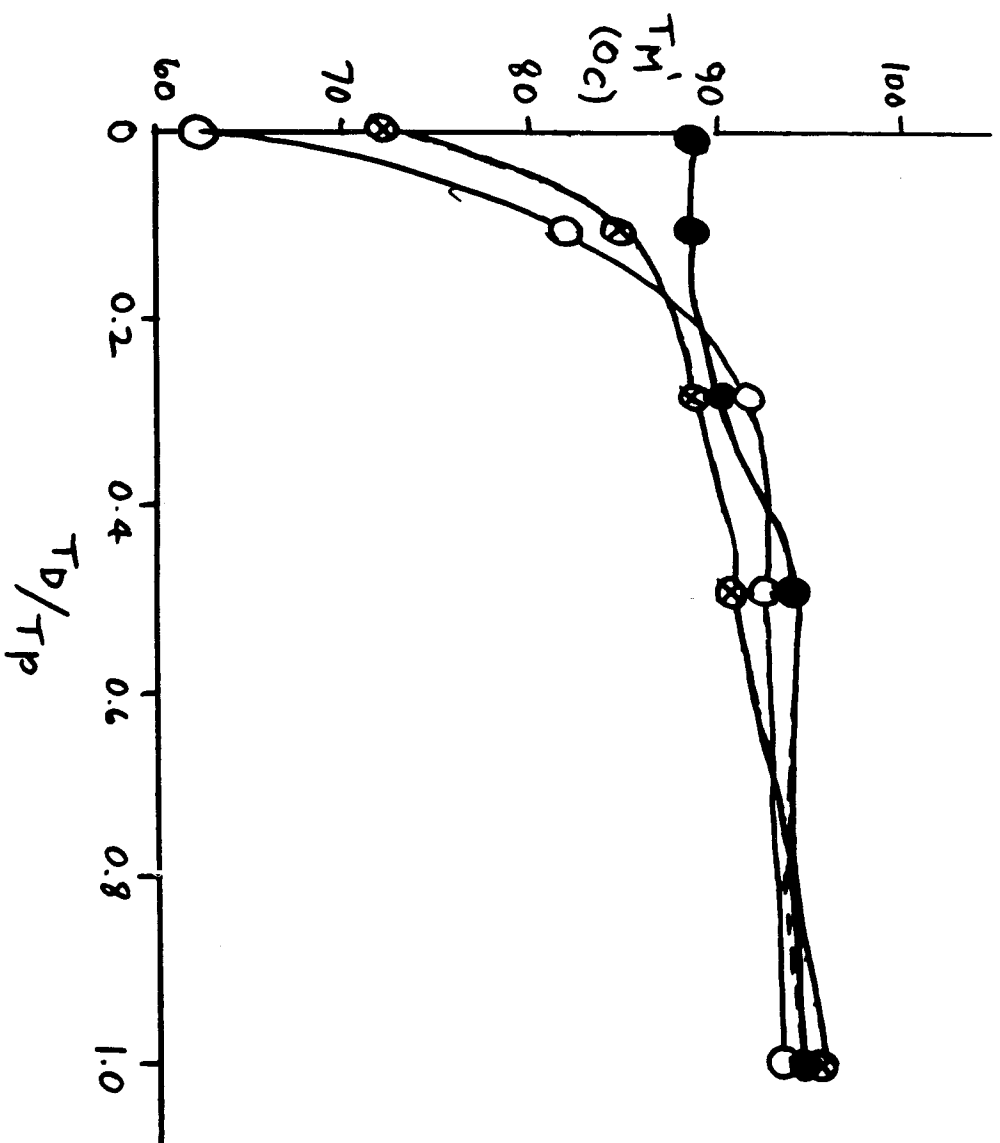


FIGURE 37.

Change in the melting temperature (ΔT_m) of C1.
perfringens DNA due to complex formation with
daunomycin as a function of daunomycin/DNA ratio
(T_D/T_p).

o-o-o, $\mu = 0.005$; \odot - \odot - \odot , $\mu = 0.05$; \bullet - \bullet - \bullet , $\mu = 0.5$.

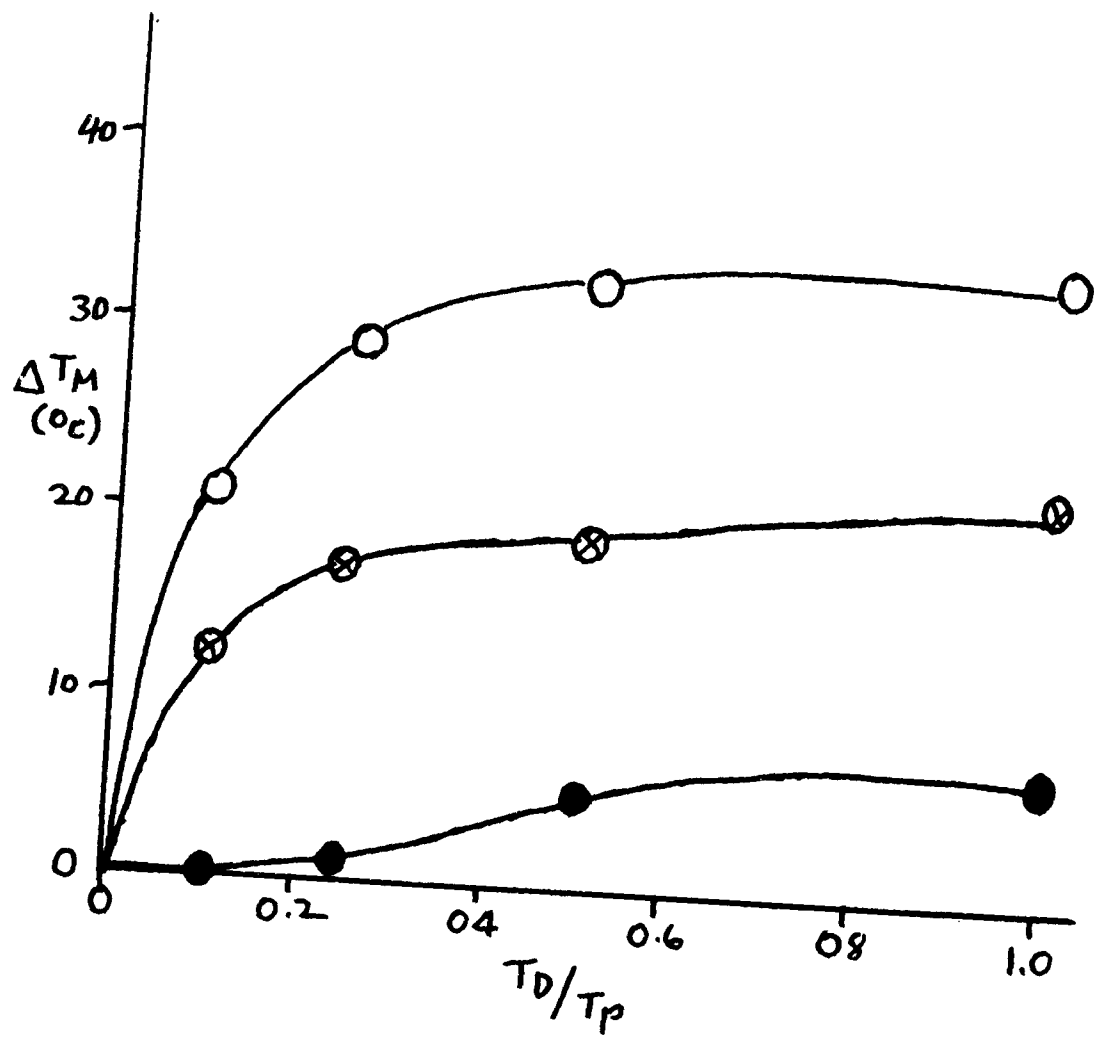


TABLE 8

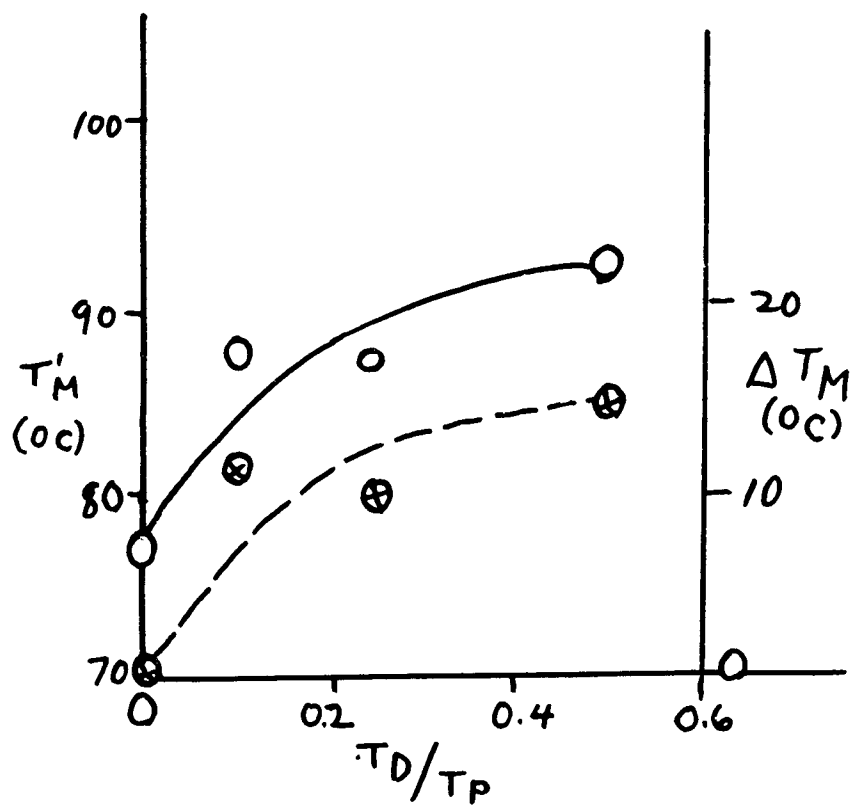
T_m DATA FOR M. LYSODEIKTICUS DNA-DAUNOMYCIN COMPLEXConcentration of DNA = $1.0 \times 10^{-4}M$

DAUNOMYCIN CONC.	[DNA]/[Dm]	°C	T _m	Δ°C	DENATURATION %	Δ%	RENATURATION %	Δ%
$\mu = 0.005$								
NONE	0	76.3	-	-	25.9	-	57.6	-
$10^{-5}M$	10:1	87.5	11.2	35.2	9.3	73.6	16.0	
$2.5 \times 10^{-5}M$	4:1	86.5	10.2	38.2	12.3	71.5	17.9	
$5 \times 10^{-5}M$	2:1	91.7	15.4	37.1	11.2	75.0	17.4	

All values are averages of two separate runs.

FIGURE 38.

Melting temperature (T_m') of the M. lysodeikticus DNA-daunomycin complex, o-o-o; and the change in the melting temperature (ΔT_m) of M. lysodeikticus DNA due to complex formation with daunomycin, ●-●-●, as a function of daunomycin/DNA (T_D/T_p) ratio. Ionic strength was 0.005.



daunomycin was increased.

d. Comparisons

Figures 39 and 40 are comparisons of the three DNA's tested. It is clear that M. lysodeikticus DNA was very different from the other two. The ΔT_m values for its complex with daunomycin were much lower than those for the other DNA's. Both calf thymus DNA and Cl. perfringens DNA reached an identical maximum T_m' of 96.8° at $T_D/T_P = 1.0$. The T_m' vs. T_D/T_P curves for these two DNA's were very much alike. It is of interest that although M. lysodeikticus DNA had a much higher T_m (76.3° vs. 65.3° for calf thymus DNA and 61.0° for Cl. perfringens DNA) in the absence of daunomycin, at T_D/T_P ratios above 0.25 the T_m' values were lower than those of the other DNA's (figure 38). This might indicate a decreased stabilization effect by daunomycin when it formed a complex with M. lysodeikticus DNA.

c. Effect of ionic strength

Tables 6-8 and figures 34-37 also indicate the effect of ionic strength on the T_m on the various DNA's .

a. Calf thymus DNA.

Increasing the ionic strength caused an increase in the T_m value for free calf thymus DNA (from 65.3° at $\mu = 0.005$ to 94.9° at $\mu = 0.5$). The T_m' also increased as a function of ionic strength, however, the ΔT_m , which is a measure of the increased stability as a result of complex formation, steadily decreased (table 6).

FIGURE 39.

Increase in the melting temperature (ΔT_m) of DNA due to complex formation with daunomycin. Effect of daunomycin on DNA's of varying GC content. o-o-o, Cl. perfringens DNA (32% GC); ⊗-⊗-⊗, calf thymus DNA (43%); ●-●-●, M. lysodeikticus DNA (72%). Ionic strength was 0.005.

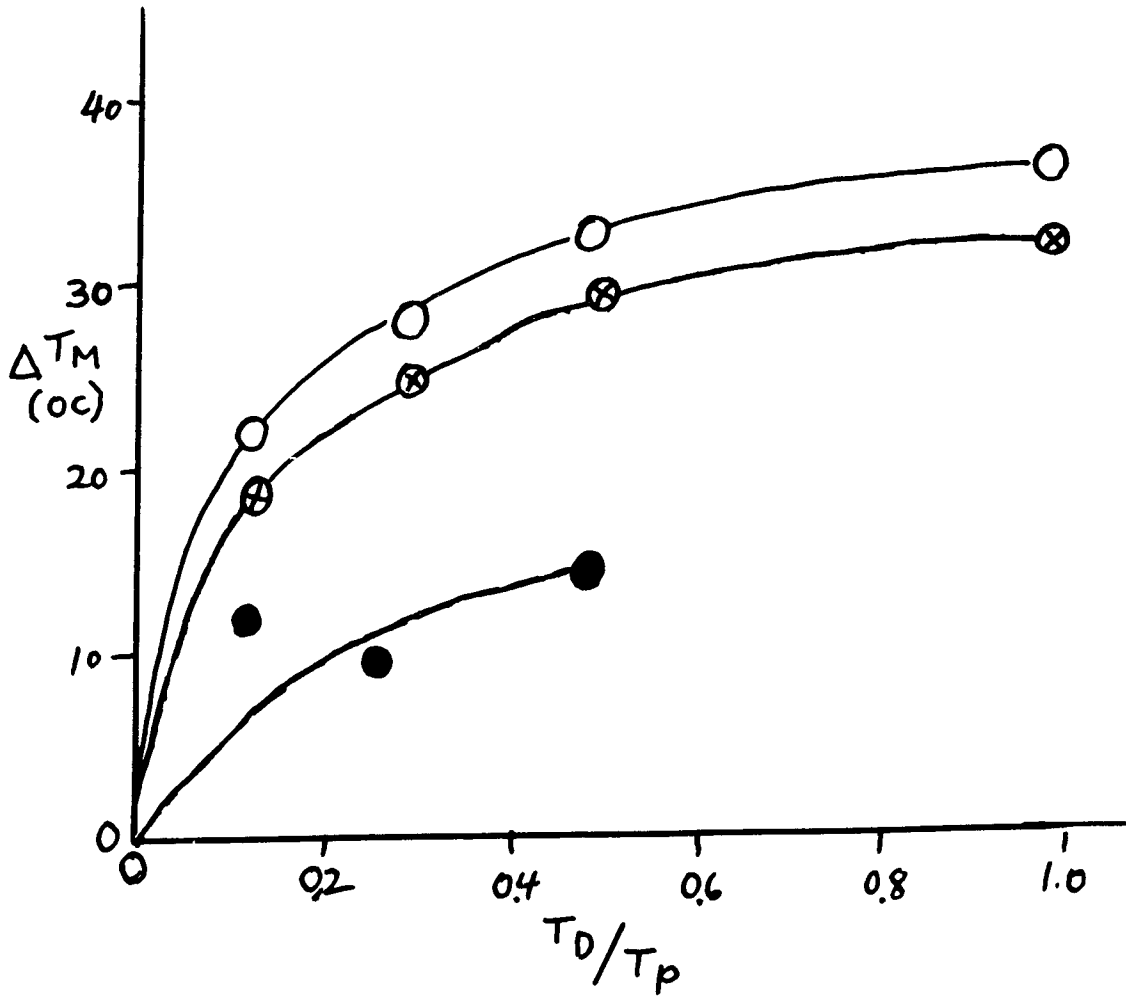
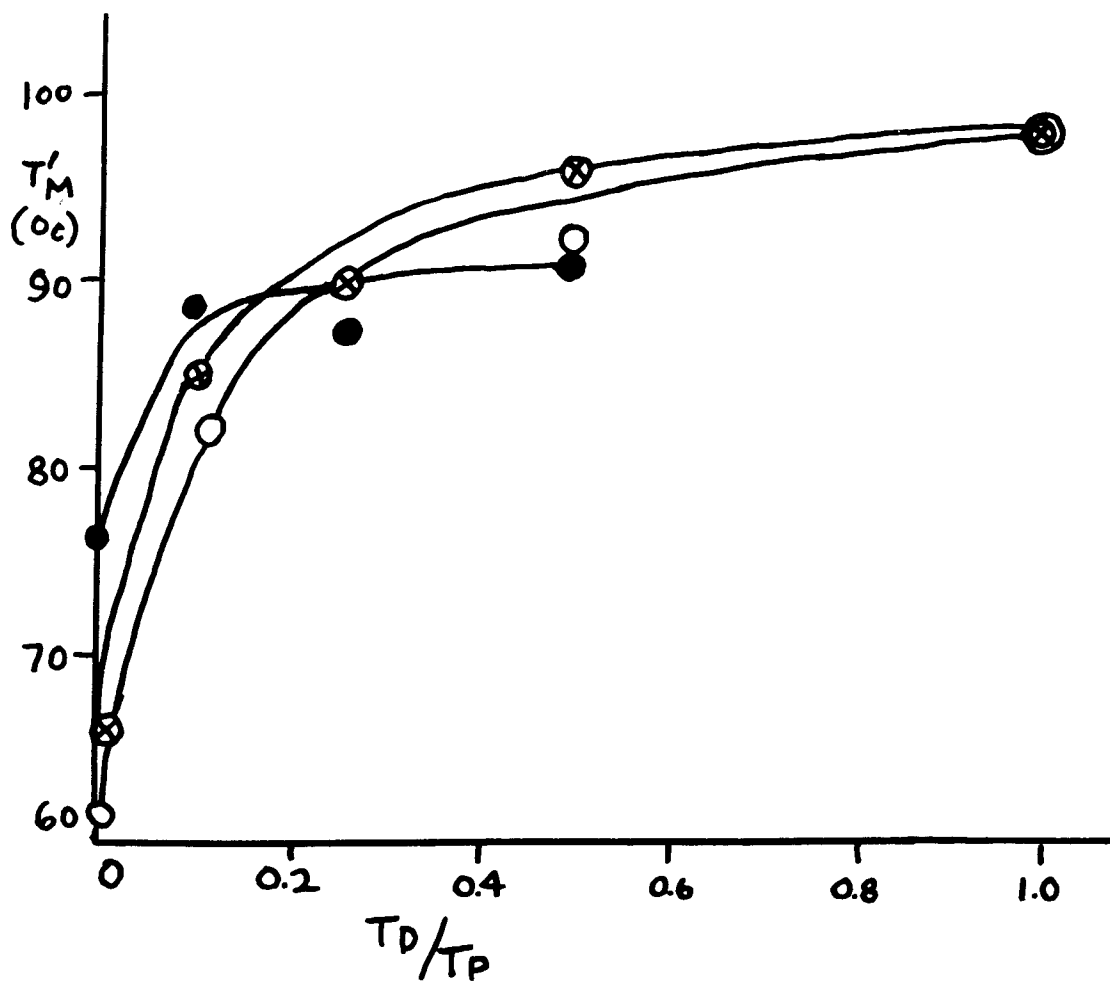


FIGURE 40.

Melting temperatures (T_m') of daunomycin-DNA complexes as a function of T_D/T_p . Effect of daunomycin on DNA's of varying GC content. o-o-o, C1. perfringens DNA (32% GC); ⊗-⊗-⊗, calf thymus DNA(43%); ●-●-●, M. lysodeikticus DNA (72%).
Ionic strength was 0.005.



The effect of ionic strength was further illustrated in figure 34. At $T_D/T_P < 0.25$ there was a sharp increase in T'_m as a function of T_D/T_P at $\mu = 0.005$. However, at $\mu = 0.5$, the plot showed no change. Figure 35 indicates that the ΔT_m was lower for higher ionic strengths. For $\mu = 0.005$, the ΔT_m increased with increasing T_D/T_P until a plateau was reached at high T_D/T_P . The same appeared to be true at $\mu = 0.05$ but at the highest ionic strength, 0.5, there was no significant ΔT_m until the higher T_D/T_P was reached.

b. C1. perfringens DNA

Table 7 and figures 36 and 37 show that C1. perfringens DNA was similar to calf thymus DNA with respect to the effect of ionic strength. The T'_m showed only slight variations at $\mu = 0.5$ while at $\mu = 0.005$ there was a sharp increase in T'_m up to $T_D/T_P = 0.25$ after which it leveled off (figure 36). The shape of the ΔT_m vs. T_D/T_P plots were the same at $\mu = 0.005$ and 0.05 (although the ΔT_m decreased with increased ionic strength). However, at $\mu = 0.5$, the ΔT_m did not increase until $T_D/T_P = 0.25$ (figure 37).

From figure 36 it appears that there was a single T_m value for all $T_D/T_P \geq 0.25$ which did not vary with ionic strength. This was a significant difference from calf thymus DNA. A glance at figure 34 shows that this was not the case with calf thymus DNA in that increasing

the ionic strength at equivalent T_D/T_P ratios resulted in an increase in T_m' .

D. Renaturation

Another measure of the daunomycin effect was the extent of renaturation on slow cooling. This can be measured by following the decrease in absorbance when a DNA (or DNA-daunomycin) solution was slowly cooled after its initial heating. This is shown in figures 32 and 33. For free calf thymus DNA there was almost no renaturation. However, the addition of daunomycin may have resulted in extensive renaturation (42%). This behavior was observed with Cl. perfringens and M. lysodeikticus DNA as well.

As indicated in tables 6-8, when more daunomycin was added to a solution of DNA there was greater renaturation, i.e. the presence of daunomycin aided the renaturation process. As with the T_m' values, % renaturation increased with increasing ionic strength in both the presence and absence of daunomycin, but the $\Delta\%$ renaturation decreased as the ionic strength was increased.

IX. Equilibrium Dialysis.

In the initial set of equilibrium dialysis experiments the concentration of daunomycin was held constant at $2.5 \times 10^{-5}M$ and that of the nucleic acid was varied from $5 \times 10^{-6}M$ to $2.5 \times 10^{-4}M$. For all these studies as r approached zero, r/c also decreased and thus Scatchard

plots could not be constructed.

A second set of dialysis experiments were performed in which the concentration of daunomycin was varied from $10^{-5}M$ to $5 \times 10^{-5}M$ and that of the nucleic acid was held constant at $10^{-4}M$. These experiments also failed for the same reason, namely, as r decreased, so did r/c .

As discussed in the methods section (p.52) the data from equilibrium dialysis experiments were obtained by measuring absorbances of the solutions on either side of the dialysis membrane. The most likely explanation for the failure of the experiments is that absorbance was not a sensitive enough method of measurement for this type of study and thus the margin of error was too large.

It should be noted that Zunino, et al. (86) have reported binding data for the daunomycin-DNA interaction obtained on the basis of equilibrium dialysis studies. However, they used tritiated daunomycin in their experiments which is more sensitive to small changes in concentration.

DISCUSSION

I. Effect of Ions on the DNA-Daunomycin Complex.

A. Effect of Cu^{++}

The addition of Cu^{++} to a solution of daunomycin resulted in complex formation between Cu^{++} and daunomycin (figure 9). Since Cu^{++} forms complexes with many nitrogen containing compounds, e.g. nitrogen bases, the amino group on the sugar moiety of daunomycin would provide a likely binding site for Cu^{++} .

The further spectral changes which were observed when DNA was added to a Cu^{++} -daunomycin complex depended on whether the added DNA was in the native or denatured state (figure 9) and this difference could be traced to the way in which Cu^{++} binds to DNA. It has been pointed out by Eichhorn (74, 75) that Cu^{++} can interact with the phosphate groups on DNA (as Cu^{++} concentration was increased), although the preferred binding sites are the nitrogen atoms in the bases. It appears that with native DNA the Cu^{++} bound to the phosphate groups (since the bases were involved in hydrogen bonding) which was a rather non-specific interaction and this resulted in the spectrum of the type seen in figure 9, i.e. a decrease in absorbance at all wavelengths with no discernible peaks. On the other hand, with denatured DNA, the bases were available for Cu^{++} binding and the spectral effects were more pronounced.

For both the Cu^{++} -Dm and DNA-Dm complexes, the maximum quenching of fluorescence occurred between pH 6.5-6.8. This seemed to indicate that whichever group on the daunomycin molecule was responsible for the decrease in fluorescence, it was similarly affected by the addition of either Cu^{++} or DNA, although the quenching was greater with DNA. However, based on the fluorescence data which are shown in Table 1, it appears that addition of both Cu^{++} and DNA together resulted in an even greater quenching effect than when they were added alone. This indicates that the Cu^{++} was bound to sites on the DNA or daunomycin other than those involved in the DNA-Dm complex. This was also supported by the observation that Cu^{++} did not split the Dm-DNA complex. Consideration was given to the maximum quenching between pH 6.5-6.8. However, a survey of the pK values for the nucleic acid bases and various Cu^{++} -amine complexes did not indicate any likely group which could account for the observed maximum.

B. Effect of Mg^{++}

Mg^{++} induced spectral effects in the range of 530-600 nm which were similar to those observed with Cu^{++} . However, these changes occurred in both the presence or absence of DNA (figure 16). This indicated a gradual release of DNA from its complex with daunomycin with the formation of a Mg^{++} -Dm complex instead. It would appear that Mg^{++} had a preferred binding with some sites on

daunomycin, most possibly the oxygen atoms, which resulted in the inability of daunomycin to remain complexed to DNA. This was supported by the fluorescence data (Table 1) which showed that the addition of Mg^{++} to a DNA-Dm complex resulted in enhanced fluorescence, presumably by releasing DNA from the complex. However, the fluorescence intensity in the presence of DNA was lower than in its absence and so there was still some degree of DNA binding. This was evident even below pH 5.8 at which Mg^{++} did not affect the visible spectrum of the DNA-Dm complex.

C. Comparison of the Cu^{++} and Mg^{++} effects:

Although both Cu^{++} and Mg^{++} induced similar spectral effects there were some important differences with regard to concentration, pH, and the state of the DNA (i.e., native or denatured). The concentration necessary to elicit these spectral changes was three orders of magnitude greater for Mg^{++} than for Cu^{++} (0.1M vs. $1 \times 10^{-4}M$). The pH at which the spectral changes took place was different, occurring at pH 7.8 with Mg^{++} but at pH 5.2 with Cu^{++} . At pH 5.2, Mg^{++} exhibited no effect at all on the DNA-Dm spectrum and it was assumed, therefore, that no binding occurred at this pH. Mg^{++} showed these changes in the presence of both native or denatured DNA. Cu^{++} , on the other hand, exhibited its effect only when denatured DNA was used. In addition, Mg^{++} caused the release of DNA from its complex with daunomycin unlike Cu^{++} which allowed the DNA to remain

complexed to daunomycin and formed what could be termed a ternary complex.

D. Binding sites for Cu^{++} and Mg^{++}

It appears, therefore, that both Mg^{++} and Cu^{++} were bound to daunomycin and DNA but the binding occurred at different sites. Mg^{++} could be bound to the oxygen of the keto or hydroxyl groups in the chromophore whereas Cu^{++} would most likely be bound to the amino group on the sugar moiety. Mg^{++} binding with the chromophore would make intercalation with DNA sterically unlikely because of the extra bulkiness of the planar chromophore. With Cu^{++} , however, the binding which would occur at the sugar residue would not exclude intercalation although it might result in reduced binding to DNA. Mg^{++} not only caused a decrease in fluorescence intensity for daunomycin but also resulted in an altered emission spectrum (figure 20). Cu^{++} did not cause such a change. Since the chromophore portion of daunomycin is what gives rise to the fluorescence spectrum, this furnishes additional evidence for Mg^{++} binding to the chromophore as opposed to Cu^{++} binding to the sugar moiety.

This points to the dual effects that ions seem to induce on the DNA-Dm interaction. They can bind to either the DNA or daunomycin, or both. Depending on the binding preference of the ion, this can result in alteration of the complex or its splitting. Below pH 5.8, even though Mg^{++} can no longer bind to daunomycin it can still be bound to

the phosphate groups on DNA. If, as suggested by Calendi, et al.(19), daunomycin does indeed bind to phosphate in addition to binding by intercalation, there would be competition between Mg^{++} and daunomycin for these phosphate sites and this would result in reduced binding of daunomycin to DNA.

It is of interest to note that Cu^{++} showed a preference for the denatured DNA-Dm complex as opposed to the native DNA complex. This was similar to that which was found with the actinomycin-DNA complex (83). However, with actinomycin-DNA, the addition of Cu^{++} caused a return of the spectrum to that of free actinomycin whereas with Dm-DNA, Cu^{++} induced additional spectral changes. Similar spectral effects were found for Ag^+ and Hg^{++} (84), both of which bind to the DNA bases (65). The addition of Ag^+ resulted in the release of either actinomycin or daunomycin from their complexes with DNA. Hg^{++} , however, caused the release of actinomycin but had no effect on the daunomycin complex. Rusconi (84) took this as evidence for different binding sites on DNA for actinomycin and daunomycin. The results presented here for Cu^{++} , in conjunction with the studies on actinomycin (83), tend to substantiate this conclusion. If both daunomycin and actinomycin bind to DNA by intercalation, as indicated by various studies (50, 63, 86) Hg^{++} and Cu^{++} should have affected their complexes with DNA similarly. In as much as this was not the case, it would indicate that in addition to the insertion of the

the planar portion of these antibiotics between the base pairs, other portions of the molecule were also involved in binding to the DNA and that this additional binding was essential for the complex. In the actinomycin molecule, the peptide lactones were undoubtedly involved and; the essential group in daunomycin was the amino group on the sugar residue.

II. Binding of Nucleic Acid Units and Polynucleotides to Daunomycin.

No binding to daunomycin was observed for nucleic acid bases, nucleosides, and nucleotides. There have been previous reports that daunomycin bound to purine mononucleotides (19, 85). In this study, no such interaction was found. In the work by Calendi, et al. (19) the molar ratio of purine to daunomycin was approximately 400:1. This undoubtedly accounts for the disparity in results.

It should be noted that purines exhibit extensive self-association in aqueous solvents and this was shown to occur in the form of vertical stacking (96). At the high concentrations of purines employed in the previous studies it is likely that daunomycin binding was occurring to vertically stacked purines rather than to individual purine mononucleotides. In this sense, the binding observed here to polynucleotides can be similar to that found with high concentrations of mononucleotides.

Greater quenching of fluorescence was observed with

the purine polynucleotides than with the pyrimidine polynucleotides and this may also be due to more extensive stacking interactions for purines as opposed to pyrimidines. This can result in more stable structures for daunomycin intercalation and thus result in greater quenching. One would expect the intrinsic association constants for the binding of the various polynucleotides to reflect this difference between purines and pyrimidines but they did not.

III Spectrophotometric Titrations.

A. Polynucleotide-daunomycin interaction.

The values for the association constants (k) for the various polynucleotides indicated that there was no base preference for the polynucleotide-daunomycin interaction since all the k values were comparable (Table 4). In addition, these values did not vary with changes in ionic strength. The one exception to this was poly I. Sarkar and Yang (99) found that, at low ionic strength, Poly I had very little organized structure. On the other hand, at elevated ionic strengths, Rich (100) demonstrated that this polynucleotide forms a unique triple-stranded molecule. These studies indicated that there was a gradual organization of structure as the ionic strength was increased. It appears that at the low ionic strength poly I exhibited a lower level of binding because of lack of organized structure but as the ionic strength was increased the secondary structure formed and so stronger binding was able to occur. When the triple-

stranded helix was formed at $\mu = 0.5$, however, binding disappeared because it was sterically impossible for daunomycin to intercalate into such a structure. Waring (47) observed similar behavior for the binding of ethidium bromide to poly I and Lerman (25) was unable to detect any binding between 9-aminoacridine and poly A·2 poly U which was also a triple-stranded structure.

B. DNA-daunomycin interaction

An intercalative mode of binding was indicated by the binding isotherms and binding parameters, k and n , calculated for the daunomycin-DNA interaction. The existence of two distinct binding processes (figure 23 and 24), one at low values of c and another at high values of c , was similar to what has been found with the acridine dyes (30).

It would appear that a qualitative observation may be made based on the slopes for the second binding process at high values of c . Firstly, for native DNA, as the ionic strength was increased this portion of the isotherm decreased, pointing to a decreased contribution by electrostatic binding at the higher ionic strength; this was to be expected. Secondly, the secondary binding was a much more prominent feature of the denatured DNA isotherms (figure 24) indicating a greater importance for electrostatic binding for the complex of denatured DNA with daunomycin. This is not meant to minimize the significance of such binding for the native DNA complex. The decrease in the association constant for native

DNA (table 4), when the ionic strength was increased, indicated that electrostatic forces did indeed play a role in the binding of native DNA to daunomycin.

There were more binding sites available for daunomycin binding in its interaction with denatured DNA than with native DNA as indicated by their respective n values (table 4). This was in agreement with other studies on the acridine-DNA interaction (26,27). Drummond, et al. (26) attributed this increase to the relative lack of steric hindrance in denatured DNA, which is a more open structure. This would remove some of the geometric constraints imposed by a double helical structure but the lack of such a structure would not preclude binding by intercalation. The decrease in the number of binding sites which was observed for both native and denatured DNA as the ionic strength was increased could also be the result of a more open structure, since, at low ionic strength, there is greater repulsion between the phosphate groups.

C. Comparison of the DNA and polynucleotide complexes.

The Scatchard plots for both DNA and the polynucleotides were convex to the x-axis indicating the existence of heterogeneous binding sites. It would be expected that at high ionic strength, electrostatic binding should be effectively abolished leaving homogeneous binding sites. For the polynucleotides, where only one binding process

was indicated, the Scatchard plots should therefore have yielded a straight line. Peacocke noted similar results in his studies with acridines (30). He attributed this inherent heterogeneity to a continuous change in k as more dye became bound as a result of alterations in the structure of the nucleic acid. A similar process may be taking place in this study.

Another difference between DNA and the ribopolynucleotides was in the number of sites available for daunomycin binding. There were more sites available in the polynucleotides and, in fact, n exceeded the maximum allowable value for an intercalation process. The insertion of one daunomycin molecule between two base pairs should exclude binding at the adjacent base pairs due to the distortion of the helix which occurs with intercalation. Consequently, only one molecule can intercalate for every two base pairs and the maximum n value should be 0.25. LePecq and Paoletti (53) calculated that intercalation should occur only once in every four base pairs. Thus, the high n values achieved with the polynucleotides suggested that a large degree of the binding was a result of electrostatic interactions for which there is essentially no limit. (It has often been assumed that the limit for this type of binding is 1.0, but if aggregation of dye molecules can occur on the DNA molecule, which is essentially a surface phenomenon, this value can be higher. Peacocke and Skerrett (23) reported values

greater than 1.0 with proflavine). This was verified by the large decrease in n which occurred when the ionic strength was raised. There were fewer sites at the higher ionic strengths because of the exclusion of many of the electrostatic interactions in this environment. In fact, at $\mu = 0.05$ and 0.5 , the n values were lower for the ribopolynucleotides than for DNA. This showed the greater relative importance for the intercalation process for DNA vis a vis the polynucleotides.

The secondary structure of the nucleic acid was, therefore, of primary importance and governed the type and extent of interaction daunomycin had with the DNA or polynucleotide. This was further illustrated by the fact that the association constant for native DNA was significantly higher at $\mu = 0.005$ than those of either denatured DNA or the polyribonucleotides. This demonstrated that a double-helical structure was necessary for type I binding and that single stranded structures, although they can exhibit type I binding, will have diminished interaction. Zunino, et al. (86) reached the same conclusion based on similar data for the DNA-Dm interaction.

IV. Spectrofluorimetric Titrations.

A. Binding of ribo- vs. deoxy-ribopolymer duplexes to daunomycin.

The importance of the sugar residue of the nucleic acid for the interaction with daunomycin was evaluated by

comparing poly rA·poly rU, poly dA·poly dT, and poly rA·poly dT. It should be noted that except for a 5-methyl group, uracil and thymine are structurally similar and so any differences amongst these compounds should be due to the differences in their sugar moieties. In a study of the relative stabilities of deoxyribo- vs. ribo- homopolymer-duplexes, Chamberlain (103) found that the hybrid duplexes had T_m values intermediate between those for the ribopolymer and the deoxyribopolymer. However, the association constants for poly rA·poly dT were lower than those for the other two. The finding here then was rather surprising. Perhaps, even though the hybrid molecules structure is stable it may be somewhat altered owing to the differences between the sugar residues in the two strands. This could account for a weaker interaction. There were more binding sites available with poly rA·poly dT and this could indicate a more open structure as was the case with denatured DNA. Denatured DNA also exhibited a weaker binding relative to native DNA but provided more sites for daunomycin binding.

Poly rA·poly rU and poly dA·poly dT were very similar to each other at $\mu = 0.05$. However, at $\mu = 0.005$, the ribohomopolymer pair had a k value twice that for poly dA·poly dT. Chamberlain's study found, based on T_m values, that in all cases RNA homopolymer pairs were more stable than the corresponding DNA homopolymer pairs. Schmechel and Crothers (44) found that poly rA·poly rU had an association constant

similar to that for DNA in its interaction with proflavine. My studies indicate that poly rA·poly rU has a very stable structure and under many conditions will be more stable than the corresponding DNA homopolymer duplex. It should be noted that at elevated ionic strength the duplex can add another strand of poly U and become a triple stranded structure and therefore undesirable for purposes of comparison (104). For this reason, all experiments with poly rA·poly rU were performed at $\mu \leq 0.05$.

B. Base preference for the binding of polynucleotides to daunomycin.

Of those synthetic double stranded polynucleotides which were studied, poly dG·poly dC had the highest association constant. Poly dG·poly dC has a very stable double-helical structure, closely resembling that of native DNA. It has an exceptionally high T_m even at low ionic strengths (101) at $\mu = 1 \times 10^{-3}$ ($T_m \approx 90^\circ$). Since poly dG·poly dC has such a stable structure, it was not surprising that daunomycin formed its strongest complexes with this compound as compared to other double stranded polynucleotides studied (table 5). The n values for this polynucleotide duplex showed minimal variation with ionic strength and this again might be attributed to its highly stable structure, even at low ionic strength.

The observation that poly dG·poly dC had consistently higher k values than those of the polynucleotide duplexes consisting of AT base pairs could be interpreted as a pre-

erence for GC base pairs as the daunomycin binding sites. It seems much more reasonable, however, to attribute the increased binding strength of poly dG·poly dC to its very stable secondary structure, a structure very similar to that of native DNA. Poly (dA-dT)·poly (dA-dT) also possesses DNA-like structure (102) and indeed was found to have an association constant comparable to that for poly dG·poly dC, at $\mu = 0.05$. It, however, was more sensitive to changes in ionic strength and in this sense was different from poly dG·poly dC.

C. Criteria for formation of type I complex.

Both the spectrophotometric and spectrofluorimetric titration studies indicated that, rather than a base preference or selectivity for a particular sugar moiety (ribose vs. deoxyribose), the major criterion in determining the type and extent of binding of daunomycin to a nucleic acid was the secondary structure of the latter. Throughout these studies, those nucleic acids with the most stable secondary structures showed the greatest interaction with daunomycin. This was consistent with an intercalation model which requires a stable double stranded helical structure for maximum binding.

The binding data obtained by spectrofluorimetric titration could not be compared to those obtained by absorbance. The dye concentration used in the fluorescence studies was $1 \times 10^{-6}M$ as compared to $2.5 \times 10^{-5}M$ in the absorbance experiments. As a result, the values for c , concentration

of free dye, were much lower with the former which of necessity changed the extent of the interaction. At the low values of c obtained by this method, there should be very little, if any, type II interaction between daunomycin and the nucleic acid. The Scatchard plots and some of the binding isotherms (figures 28 and 29), however, did indicate two distinct binding processes. This tended to verify the point made earlier about the value for the association constant varying as more daunomycin became bound thus resulting in an inherent heterogeneity.

V. T_m Studies.

A. Biphasic melting profiles.

Figures 32 and 33 show the T_m plots for the calf thymus-DNA-Dm complexes at $T_D/T_P = 0.1$ and $T_D/T_P = 1.0$, respectively. Two characteristics of these curves should be noted. At $T_D/T_P \geq 0.5$ (figure 33), a biphasic character to the T_m curves was observed. DNA alone at all ionic strengths showed nearly no change in absorbance until the T_m transition was reached. In addition, the width of the T_m transition, i.e. the number of degrees over which the transition occurred, was very broad at low T_D/T_P , occurring over a range of $\sim 35^\circ$, whereas the transition at the higher T_D/T_P ratio took place in $\sim 8^\circ$. The increase in absorbance for the DNA-Dm complex could be interpreted as an initial destabilization of the DNA helix at pre-melting temperatures but the overall effect of the

binding was still stabilization as evidenced by an increase in T_m^i at these higher ratios. Kleinwachter and co-workers (38) found a similar behavior with acridine orange and proflavine at high values of r . They explained this as being due to a decrease in r in the pre-melting range which resulted in a release of the more weakly bound dye. A similar process was probably occurring in these studies.

Kleinwachter et al. (38) also noted a difference in the sharpness of the helix-coil transition at low and high values of r . This appeared to be a result of heterogeneity between the various base pairs in the DNA at low r values. In this range only a few dye molecules are intercalated and those base pairs adjacent to intercalated dye molecules would be more stable than those which weren't. Thus the melting would occur over a wide range of temperature. However, at high T_D/T_P , when DNA is saturated with dye, the heterogeneity would disappear and, in fact, the base pairs would be more similar to each other than they would be in free DNA since the binding of dye minimizes the stability differences between AT and GC base pairs.

B. Renaturation.

Another property of the daunomycin-DNA interaction was the apparent increase in the extent of renaturation on slow cooling as the concentration of daunomycin in the complex was increased (tables 6-8). The two strands of DNA had an increased probability of rejoining properly because

the daunomycin was holding them in proximity to each other. Although denaturation, unwinding, and strand separation, did take place in the presence of daunomycin, it is likely that at those points along the DNA molecule where daunomycin was bound complete separation did not occur. The helix thus had a greater opportunity to reform.

C. Stabilization due to AT base content.

It should be noted here that there was a difference in the renaturation behavior between the DNA's of varying GC content. A comparison of the % renaturation values in the presence of daunomycin at equivalent T_D/T_p ratios and ionic strength showed that the values were higher for calf thymus DNA (table 6) than for M. lysodeikticus DNA (table 8). The values for C1. perfringens DNA were even higher (table 7). This was especially true at low T_D/T_p ratios. This indicated that daunomycin aided the renaturation of C1. perfringens DNA to a greater extent than the others and this was even more striking in view of the fact that this DNA had less of a tendency to renature than the other DNA's when in the free state. The pattern toward increased renaturation follows the relative AT content of the DNA's, i.e. M. lysodeikticus DNA (28%) > calf thymus DNA (57%) > C1. perfringens DNA (68%). This could indicate that in the binding of daunomycin to DNA there was a preference for AT pairs. Since a DNA with more AT sites would have a greater amount of daunomycin bound, it follows that

there would be a greater degree of renaturation. This would be the situation particularly at low T_D/T_P ratios where the DNA was not yet saturated with daunomycin and it was bound preferentially to those sites for which it had the greatest affinity.

A further comparison on the basis of AT content was shown in figures 39 and 40. The plot of ΔT_m vs. T_D/T_P is hyperbolic for the three DNA's as is that for T_m' vs. T_D/T_P . The ΔT_m values were higher for Cl. perfringens DNA than the others, the trend being very similar to that described above with renaturation. As the %AT in a DNA decreased, the ΔT_m and the initial slope of the plot both decreased and this again implied a greater stabilization effect for a DNA with a higher AT base content. However, figure 40 indicates that this was not the case. At $T_D/T_P \geq 0.25$ the T_m' values for Cl. perfringens DNA and calf thymus DNA were almost identical. This indicated that at equivalent daunomycin concentrations the helix stability was the same in both DNA's. It thus seemed possible that increased stabilization, as manifested by a higher ΔT_m , for Cl. perfringens DNA was the result of lower stability of the free DNA (since Cl. perfringens DNA has a lower %GC it is less stable as attested to by its lower T_m in the free state). A greater ΔT_m may not, therefore, reflect an increased affinity for AT base pairs. A similar explanation could be proposed for the renaturation phenomenon as well.

D. Effect of ionic strength on T_m' and ΔT_m .

Another feature common to both DNA's was the increase in T_m' and a decrease in ΔT_m when the ionic strength was raised. At $\mu = 0.5$ and $T_D/T_P \leq 0.25$, the ΔT_m for both calf thymus and *Cl. perfringens* DNA was essentially zero. Chambron, et al. (36) studied the effect of ionic strength on the T_m of the proflavine-DNA complex. They measured the difference between the temperature at which proflavine was dissociated from the complex and the T_m of free DNA. This value was essentially a ΔT_m . The results found in this study were in agreement with Chambron et al.; at high ionic strength (≥ 0.5) $\Delta T_m = 0$. At first glance, one is tempted to conclude that at higher ionic strengths the complex was less stable and, therefore, the ΔT_m decreased. The intrinsic association constants for DNA did indeed decrease as the ionic strength was increased. However, Chambron, et al. (36) have pointed out that a good deal of the stabilization due to proflavine binding was the result of an electrostatic effect. If this were indeed the case, then it is easy to see how an increase in ionic strength can result in destabilization. It is clear, however, that, if anything, increasing ionic strength should stabilize the helix, as evidenced by a higher T_m for free DNA at elevated ionic strength. Based on this, another possible explanation is that since free DNA was already more stable at the higher ionic strength the extra stability to be gained by daunomycin binding was not so great.

In line with this, a glance at the T_m' values for C1. perfringens DNA-Dm complexes at all ionic strengths is informative (table 7). Although the ΔT_m decreased with increasing ionic strength, the T_m' values, at constant T_D/T_p ratios, ($T_D/T_p > 0.2$) were essentially the same at all ionic strengths (figure 36). This indicated that there was a maximum stability which could be attained and this was not dependent on ionic strength. Thus, there was no decrease in the stability of the complex at elevated ionic strengths. This behavior was not found with calf thymus DNA (table 6 and figure 34). This indicated that, for calf thymus DNA, stability could be enhanced even at higher ionic strengths and this might be a function of the base content of the DNA (calf thymus DNA having a higher %GC). This would mean that the ΔT_m decrease was indeed an indication of a decrease in stability of the complex. On the other hand, the values for T_m' at the higher ionic strengths were above 100° for $T_D/T_p > 0.5$. and it is possible that there was a maximum T_m' at the higher ionic strengths which were not measurable by the techniques used. Unfortunately, the experiments with M. lysodeikticus DNA were limited to low ionic strength and thus the possibility of GC dependence could not be clearly ascertained.

E. T_m stabilization is result of intercalation.

The T_m of a DNA solution increased as more daunomycin was added but eventually reached a plateau. For calf

thymus DNA at $\mu = 0.005$ and $\mu = 0.05$, the plateaus in the T_m' vs. T_D/T_p plots (figure 34) occurred at an r value corresponding to 0.42 and 0.3, respectively. This was the same as the n values obtained by spectral titrations. This n value is the maximum number of binding sites for type I, or intercalative, binding. A similar correlation can be made for C1. perfringens DNA (figure 36) at $\mu = 0.005$ and with less certainty at $\mu = 0.05$, the n values in this case being 0.24 and 0.1, respectively. The correspondence between the r from T_m data and the r from spectral titrations indicated that the stabilization induced by daunomycin, as evidenced by the increase in T_m , was due mainly to binding by intercalation since the stabilization leveled off at the point at which type I binding sites had become saturated. The same behavior was noted for acridine dyes and a similar explanation was proposed by Jordan (39).

Thus, much of the T_m results presented here are in accord with an intercalative mode of binding for daunomycin to DNA. Similar conclusions were drawn by various workers concerning the binding of acridine dyes to DNA, based on melting studies (36,37,38). Tubbs, and co-workers (42), on the basis of fluorescence studies, concluded that there was a preference for AT base pairs in the binding of acriflavine with DNA although this was modified subsequently (97). Gersh and Jordan (98) calculated that an intercalated proflavine should have a greater stabilization effect on AT

pairs relative to GC pairs. It is clear from the many investigations described in the introduction that the binding of acridine dyes occurs by means of intercalation. If the same is true for daunomycin, as appeared to be the case based on the present studies, then it is not surprising to find similar behavior for daunomycin and acridines in terms of base preference. Indeed, the results obtained by Kleinwachter, et al. (38) with proflavine and acridine orange were almost identical to those presented here for daunomycin. They point out, however, that in a scheme for intercalation the binding of dye to DNA proceeds in a random manner and thus the probability for intercalation into sites adjacent to either GC or AT base pairs should be equal. Therefore, there should not be any preference for AT pairs. Once random intercalation has occurred, however, it is likely that AT pairs gain more stabilization from this process than do GC pairs.

REFERENCES

1. A. DiMarco, M. Gaetani, P. Orezzi, B. Scarpinato, R. Silvestrini, M. Soldati, T. Dasdia and L. Valentini. *Nature* 201: 706, 1964.
2. F. Arcamone, G. Franceschi, P. Orezzi, G. Cassinelli, W. Barbieri and R. Mondelli. *J. Amer. Chem. Soc.* 86: 5334, 1964.
3. F. Arcamone, G. Cassinelli, P. Orezzi, G. Franceschi and R. Mondelli. *J. Amer. Chem. Soc.* 86: 5335, 1964.
4. F. Arcamone, G. Franceschi, P. Orezzi, S. Penco and R. Mondelli. *Tetrahedron Lett.* 30: 3349, 1968.
5. F. Arcamone, G. Cassinelli, G. Franceschi, P. Orezzi and R. Mondelli, *Tetrahedron Lett.* 30: 3353, 1968.
6. A. DiMarco. in *Antibiotics Vol. 1*, Ed. D. Gottlieb and P.D. Shaw, Springer-Verlag, Berlin, 1967, p. 190.
7. A. Cohen, E.H. Harley and K. Rees. *Nature* 222: 36, 1969.
8. G. Doddi, C. Intini, A.M. Isetta and M. Soldati. *Experientia*, 26: 910, 1970.
9. C. Tan, H. Tasaka, K. Yu, M. Murphey and D. Karnofsky *Cancer*, 20: 333, 1967.
10. T. Vietti, K. Starbing, J.R. Wilbur, D. Lonsdale and D.M. Lane. *Cancer*, 27: 602, 1971.
11. G. Hartmann, H. Goller, K. Koschel, W. Kersten and H. Kersten. *Biochem. Z.* 341: 126, 1965.
12. A. Rusconi and E. Calendi. *Biochemica et Biophysica Acta*, 119: 413, 1966.

13. J.H. Kim, A.S. Gelbard, B. Djordjevic, S.H. Kim and A.G. Perez. *Cancer Research* 28: 2437, 1968.
14. L.E. Crook, K.R. Rees and A. Cohen. *Biochem. Pharm.* 21: 281, 1972.
15. H. Bosmann and D. Kessel, *FEBS Lett.* 15: 273, 1971.
16. P. Chandra, F. Zunino, A. Gotz, D. Gericke, R. Thorbeck and A. DiMarco. *FEBS Lett.* 21: 264, 1972.
17. A. DiMarco, R. Silvestrini, S. DiMarco and T. Dasdia. *J. Cell Bio.* 27: 545, 1965.
18. R. Silvestrini, A. DiMarco and T. Dasdia. *Cancer Res.* 30: 966, 1970.
19. E. Calendi, A. DiMarco, M. Reggiani, B. Scarpinato and L. Valentini. *Biochem. et Biophys. Acta.* 103: 25, 1965.
20. L. Michaelis, *Cold Spring Harbor Symposium on Quantitative Biology*, 12: 131, 1947.
21. S. Brenner, L. Barnett, F.H.C. Crick and A. Orgel. *J. Mol. Biol.* 3: 121, 1961.
22. F.H.C. Crick, L. Barnett, S. Brenner and R.J. Watts-Tobin, *Nature.* 192: 1227, 1961.
23. A.R. Peacocke and J.N.H. Skerrett, *Trans. Farad. Soc.* 52: 261, 1956.
24. L.S. Lerman. *J. Mol. Biol.* 3: 18, 1961.
25. L.S. Lerman. *J. Cell.Comp. Physiol.* 64: Suppl. 1: 1, 1964.
26. D.S. Drummond, V.F.W. Simpson-Gildemeister and A.R. Peacocke. *Biopolymers*, 3: 135, 1965.

27. S. Ichimura, M. Zama, H. Fujita and T. Ito, *Biochim. et Biophys. Acta* 190: 116, 1969.
28. R.W. Armstrong, T. Kuruesev and U.P. Strauss. J. *Amer. Chem. Soc.* 92: 3174, 1970.
29. J. Chambron, M. Daune and C. Sadron. *Biochim. et Biophys. Acta.* 123: 306, 1966.
30. A. Blake and A.R. Peacocke, *Biopolymers* 6: 1225, 1968.
31. G. Lober and G. Achtert. *Biopolymers* 8: 595; 1969.
32. H.J. Li and D.M. Crothers. *Biopolymers* 8: 217, 1969.
33. I. Tinoco.J. *Amer. Chem. Soc.* 82: 4785, 1960.
34. P. Doty, H. Boedtker, J. Fresco, R. Haselkorn and M. Litt. *Proc. Nat. Acad. Sci* 45: 482, 1959.
35. J. Marmur and P. Doty. *J. Mol. Biol.* 5: 109, 1962.
36. J. Chambron, M. Daune and C. Sadron. *Biochim. et Biophys. Acta* 123: 319, 1966.
37. D.O. Jordan and L.N. Sansom. *Biopolymers* 10: 399, 1971.
38. V. Kleinwachter, Z. Balcarova and J. Bohacek. *Biochim et Biophys. Acta* 174: 188, 1969.
39. D.O. Jordan. in *Molecular Associations in Biology* Ed. B. Pullman, Academic Press, New York, 1968 p. 221.
40. G. Lober, H. Schutz and V. Kleinwachter. *Biopolymers* 11: 2439, 1972.
41. T.T. Herskovits. *Arch. Biochem. Biophys.* 97: 474, 1962.
42. R.K. Tubbs, W.E. Ditmars and Q. Van Winkle. *J. Mol. Biol.* 9: 545, 1964.
43. N.F. Ellerton and I. Isenberg. *Biopolymers* 8: 767, 1969.

44. D.E.V. Schmechel and D.M. Crothers. *Biopolymers* 10: 465, 1971.
45. H.J. Li and D.M. Crothers. *J. Mol. Biol.* 39: 461, 1969.
46. M.J. Waring, *Biochim et Biophys Acta* 87: 358, 1964.
47. M.J. Waring, *Biochim et Biophys. Acta* 114: 234, 1966.
48. G. Kreishman, S. Chan and W. Bauer, *J. Mol. Biol.* 61: 45, 1971.
49. W. Fuller and M.J. Waring. *Ber. Bunsenges. Physik. Chem.* 68: 805, 1964.
50. M.J. Waring. in *FEBS Symposium, Macromolecular Structure and Function*. Ed. S. Ochoa, 21: 143, 1970.
51. M.J. Waring. *J. Mol. Biol.* 54: 247, 1970.
52. J. Paoletti and J.B. LePecq. *J. Mol. Biol.* 59: 43, 1971.
53. J.B. LePecq and J. Paoletti. *Biochimie* 53: 973, 1971.
54. J. Hurwitz, J. Furth, M. Malamy and M. Alexander. *Proc. Nat. Acad. Sci*, 48: 1222, 1962.
55. E. Kahan, F. Kahan and J. Hurwitz. *J. Biol. Chem* 238: 2491, 1963.
56. E. Reich and I.H. Goldberg. *Progress in Nucleic Acid Research and Molecular Biology* 3: 183, 1964.
57. W. Kersten, H. Kersten and W. Szybalski. *Biochemistry* 5: 236, 1965.
58. A. Cerami, E. Reich and I.H. Goldberg. *Proc. Nat. Acad. Sci.* 57: 1036, 1967.
59. E. Reich, A. Cerami and D.C. Ward. in *Antibiotics vol. 2* Ed. D. Gottlieb and P.D. Shaw. Springer-Verlag, Berlin

1967, p. 714.

60. L. Hamilton, W. Fuller and E. Reich. *Nature* 198: 538, 1963.
61. R.D. Wells. *Science* 165: 75, 1969.
62. R.D. Wells and J.E. Larson. *J. Mol. Biol.* 49: 319, 1971.
63. W. Muller and D.M. Crothers. *J. Mol. Biol.* 35: 251, 1968.
64. J.C. Wang, *Biochim et Biophys. Acta* 232: 246, 1971.
65. R.M. Izatt, J.J. Christensen and J.H. Rytting. *Chem. Rev.* 71: 439, 1971.
66. G.L. Eichhorn, *Nature* 194: 474, 1962.
67. R.B. Inman and D.O. Jordan. *Biochim. Biophys. Acta* 42: 421, 1960.
68. W.F. Dove and N. Davidson. *J. Mol. Biol.* 5: 467, 1962.
69. J. Eisinger, R.G. Shulman and W.E. Blumberg. *Nature* 192: 963, 1961.
70. C.A. Thomas, *J. Amer. Chem. Soc.* 76: 6032, 1954.
71. T. Yamane and N. Davidson. *J. Amer. Chem. Soc.* 83: 2599, 1961.
72. T. Yamane and N. Davidson, *Biochim. et Biophys. Acta* 55: 609, 1962.
73. R.H. Jensen and N. Davidson. *Biopolymers* 4: 17, 1966.
74. G.L. Eichhorn and Y.A. Shin, *J. Amer. Chem. Soc.* 90: 7323, 1968.
75. G.L. Eichhorn, P. Clark and E.D. Becker. *Biochemistry* 5: 245, 1966.
76. M.M. Fishman, J. Isaac, S. Schwartz and S. Stein. *Biochem. Biophys. Res. Commun.* 29: 378, 1967.

77. A.M. Willemssen and G.A.J. Van Os, *Biopolymers* 10: 945, 1971.
78. S. Hiai, *J. Mol. Biol.* 11: 672, 1965.
79. C. Zimmer and H. Venner. *Eur. J. Biochem.* 15: 40, 1970.
80. M. Sundaralingam and J.A. Carrabine. *J. Mol. Biol.* 61: 287, 1971.
81. N.A. Berger and G.L. Eichhorn. *Biochemistry* 10: 1847. 1971.
82. N.A. Berger and G.L. Eichhorn. *Biochemistry* 10: 1857, 1971.
83. M.M. Fishman and L. Rosenwasser. *Biochim. et Biophys. Acta* 166: 584, 1968.
84. A. Rusconi, *Biochim. Biophys. Acta* 123, 627, 1966.
85. D. C. Ward, E. Reich and I.H. Goldberg. *Science* 149: 1259, 1965.
86. F. Zunino, R. Gambetta, A. DiMarco and A. Zaccara. *Biochim. et Biophys. Acta* 277: 489, 1972.
87. W. Kersten and H. Kersten. *Biochem. Z.* 341: 174, 1965.
88. F. Zunino. *FEBS Lett.* 18: 249, 1971.
89. A. DiMarco, F. Zunino, R. Silvestrini, C. Gambarucci and R.A. Gambetta. *Biochem. Pharm.* 20: 1323, 1971.
90. W.J. Pigram, W. Fuller and L.D. Hamilton. *Nature New Biology* 235: 17, 1972.
91. J.T. Edsall and J. Wyman, *Biophysical Chemistry*, vol. 1 Academic Press, New York, 1958, pp. 610-616.
92. K.E. Van Holde. *Physical Biochemistry*, Prentice-Hall

- Englewood Cliffs, New Jersey, 1971, pp. 57-62.
93. C. Tanford, *Physical Chemistry of Macromolecules*.
J. Wiley and Sons, New York, 1961, pp. 540-545.
94. G. Scatchard, *Annals of New York Acad. Sci.* 51: 660, 1949.
95. T. Forster, *Fluoreszenz Organischer Verbindungen*,
Vandenhoeck and Ruprecht, Gottingen, 1951.
96. P.O.P. T'so, in *Molecular Associations in Biology*, Ed.
B. Pullman, p. 39, Academic Press, New York & London,
1968.
97. L.M. Chan and Q. Van Winkle, *J. Mol. Biol.* 40: 491,
1969.
98. N.F. Gersh and D.O. Jordan. *J. Mol. Biol.* 13: 138,
1965.
99. P.K. Sarkar and J.T. Yang. *Biochemistry* 4: 1238, 1966.
100. A. Rich, *Biochim. et Biophys. Acta* 29: 502, 1958.
101. C.M. Radding, J. Josse and A. Kornberg. *J. Biol.*
Chem. 237: 2869, 1962.
102. H.K. Schachman, J. Adler, C.M. Radding, I.R. Lehman, and
A. Kornberg. *J. Biol. Chem.* 235: 3242, 1960.
103. M. Chamberlain, *Fed. Proc.* 24: 1446, 1965.
104. A. M. Michelson, J. Massoulie and W. Guschlbauer.
Progress in Nucleic Acid Research and Molecular Biology
6: 83, 1967.